


5-2017

## ANALYSIS OF THE BIOCHEMICAL AND CELLULAR ACTIVITIES OF SUBSTRATE BINDING BY THE MOLECULAR CHAPERONE HSP110/SSE1

Veronica M. Garcia

Follow this and additional works at: [https://digitalcommons.library.tmc.edu/utgsbs\\_dissertations](https://digitalcommons.library.tmc.edu/utgsbs_dissertations)

 Part of the [Biochemistry Commons](#), [Medicine and Health Sciences Commons](#), [Microbiology Commons](#), [Molecular Biology Commons](#), and the [Molecular Genetics Commons](#)

---

### Recommended Citation

Garcia, Veronica M., "ANALYSIS OF THE BIOCHEMICAL AND CELLULAR ACTIVITIES OF SUBSTRATE BINDING BY THE MOLECULAR CHAPERONE HSP110/SSE1" (2017). *The University of Texas MD Anderson Cancer Center UTHealth Graduate School of Biomedical Sciences Dissertations and Theses (Open Access)*. 771.

[https://digitalcommons.library.tmc.edu/utgsbs\\_dissertations/771](https://digitalcommons.library.tmc.edu/utgsbs_dissertations/771)

This Dissertation (PhD) is brought to you for free and open access by the The University of Texas MD Anderson Cancer Center UTHealth Graduate School of Biomedical Sciences at DigitalCommons@TMC. It has been accepted for inclusion in The University of Texas MD Anderson Cancer Center UTHealth Graduate School of Biomedical Sciences Dissertations and Theses (Open Access) by an authorized administrator of DigitalCommons@TMC. For more information, please contact [digitalcommons@library.tmc.edu](mailto:digitalcommons@library.tmc.edu).

ANALYSIS OF THE BIOCHEMICAL AND CELLULAR ACTIVITIES OF SUBSTRATE BINDING BY  
THE MOLECULAR CHAPERONE HSP110/SSE1

By

Veronica Margarita Garcia, B.S.

APPROVED:

---

Supervisory Professor  
Kevin A. Morano, Ph.D.

---

Catherine Denicourt, Ph.D.

---

Theresa M. Koehler, Ph.D.

---

Michael C. Lorenz, Ph.D.

---

Ambro van Hoof, Ph.D.

APPROVED:

---

Dean, The University of Texas  
MD Anderson Cancer Center UTHealth Graduate School of Biomedical Sciences

ANALYSIS OF THE BIOCHEMICAL AND CELLULAR ACTIVITIES OF SUBSTRATE BINDING BY  
THE MOLECULAR CHAPERONE HSP110/SSE1

A

Dissertation

Presented to the Faculty of

The University of Texas

M.D. Anderson Cancer Center

Graduate School of Biomedical Sciences

in Partial Fulfillment

of the Requirements

for the Degree of

DOCTOR OF PHILOSOPHY

By

Veronica Margarita Garcia, B.S.

Houston, TX

May, 2017

I dedicate this work to Ozmin Jr., Emily and Victoria Salinas.

May you always dream big and recognize that your dreams are achievable.

## **Acknowledgments**

I would like to thank my mentor Dr. Kevin A. Morano for support and guidance throughout my graduate career and for accepting me into your laboratory when I was without a home. I would like to thank Drs. Catherine Denicourt, Theresa M. Koehler, Michael C. Lorenz, and Ambro van Hoof for all the time you invested in me. Thank you for serving on my committee, for all of your input in my research, and for all the recommendation letters you had to write. The successes I've had could not have happened without the five of you.

To the members of my lab, Yanyu Wang, Jacob Verghese, Jennifer Abrams, Kimberly Cope, Sara Pepper, Amy Ford, Unekwu Yakubu, Julie Heffler, Mike McCarthy, and Justin Nguyen, it has been a pleasure working with and getting to know you. Thank you for all your help and contributions to my research. Each of you has added greatly to my professional and scientific development.

I am grateful to the organizations that funded my graduate studies through awards Ruth L. Kirschstein National NRSA Predoctoral Fellowship, Robert D. Watkins Graduate Research Fellowship, Harry S. & Isabel C. Cameron Foundation. Thank you for funding my ideas. Without your support, there would be less scientific exploration.

I want to thank the MMG department. The faculty pushed me to do more and think beyond the obvious. The research we conduct as students would be significantly more difficult if we did not have the support of our departmental staff. I also want to thank my fellow students. I have learned so much from interacting with you. Thank you for the fun times, the scientific challenges, and the help you provided when I needed it.

I met three amazing people during my time in graduate school. Jennifer Abrams, I love your heart. Thank you for being the friend that I could always count on. Veronica Rowlett, you're my friend, my workout partner, my collaborator, and my homodimer. Katie McCallum, thank you for keeping me grounded and a little less insane. These women were excellent contemporaries and

better friends than I deserved. Thank you for always being available for science talks, guidance, venting sessions, and most importantly to share a beer.

Dr. Sarah Castro, Dr. Mark Ott, Willy Wong, and Tatyana Modlin your professional as well as personal support is greatly appreciated. My years at Johnson Space Center were a pleasure because I was able to work with a great team, and I was lucky to have mentors like you. Sarah, I'm ready for the Fusion Institute!

Dr. Serenella Sukno and Dr. Carlos Gonzales thank you for noticing and believing in my potential. Dr. Sukno, your teachings were the foundation of my scientific career something for which I am very grateful.

Erin, I want to thank you for your friendship. We met almost 15 years ago, and your support and encouragement has never faltered. In you, I have a friend and another sister.

I want to thank my partner. You celebrate my accomplishments and feel my frustrations as if they were your own. Thank you for being there every step of the way and for holding my hand when things get tough. Jay, I love you.

Erika, Claudia, Miguel, Ozmin, and Kristin, you're the best crew. Thank you for pointing out my flaws, as siblings should, and accepting me in spite of them. Thank for supporting me and cheering me on during the difficult times. I hope that I can pay it back someday. I am lucky to have grown up with you, and I look forward to us growing older and weirder together.

Mami y Papi, estoy muy agradecida de la educación que me dieron, del apoyo que siempre me brindaron, y del amor que han mostrado. Los quiero con todo mi corazón. Todo lo que eh logrado a sido posible porque tengo los mejores padres del mundo.

ANALYSIS OF THE BIOCHEMICAL AND CELLULAR ACTIVITIES OF SUBSTRATE BINDING BY  
THE MOLECULAR CHAPERONE HSP110/SSE1

Veronica Margarita Garcia, B.S.

Advisory Professor: Kevin A. Morano, Ph.D.

Molecular chaperones ensure protein quality during protein synthesis, delivery, damage repair, and degradation. The ubiquitous and highly conserved molecular chaperone 70-kDa heat-shock proteins (Hsp70s) are essential in maintaining protein homeostasis by cycling through high and low affinity binding of unfolded protein clients to facilitate folding. The Hsp110 class of chaperones are divergent relatives of Hsp70 that are extremely effective in preventing protein aggregation but lack the hallmark folding activity seen in Hsp70s. Hsp110s serve as Hsp70 nucleotide exchange factors (NEF) that facilitate the Hsp70 folding cycle by inducing release of protein substrate from Hsp70, thus recycling the chaperone for a sequential round of folding and allowing successfully folded substrates to exit the folding cycle. In the model organism *Saccharomyces cerevisiae*, Hsp110 is represented by the proteins Sse1 and Sse2, which possess an Hsp70-like substrate binding domain (SBD), making them unique among other functionally similar, but structurally distinct, NEFs. Studies of Hsp110 and Sse1 have demonstrated that this chaperone/NEF family can bind polypeptides and prevent proteins from aggregating *in vitro* and that this ability is conferred by the SBD. However, attempts to study Hsp110 protein binding *in vivo* have not been successful. To date, the impact of peptide binding by Hsp110 is unknown. This study elucidates and defines substrate binding by the yeast Hsp110 and addresses the contributions of this activity toward protein and cellular homeostasis as well as begins inquiries into substrate binding by the *Drosophila melanogaster* Hsp110, Hsc70cb. As a major partner of Hsp70, determining cellular Hsp110 activities is a prerequisite to a full understanding of chaperone-mediated protein homeostasis. By studying chaperone functions and activities in yeast and animal

models, we can understand human cellular protein quality control systems which can then be pharmacologically targeted to combat protein conformational disorders, including Alzheimer's, Huntington's, and Parkinson's diseases.



## Table of Contents

Approval Sheet	i
Title Page	ii
Dedication	iii
Acknowledgements	iv
Abstract	vi
Table of Contents	viii
List of Figures	x
List of Tables	xii
Chapter I: Introduction	1
Stress and protein quality control	2
The Hsp70 machine	4
Hsp70•Hsp40•NEF complexes throughout the yeast cell	9
Sse1/Hsp110 as a nucleotide exchange factor and holdase	12
Biomedical Significance	13
Chapter II: Materials and Methods	18
Chapter III: Semi-automated microplate monitoring of protein polymerization and aggregation	30
Introduction	31
Results	32
Discussion	39
Chapter IV: Substrate binding by the yeast Hsp110 nucleotide exchange factor and molecular chaperone, Sse1, is not obligate for its biological activities	40
Introduction	41

Results	43
Discussion	61
Chapter V: A carboxy-terminus regulated fluorescence affinity tag affects Sse1 functions	64
Introduction	65
Results	67
Discussion	85
Chapter VI: Characterization of the <i>Drosophila melanogaster</i> Hsp110	87
Introduction	88
Results	89
Discussion	96
Chapter VII: Discussion and Future Directions	99
Summary	100
Hsp110 as a nucleotide exchange factor and a substrate chaperone	101
Hsp110 contribution to Hsp70 functions	102
The metazoan disaggregase	105
Implications of Hsp110 in molecular progression of neurodegeneration	107
Hsp110 holdase as a clinical tool	108
Bibliography	109
Vita	129

## List of Figures

<b>Figure 1-1.</b> Comparative representation of Hsp70 and Hsp110 proteins	5
<b>Figure 1-2.</b> Cooperative folding by Hsp70, Hsp40 and Hsp110	7
<b>Figure 1-3.</b> Crystal structure of Hsc70-Hsp110 complex	14
<b>Figure 2-1.</b> Allele recombination to produce Sse1 variant strains	21
<b>Figure 3-1.</b> Monitoring aggregation of firefly luciferase	34
<b>Figure 3-2.</b> Aggregation of model chaperone substrates rhodanese and citrate synthase	36
<b>Figure 3-3.</b> Monitoring aggregate prevention of citrate synthase and protection by Sse1	38
<b>Figure 4-1.</b> Novel Sse1 substrate binding mutant retains Hsp70 nucleotide exchange capacity	44
<b>Figure 4-2.</b> Purification of recombinant Hexa-histidine tagged Sse1 proteins	45
<b>Figure 4-3.</b> Sse1 substrate binding domain mutant exhibits impaired chaperone holdase activity towards firefly luciferase	47
<b>Figure 4-4.</b> Sse1 substrate binding domain mutant exhibits impaired chaperone holdase activity towards citrate synthase	48
<b>Figure 4-5.</b> Sse1 <sub>sbd</sub> is stable and interacts with endogenous yeast Hsp70 proteins in vivo	51
<b>Figure 4-6.</b> Sse1 <sub>sbd</sub> supports growth at normal but not heat shock temperatures	53
<b>Figure 4-7.</b> Loss of Sse1 holdase activity results in mild proteotoxicity	55
<b>Figure 4-8.</b> SBD function is not required for Hsp90-dependent glucocorticoid activation via Sse1	57
<b>Figure 4-9.</b> Sse1 SBD function is not required for clearance of the misfolded CPY <sup>+</sup> -GFP reporter	59
<b>Figure 4-10.</b> Sse1 SBD function is not required for clearance of the CPY <sup>+</sup> -GFP aggregates	60
<b>Figure 5-1.</b> Model of Sse1 fused to a carboxyl-terminus regulated fluorescence affinity (RFA) tag	68
<b>Figure 5-2.</b> Sse1-RFA phenocopies the sensitivity to heat stress of the Sse1 substrate binding mutant	70

<b>Figure 5-3.</b> Similar to a substrate binding mutant, Sse1-RFA is sensitive to formamide	71
<b>Figure 5-4.</b> <i>SSE1-RFA</i> cells grow like wild-type cells and demonstrate a negligible HSR activation	74
<b>Figure 5-5.</b> Sse1-RFA is capable of activating the Hsp90-dependent glucocorticoid receptor via Sse1	76
<b>Figure 5-6.</b> Sse1-RFA is non-functional in clearing the misfolded CPY <sup>+</sup> -GFP substrate	78
<b>Figure 5-7.</b> TMP does not rescue the clearance defect of <i>SSE1-RFA</i> cells	80
<b>Figure 5-8.</b> The Sse1-RFA domains are accessible in vivo	82
<b>Figure 5-9.</b> A GFP tag on the C-terminus of <i>SSE1</i> results in growth phenotypes similar to the <i>SSE1-RFA</i> strain	84
<b>Figure 6-1.</b> Characterizing the substrate binding domain in yeast, fly and human biology	90
<b>Figure 6-2.</b> Hsp70cb does not complement an <i>sse1Δ</i> or interact with the yeast Hsp70s	92
<b>Figure 6-3.</b> Substrate holding function is conserved in Hsp70cb	94
<b>Figure 6-4.</b> Recombinant protein purification of Hexa-histidine tagged Hsc70cb	95
<b>Figure 6-5.</b> Proposed mutants to study the substrate interactions of Hsp70cb	97

## **List of Tables**

<b>Table 2-1.</b> Strains used in this study	18
<b>Table 2-2.</b> Plasmids used in this study	19

## **Chapter 1: Introduction**

## *Stress and protein quality control*

Most cellular functions are carried out by proteins which must fold into a proper three-dimensional configuration, or native state. Nascent polypeptides possess all the biophysical information required to achieve the native state, but the process of protein folding is complex and often vulnerable to translation errors and environmental factors (1-4). As newly synthesized proteins exit the ribosome, these unfolded polypeptides run the risk of misfolding or aggregating. Large complex polypeptides cannot acquire their proper secondary or tertiary structure until the entire necessary domain or domains required for proper folding have exited the ribosome (5, 6). Exponentially growing yeast contain approximately  $10^5$  active ribosomes per cell (7, 8). In typical mammalian cells approximately  $10^6$  to  $10^7$  ribosomes are translating RNA into protein (9). This much ribosomal activity within one cell necessitates the aid of a network of molecular chaperones to maintain a functional proteome. Molecular chaperones help other proteins achieve their native conformations by stabilizing folding intermediates without becoming part of the final structure of those proteins (5).

Under optimal conditions, molecular chaperones help in *de novo* protein folding, repairing misfolded substrates, maturation and translocation of proteins, and promoting the degradation of irreparable proteins (5, 10). Chaperones act as a cellular quality control system and protect newly synthesized polypeptides by binding the exposed hydrophobic regions of unfolded proteins. They preventing aggregation and allow proteins to fold in a protective environment thus preventing premature degradation (11). In addition to promoting nascent polypeptide folding, chaperones repair proteins that are damaged post-translation. For example, when cells are exposed to heat stress, damaged proteins segregate into aggregates until chaperones rescue and refold them (12-14). Producing proteins is energy and resource intensive therefore the protein quality control machinery first attempts to repair proteins where energy has already been spent (15). While chaperones

typically function as protein folding machines, they play an important role in determining when a protein is fatally damaged and repair is not a possibility. Chaperones have to recognize misfolded proteins and facilitate their refolding to avoid protein aggregates. When this fails or the misfolding is irreversible, chaperones have to recognize this terminal state and target the protein for degradation (16). Irreparably misfolded proteins are delivered for proteolysis and eradicated by the ubiquitin proteasome system which tags substrates with ubiquitin and delivers them to the 26S proteasome (17). This process is part of protein quality control and depends on molecular chaperones cooperating with specific ubiquitin protein ligases (18-20).

Proteostasis can be defined as the balance of biosynthetic and turnover activities of the proteome (21). Proteomic stress such as fluxes in pH, temperature, or reactive chemical compounds can wreak havoc on proteostasis and may cause proteins to misfold and aggregate. These stresses induce the expression of chaperones through activation of the unfolded protein response (UPR) or the heat shock response (HSR) in the ER or the cytosol respectively (22-24). The heat shock response is a transcriptional activation that induces protective genes encoding molecular chaperones, or the Heat shock Protein (HSPs) (25). Chaperones are classified according to their molecular weight, i.e. Hsp40, Hsp70, Hsp90, and Hsp110 and into classes by functional similarity. Stress-induced stimulation of the HSR is important to combat the serious risk of unfolded protein accumulation that can result in the formation of aggregates that can be detrimental to cell health (26). Furthermore, aggregate associated sequestration of chaperones can lead to a deficit of chaperone-mediated activities. For instance, cellular functions such as clathrin-mediated endocytosis are dependent on a consistent pool of chaperones (27). The HSR and HSPs are required for cells to recover from, adapt to, and resume growth under stress conditions that may perturb cellular proteostasis (28).



### *The Hsp70 machine*

Heat shock protein 70 (Hsp70) chaperones are highly conserved and ubiquitous, and they possess an astounding functional diversity considering the high level of conservation among homologs and across species. These chaperones are central players in proteome maintenance as they are involved in folding of nascent polypeptides, delivering proteins to different organelles, refolding damaged proteins, and targeting proteins for degradation that are terminally misfolded.

Hsp70 recognizes its substrates by the exposed hydrophobic regions of unfolded polypeptides and binds a stretch of approximately seven amino acids rich in aliphatic residues (29-30). Its function is fundamentally an activity executed by nucleotide-dependent cycles of substrate binding and release. Hsp70 requires the J-domain (also known as J-proteins and Hsp40) and nucleotide exchange factor (NEF) to drive the ATP cycle and the promiscuous client recognition.

The canonical Hsp70 protein is divided into two major domains. The amino-terminal ATPase is known as the nucleotide binding domain (NBD) (44 kDa) whereas the carboxy-terminus includes a substrate binding domain (SBD) (27 kDa) that can be subdivided into a  $\beta$ -domain and an  $\alpha$ -domain (Figure 1-1) (31, 32). Hsp70 possess a nucleotide-driven interdomain communication that causes conformational changes based on its ATP or ADP binding state (33-35). The SBD binds substrates through a binding cleft in the SBD  $\beta$ . When Hsp70 is ADP-bound, substrate binding switches to a high affinity state due to a domain reorientation which is driven by ATP hydrolysis in the NBD. The conformational change in Hsp70 induces a “clamping down” of the SBD  $\alpha$  on the SBD  $\beta$  to confer high-affinity substrate binding (34-37). Hsp70 must cycle between high- and low-binding affinity states in order to allow protein clients to fold.



**Figure 1-1 Comparative representation of Hsp70 and Hsp110 proteins.** Both proteins are structurally divided into two major domains which are the nucleotide binding domain (NBD) at the N-terminus and the substrate binding domain (SBD) at the C-terminus. Hsp110 possess an extender spacer region between the beta sandwich (SBD β) and the alpha helical bundle (SBD α) at the C-terminus.

The different nucleotide-dependent binding states are regulated by cochaperones. At basal levels, Hsp70 has a very low rate of ATPase activity and nucleotide exchange. The basal ATP hydrolysis rate of the bacterial Hsp70 is  $0.040 \pm 0.007 \text{ min}^{-1}$  and the nucleotide dissociation rates of various yeast and human Hsp70s ranges from  $0.2\text{-}0.5 \text{ s}^{-1}$  (33, 38-40). This characteristic low level of ATPase and nucleotide exchange activity is accelerated by the Hsp40 chaperones (also known as J-proteins) and nucleotide exchange factors to accelerate both activities and promote functional cycling (Figure 1-2). Hsp40 proteins induce the intrinsic ATPase of Hsp70 causing a conformational change that increases the affinity of client binding (41-43). The NEFs promote a recycling of Hsp70 by triggering the release and exchange of ADP for ATP (39, 44-46). They bind to the Hsp70 NBD inducing a conformational change in that domain that triggers the release of the ADP nucleotide (47). When the nucleotide is ejected from the NBD, Hsp70 returns to a low affinity binding state and the bound substrate is released (40, 48). A new ATP molecule is bound by the NBD and a new Hsp70 folding cycle begins. Hsp70 functional specificity can be ascribed to these cochaperones which are more adapted to specific functions.

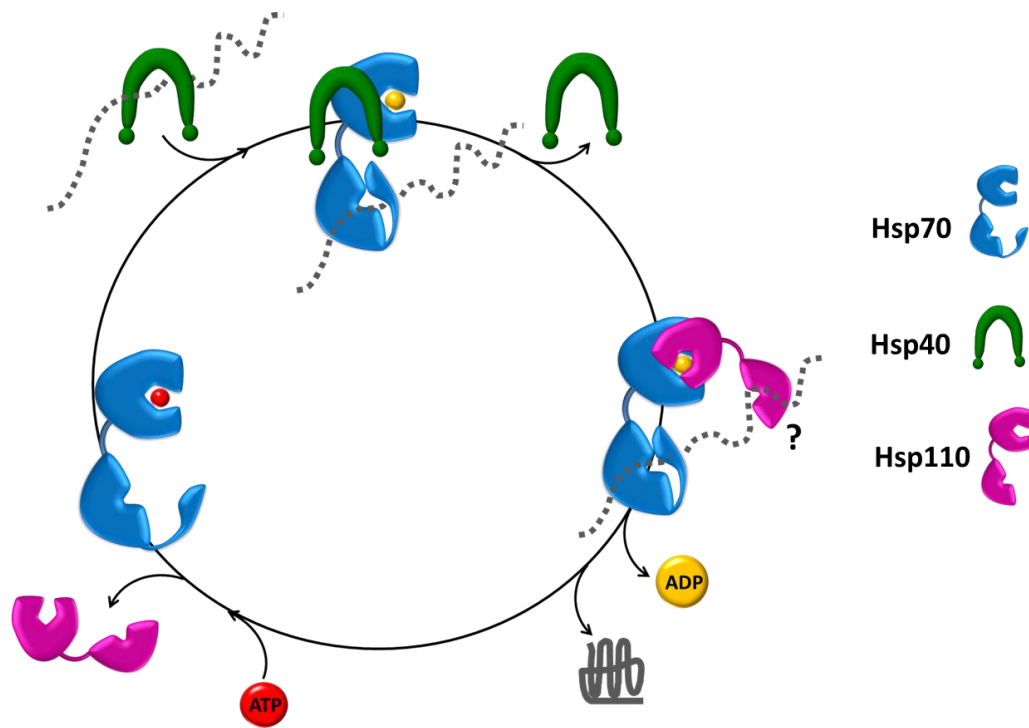


**Figure 1-2. Cooperative folding by Hsp70, Hsp40, and Hsp110.** The nucleotide dependent Hsp70 protein folding cycle proceeds with the help of the cochaperones Hsp40 and nucleotide exchange factors (NEF) to produce a folded protein. The NEF depicted here is the Hsp110. The unfolded polypeptide is depicted as a dotted line and as a solid line when fully folded.

Hsp40 chaperones are classified based on the J-domain, a 70-amino acid domain containing a conserved histidine-proline-aspartate (HPD) tripeptide sequence modeled in the bacterial DnaJ (42). All Hsp40s have the J-domain in common, but they can have many other domain variations. Additionally, Hsp40s are classified as type I, type II, or type III by the similarity of each chaperone to DnaJ outside of the J-domain (49). The HPD allows J-proteins to interact with the Hsp70 NBD, prompting its intrinsic ATPase activity (50, 51). Hsp40s induce the ATPase of Hsp70 to increase substrate binding affinity but can also bind substrate clients themselves (52). Based on *in vitro* characterization, a triprotein complex is formed where Hsp40 recognizes and binds unfolded proteins and presents the substrate during the interaction with the Hsp70 NBD (53, 54). J-domain proteins increase the effectiveness of the Hsp70 protein folding machine by binding chaperone substrates and delivering them to Hsp70 (52, 55-56). In yeast, either of the two major cytosolic Hsp40s, Ydj1 or Sis1, and their substrate binding function is required to maintain cell viability (57). These data are evidence that Hsp40 activities include inducing ATP hydrolysis in Hsp70 and facilitating substrate recognition and binding by Hsp70.

Although Hsp70 possesses a low rate of intrinsic nucleotide exchange activity *in vitro*, NEFs facilitate nucleotide exchange and are clearly vital for Hsp70 function *in vivo* as absence of cytosolic NEF function is lethal in yeast (33, 39, 45, 58). As previously mentioned, the NEFs allow for the quick nucleotide cycling required of Hsp70. They make contact with the bi-lobular Hsp70 NBD and cause it to collapse around the ADP molecule so the nucleotide-binding pocket cannot function (46, 59, 60). Release of the hydrolyzed nucleotide leaves the NBD free to bind another ATP molecule and begin a new Hsp70 folding cycle. NEFs can be classified into four unrelated groups: homologs of the protein GrpE from *Escherichia coli*, the human Hsp70-binding protein 1 (HspBP1), the Bcl-2 associated athanogene (BAG) proteins, or the Hsp110 proteins. Unlike the J-domain of Hsp40s, there is no functional domain that is common to the NEFs. While all NEFs make contact with the Hsp70 NBD to perform the nucleotide exchange activity, the varied structure of each NEF class dictates a different

mechanism of Hsp70 interaction (61, 62). For example, HspBP1 contains four  $\alpha$ -helical repeats that constitute an armadillo-like domain that makes contact with Hsp70 (63). Hsp110 proteins are divergent members of the Hsp70 family of proteins. They interact with Hsp70 through their own NBD and their C-terminus (59). Even though the NEFs vary in structure and domain composition, they all interact with the same region of the Hsp70 NBD (64).

#### *Hsp70•Hsp40•NEF complexes throughout the yeast cell*

In the *Saccharomyces cerevisiae* cytosol, Hsp70 is represented by two families of proteins. The Ssa family is encoded by *SSA1-4* (Stress-Seventy subfamily A) which share functional homology and are differentially transcriptionally regulated (65). The *SSA1* and *SSA2* isoforms are constitutively expressed while *SSA3* and *SSA4* are stress inducible under the control of the Hsf1 transcription factor (66). The Ssb family is encoded by *SSB1-2* (Stress-Seventy subfamily B) which are functionally interchangeable (66). Ssa chaperones can fulfill some Ssb functions, but Ssb cannot fulfill all Ssa functions as deletion of all *SSA* isoforms is lethal (67). Ssb chaperones are regulated in a similar fashion to ribosomal proteins and their transcription is reduced upon heat shock of yeast cells (68, 69). There are 13 cytosolic and nuclear Hsp40s in yeast that are involved in cytosolic general protein folding, peroxisomal import, ribosome biogenesis, and vesicle trafficking (65). Of these, Caj1 and Cwc23 are strictly localized in the nucleus (70). The yeast cytosol possesses three classes of cytosolic NEFs, with human orthologs: the Hsp110-type proteins Sse1/Sse2 (Stress-Seventy subfamily E), the HspBP1-type protein Fes1 (Factor Exchange for Ssa1p) and the BAG-1-type protein Snl1 (Suppressor of Nup116-C Lethal) (71-75).

Protein folding in the cytosol and nucleus is executed by an overlapping chaperone network. The Hsp40s, Ydj1 (Yeast DnaJ) and Sis1 (Slt4 Suppressor), help the cytosolic Hsp70 Ssa prevent protein aggregation (52). Although both Ydj1 and Sis1 enhance the ability of Ssa to reactivate unfolded

proteins, Ydj1 is more effective at inducing this Ssa behavior than Sis1. Furthermore, Ydj1 is essential to help cells cope with heat stress and in its absence are non-viable (52, 76). Large aggregate resolubilization by Hsp70 requires the concerted effort of the ATP-dependent Hsp100 family of proteins (26). In yeast, these proteins are located in the cytosol and in the mitochondrion to provide compartment-specific protection by interacting with the local Hsp70s (77). Hsp104, a member of the Hsp100 family, is greatly induced upon thermal stress and functions to reactivate aggregated proteins by translocating polypeptides through the ring formed by its hexameric complex (26). Hsp100 chaperones act cooperatively with the Hsp70 machine to disaggregate and reactivate misfolded proteins (1).

The high expression of Ssb during cell growth is consistent with its primary function of folding nascent chains on translating ribosomes along with the ribosome associated complex (RAC). RAC is a heterodimer complex that works exclusively at the ribosome and is composed of the Hsp40, Zuo1 (ZUOtin), and the atypical Hsp70, Ssz1 (Stress-Seventy subfamily Z) (78). Ribosomal interactions of Ssb through RAC are conferred exclusively via Zuo1 which induces the ATP hydrolysis in Ssb. A charged region within the Zuo1 structure mediates RAC binding to Rpl31, a protein at the ribosomal tunnel exit (79-81). Ssb binds the unfolded polypeptide, dissociates from the ribosome, and interacts with NEFs in the cytosol to complete *de novo* folding activities (45, 82, 83). Although Ssb has the prominent role in folding newly synthesized proteins and ribosomal interaction, Ssa can fulfill this function in the absence of Ssb (84). In addition to their *de novo* folding activities, Ssa and Ssb coordinate with Jjj1 (Hsp40), RAC, and NAC (Nascent Polypeptide-Associated Complex), in the assembly of new ribosomes (85).

The cytosolic Hsp70 in yeast are also responsible for endoplasmic reticulum (ER) protein translocation and for nuclear transport across the nuclear membrane (86). Ssa1 binds precursor proteins prior to their import in to the ER (87) . Ssa1 is also involved during nuclear transport by targeting protein to the nuclear membrane and during the translocation phase (88). Ssb is exported

from the nucleus because it possesses a C-terminal nuclear export sequence (NES). Removal of the NES is sufficient for Ssb to stimulate nuclear transport similar to Ssa. In the nucleus, Ssa also regulates the transcription factor Hsf1, the master regulator of the HSR. Ssa1 and Ssa2 bind Hsf1 to repress its activity during non-stress conditions (24) (unpublished data from Sara Pepper, Morano Laboratory).

Protein residents of the ER and the mitochondrion are physically separate from the cytosolic environment; therefore, they require their own chaperone network with specific Hsp70 machines. The ER is an undulating organelle where nascent proteins are folded and processed before being trafficked by Golgi vesicles. Protein processing and the maturation in the ER are facilitated by a dedicated Hsp70 network. The ER possesses one canonical Hsp70, Kar2 (KARyogamy), four Hsp40s, and two NEFs (65). Three of the four Hsp40s in the ER are membrane anchored and face the lumen whereas Scj1 is not anchored and diffusible. Scj1 cooperates with Kar2 to chaperone an array of ER luminal proteins (89). Translocation into the ER lumen occurs both co-translationally, as proteins are synthesized, and post-translationally, as a fully synthesized polypeptide released from the ribosome. During translocation, Kar2 is recruited by Sec63, an Hsp40 protein, to the translocon complex which stimulates the ATPase activity of the Hsp70 and facilitates the transport of a polypeptide chain across the ER translocon (90). Lhs1 (Luminal Hsp Seventy) and Sil1 (Suppressor of the Ire1/Lhs1 double mutant), are redundant NEFs and function as cochaperones for Kar2 during protein translocation (91).

Perturbations in the ER homeostasis that cause protein misfolding trigger the UPR, causing proteins to be ejected from the ER in a process known as ERAD (Endoplasmic Reticulum Associated Degradation). Jem1 (DnaJ-like protein of the ER Membrane) and Scj1 (*S. Cerevisiae* DnaJ) are Hsp40s that function redundantly during Kar2-mediated ERAD substrate selection (92). Lhs1 plays a role in refolding protein aggregates after stress and its substrate binding activity is vital to turnover of ER proteins through ERAD (93, 94).

Given the different environments in the mitochondrion created by the dual membrane system and its two compartments, protein folding and quality control requires a dedicated set of



chaperones. The Hsp70 machines in the mitochondrion are comprised of three Hsp70-type chaperones, Ssc1/3 (Stress-Seventy subfamily C) and Ssq1 (Stress-Seventy subfamily Q), five Hsp40-type, and one NEF; all of which localize to the mitochondrial matrix (65). The GrpE-like Mge1 (Mitochondrial GrpE) is the sole NEF, so the Hsp70s compete for interaction to fulfill their respective functions (95, 96).

The primary roles for Ssc1 are in protein translocation into the mitochondrion through interactions with the translocase complexes, Tom and Tim, followed by protein folding in the matrix (97, 98). Ssc3 is 82% identical to Ssc1 and also associates with unfolded proteins during and after translocation, but Ssc3 cannot fulfill all the functions of Ssc1 as it cannot complement the lethal *ssc1Δ* (99, 100). Ssq1 shares 52% identity to Ssc1, and while Ssc1 overexpression can rescue the growth phenotypes of *ssq1Δ* during cold stress, Ssq1 overexpression does not fix the translocation defects in cells expressing an Ssc1 mutant (101). Assembly of FeS clusters in mitochondria requires Ssq1 activity along with the Hsp40, Jac1 (102). In the mitochondrial matrix, yeast has an Hsp104 homolog known as Hsp78 which binds and stabilizes unfolded proteins to prevent aggregation (65, 77). Hsp78 has chaperone functions that overlap with those of Ssc1 such as maintaining genome integrity and respiration in the mitochondrion and conferring mitochondrial thermotolerance (77). Hsp70 is conserved throughout various compartments of the yeast cells to promote protein folding in diverse environments in coordination with cochaperones that add specificity to the Hsp70 machine.

#### *Sse1/Hsp110 as a nucleotide exchange factor and holdase*

First characterized in 1993, the Sse1/Sse2 proteins share high similarity with each other (97%) and with the Hsp70 protein Ssa1 (70%) (71). Distinct from other NEFs, Hsp110 share similar structure to Hsp70 and are divergent members of the Hsp70 superfamily. Hsp110, like Hsp70 proteins, is composed of a nucleotide binding domain (NBD) with an ATP binding pocket, and a substrate binding

domain (SBD) at the C-terminus (103) (60) (104). The NBD is followed by a linker that connects it to the SBD which can be subdivided into a  $\beta$ -domain ( $\beta$  sandwich and loop) and a  $\alpha$ -domain (Figure 1-1). The loop in the SBD  $\beta$  functions as a spacer region between the  $\beta$ -domain sandwich and  $\alpha$ -helix bundle that makes up the  $\alpha$ -domain (59).

Unlike the Hsp70s, the NBDs of Sse1 and Sse2 bind ATP but hydrolysis is not required for their NEF activity (39, 44, 47, 105). ATP binding allows the Sse1 NBD to be in a proper conformation to interact with Hsp70. The Sse1  $\alpha$ -helical lid domain contacts the Hsp70 NBD in the heterodimer complex (Figure 1-3) (60, 104). The crystal structure for the Hsp70-Sse1 complex depicts two chaperones interacting primarily through the NBDs and the Hsp70 SBD in close proximity to the Sse1  $\beta$ -domain (104, 105). In complex, the Sse1 substrate binding domain remains exposed and potentially free to bind an unfolded polypeptide, suggesting possible cooperative substrate binding. Whereas the entire SBD of Hsp70 is known to bind regions of unfolded polypeptides and accelerate substrate folding (“foldase” activity), a cellular role for the Sse1/Sse2  $\beta$ -domain has not been found but it is hypothesized to be a peptide-binding site (103). Sse1 and mammalian Hsp110 are capable of binding unfolded substrates and can act as a “holdase” *in vitro*, meaning that they can stabilize unfolded proteins independently of Hsp70 (106-108). Sse1 exhibits a preference for regions rich in aromatic residues that differ from the aliphatic residues commonly bound by Hsp70 (30, 109). The ability of Hsp110/Sse1 to bind unfolded polypeptides *in vitro*, the unique peptide preference, and the conformation of the heterodimer complex with Hsp70 suggest the possibility that Sse1 and other Hsp110s interact with substrate during the Hsp70 folding cycle. It is widely accepted that Hsp110 modulates Hsp70 function through involvement in its ATPase cycle, but it remains disputed if Hsp110 additionally influences Hsp70 substrate targeting. Biochemical studies have implicated the human Hsp110 as the single NEF that can power a metazoan disaggregase machine (110-112). Together, these data support a model wherein Sse1 binds substrate using its SBD to stabilize unfolded proteins *in vivo* thus contributing to Hsp70-mediated protein folding by function other than NEF activity.

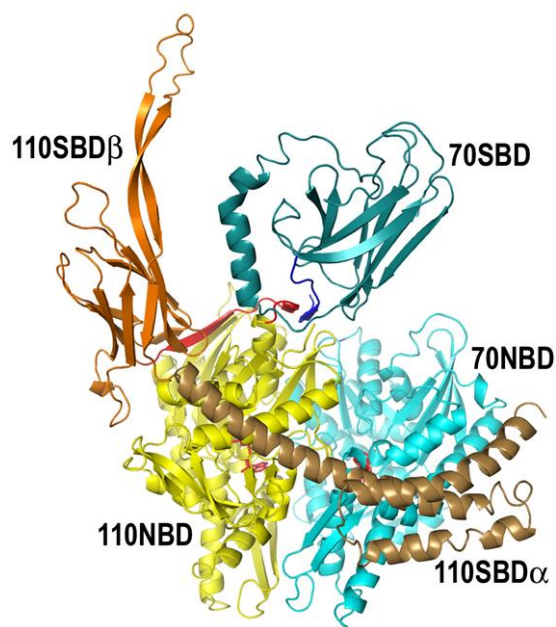


**Figure 1-3. Crystal structure of Hsc70-Hsp110 complex.** Ribbon model of the heterodimer where Hsp110 is colored in red, yellow, orange, and brown, and Hsp70 is colored in blue tones (104). This figure was obtained from Schuermann, J. P., J. Jiang, J. Cuellar, O. Llorca, L. Wang, L. E. Gimenez, S. Jin, A. B. Taylor, B. Demeler, K. A. Morano, P. J. Hart, J. M. Valpuesta, E. M. Lafer, and R. Sousa. 2008. Structure of the Hsp110:Hsc70 nucleotide exchange machine. *Mol Cell* 31: 232-243. It was printed with permission from Elsevier, the owner of Molecular Cell, through license number 4077501097759.

Sse1 is an abundant and potent Hsp70 NEF that is constitutively expressed, and both *SSE1* and *SSE2* are transcriptionally upregulated during stress conditions (113). During heat stress, *SSE1* is upregulated approximately two-fold, and *SSE2* transcripts increase by up to twelve-fold (71). Deletion of *SSE1* confers a distinct growth deficiency and a temperature sensitive phenotype, whereas a combined deletion of non-essential *SSE1* and *SSE2* is lethal (40, 44, 71). The overexpression of the cytosolic Snl1 $\Delta$ N or Fes1 NEFs can partially rescue the growth phenotype of *sse1* $\Delta$  cells grown under optimal conditions but cannot complement the nonviable *sse1* $\Delta$ *sse2* $\Delta$  (114, 115). These phenotypes indicate that Sse proteins perform a unique cellular role that other cytosolic NEFs cannot fulfill. Given that Sse proteins are unique in their ability to bind unfolded polypeptides, it stands to reason that their substrate binding functions cannot be rescued by the other cytosolic NEFs.

#### *Biomedical Significance*

The chaperone system that coordinates protein quality control during environmental stress also overcomes the folding barriers so proteins encoded by genes with mutations can properly fold (116). Protein misfolding and aggregation are linked to many human diseases. Neurodegenerative disorders such as Alzheimer's (AD), Parkinson's (PD), and Huntington's (HD) disease, and Amyotrophic Lateral Sclerosis (ALS) are examples of the deleterious effects of protein misfolding and aggregation (116, 117). AD, HD, ALS and PD are essentially diseases where misfolded proteins form fibrillar aggregates that are deposited around neurons. Alzheimer's disease is characterized by amyloid plaques or neurofibrillary tangles caused by A $\beta$ -peptide or Tau respectively (118). Lewy body formations of  $\alpha$ -synuclein are commonly found in Parkinson's disease (3, 118). When the huntingtin (Htt) protein is mutated with an expansion of CAG repeats that code for polyglutamine stretches, intracellular inclusion and cytoplasmic aggregates can form to cause the progression of Huntington's Disease (118, 119). Patients with ALS have neuronal aggregates formed by various mutant proteins

some of which are the mutant superoxide dismutase (SOD1) or fused-in-sarcoma (FUS) gene (118, 120-122). Common to all of these diseases is the neuronal impairment that protein misfolding causes due to cytotoxicity, the age-dependent onset of the disorders, and the eventually fatal course in patients.

Animal models are currently being used to further our understanding of the molecular mechanisms that drive these diseases. Stress responses and molecular chaperones, specifically Hsp110, are potent modifiers of protein aggregation and can alleviate the degenerative effects of the “gain-of function” toxic species that cause disease (28). In mice, the absence of one of the three Hsp110 homologs results in accumulation of the toxic hyperphosphorylated form of tau and enhanced neurodegeneration (123). Furthermore, Hsp110 has proved to be highly effective at preventing degeneration and toxicity in flies and mammalian cells expressing polyglutamine proteins (124-126). Similarly, nematodes expressing a mutant human SOD1 demonstrated diminished locomotion and aggregate accumulation when Hsp110 levels were reduced through RNAi knockdown (127). Hsp110 also localizes with aggregates of polyglutamine proteins and SOD1 mutants *in vivo* (124, 127). As yet, the functional role of the Hsp110  $\beta$  domain in the Hsp70 protein folding process and the physiological implications of this activity remain unknown.

The work presented here addresses long-standing questions in molecular chaperone research and expands our understanding of molecular chaperones. It characterizes Hsp110/Sse1, a cochaperone that is required for function of the ubiquitous Hsp70, through biochemical and genetic experiments using yeast and fruit fly chaperones. Chapter 3 describes a novel, micro-scale, and semi-automated method to characterize the molecular dynamics of different types of protein complexes *in vitro* using a microplate reader. The interactions between Sse1 and unfolded polypeptides and the physiological implications of this chaperone activity are investigated in chapter 4. Here, I tested the involvement of Sse1 substrate binding with respect to growth, proteome maintenance, stress response, Hsp90-mediated activities, and in clearing fatally misfolded proteins. A regulated

fluorescence affinity (RFA) tag was used to investigate Sse1 roles in maintaining cellular proteostasis as detailed in chapter 5. Finally, Chapter 6 establishes the biochemical characterization of the *Drosophila melanogaster* Hsp110 which can be later utilized to investigate the molecular dynamics in a huntingtin (Htt with polyglutamine expansions) model of disease.

## **Chapter 2: Materials and methods**

### *Strains, Plasmids and Yeast Culture*

All yeast strains are derived from either BY4741 or W303 (Table 2-1). Mutant *sse1<sub>sbd</sub>* was constructed via site directed mutagenesis by PCR using the plasmid *p413TEF-FLAG-SSE1* as a template. This *SSE1* allele and the *sse1<sub>nbd</sub>* mutant (*sse1-G233D*, previously described in (128)) were sub-cloned into the *p413TEF* vector using *SpeI/XhoI* restriction sites (129). The plasmids *p413TEF-FLAG-SSE1-RFA* and *p413TEF-FLAG-RFA* were constructed by Julie Heffler (130). The *Hsc70cb* (*Drosophila melanogaster* Hsp110) gene was PCR amplified from the plasmid pUAST-Hsc70cb (kind gift from Dr. Sheng Zhang, UTHealth) and cloned into *p413TEF* using *XbaI/SpeI*.

For immunoprecipitation experiments, *SSE1* alleles were expressed from the *p413TEF* plasmid. A FLAG epitope tag (DYKDDDDK) was added to the 5' end of the *SSE1* or *Hsc70cb* genes immediately after the start codon by using primers that included the FLAG-encoding, yeast-optimized sequence (5'-GACTACAAGGACGACGATGACAAAATG-3').

Strains expressing the various *SSE1* alleles from the endogenous locus (YPL106C) were constructed by gene replacement (Figure 2-1.A). *SSE1* amplicons were generated from plasmids containing a *CYC1* terminator sequence using primers (5'-ATAACTCTGTCCTTGCCGT-3') and (5'-TACTCTGTCAGAAACGGCCTGTACCGCCGCAAATTAAAGCC-3') to PCR-amplify from nucleotide +35 relative to the ATG in *SSE1* (forward primer) to the 3' end of the *CYC1* terminator and including an overhang with homology to the *LEU2* terminator (reverse primer). The *LEU2* cassette was PCR-amplified from plasmid DNA using a forward primer that shares homology with the *CYC1* terminator (5'-GCTTTAATTTGCGGCCGTACAGGCCGTTTCTGACAGAGTAAAATTCTTG-3') and a reverse primer with an overhang that shares homology with the endogenous *SSE1* terminator (5'-AATCTTTTTTAACTATACAGAGAAGATATTAGTATTTACACCGCATATCG-3'). The two PCR amplicons were co-transformed into the BY4741 parent strain and successful *Leu*<sup>+</sup> double recombinants were selected. Individual clones were obtained, verified by PCR amplification of the *SSE1-LEU2* junction and an area internal to *SSE1* using genomic DNA, verified by Western blot, and sequenced to ascertain



correct integration, presence of desired mutations, and absence of additional nucleotide substitutions  
(Figure 2-1.B and C).

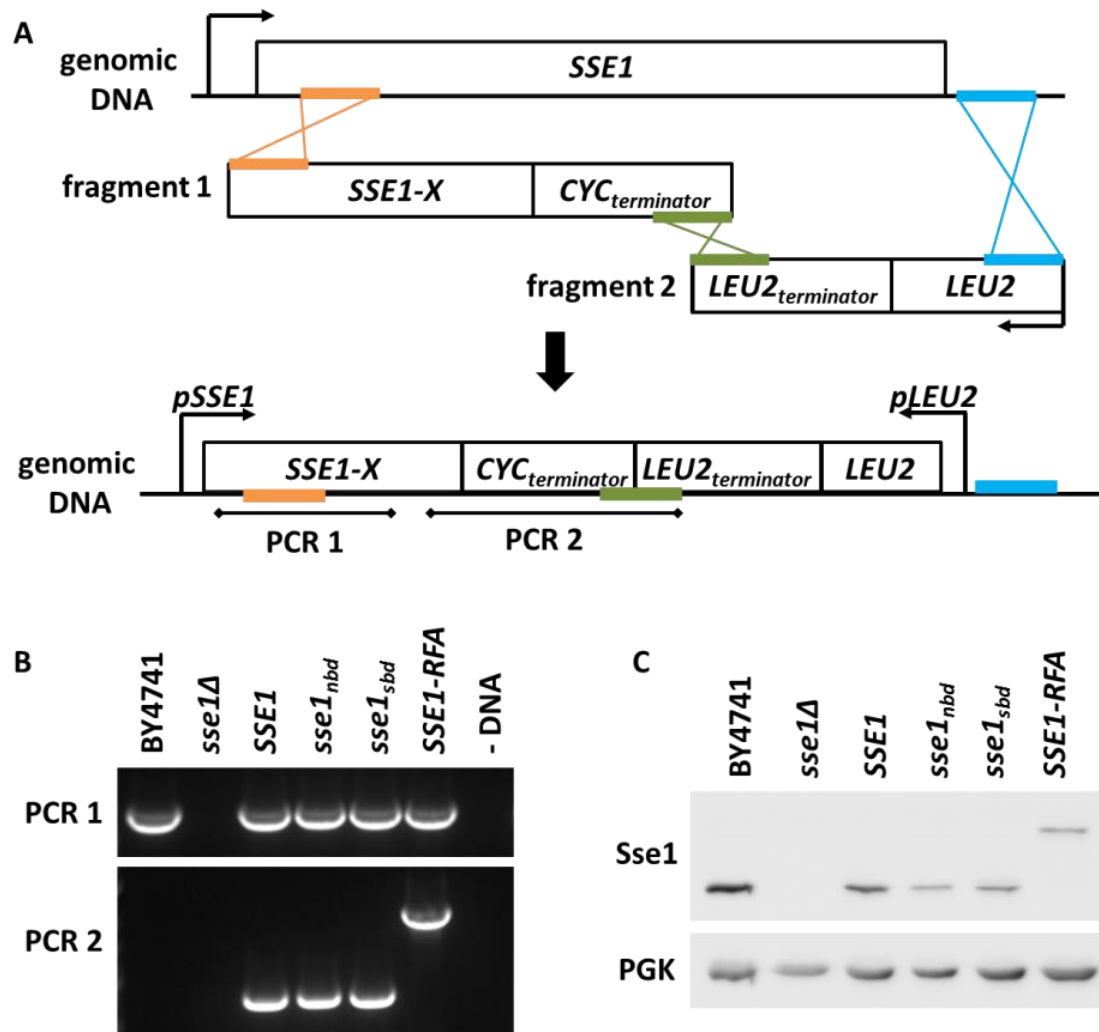


**Figure 2-1. Allele recombination to produce Sse1 variant strains.** A. Allele exchange for *SSE1* variants including areas of homology between recombinant fragments and genomic DNA in orange, green, and blue. B. Verification of proper insertion of *SSE1* and *LEU2* into the yeast genome by PCR1 and PCR2 as depicted in (A). C. Verification of protein production and proper protein length by immunoblotting with anti-Sse1 antiserum.

Table 2-1. Strains used in these studies.

strain and genotype	source
BY4741 <i>MATa ura3Δ leu2Δ his3Δ met15Δ</i>	Open Biosystems
BY4741 <i>sse1Δ::kanMX</i>	[Abrams 2014]
BY4741 <i>SSE1::LEU2</i>	this study
BY4741 <i>SSE1<sub>nb</sub>Δ::LEU2</i>	this study
BY4741 <i>SSE1<sub>sb</sub>Δ::LEU2</i>	this study
BY4741 <i>SSE1::LEU2 sse2Δ:: kanMX</i>	Unekwu Yakubu
BY4741 <i>SSE1<sub>nb</sub>Δ::LEU2 sse2Δ:: kanMX</i>	Unekwu Yakubu
BY4741 <i>SSE1<sub>sb</sub>Δ::LEU2 sse2Δ:: kanMX</i>	Unekwu Yakubu
BY4741 <i>SSE1-RFA::LEU2 sse2Δ:: kanMX</i>	Unekwu Yakubu
W303 <i>MATa ura3-52 trp1 leu2-3,112 his3-11,15 ade2-1 can1-100</i>	[Rothstein 1991]
W303 <i>sse1Δ::kanMX sse2Δ:: LEU2</i>	[Trott 2005]
BY4741 <i>pRH2081 (PTDH3-CPY<sup>+</sup>-GFP, ADE2 URA3)</i>	this study
BY4741 <i>sse1Δ pRH2081 (PTDH3-CPY<sup>+</sup>-GFP, ADE2 URA3)</i>	this study
BY4741 <i>SSE1::LEU2 pRH2081 (PTDH3-CPY<sup>+</sup>-GFP, ADE2 URA3)</i>	this study
BY4741 <i>SSE1<sub>nb</sub>Δ::LEU2 pRH2081 (PTDH3-CPY<sup>+</sup>-GFP, ADE2 URA3)</i>	this study
BY4741 <i>SSE1<sub>sb</sub>Δ::LEU2 pRH2081 (PTDH3-CPY<sup>+</sup>-GFP, ADE2 URA3)</i>	this study
BY4741 <i>SSE1-RFA::LEU2 pRH2081 (PTDH3-CPY<sup>+</sup>-GFP, ADE2 URA3)</i>	this study
BY4741 <i>SSE1::LEU2 sse2Δ pRH2081 (PTDH3-CPY<sup>+</sup>-GFP, ADE2 URA3)</i>	this study
BY4741 <i>SSE1<sub>nb</sub>Δ::LEU2 sse2Δ pRH2081 (PTDH3-CPY<sup>+</sup>-GFP, ADE2 URA3)</i>	this study
BY4741 <i>SSE1<sub>sb</sub>Δ::LEU2 sse2Δ pRH2081 (PTDH3-CPY<sup>+</sup>-GFP, ADE2 URA3)</i>	this study

**Table 2-2. Plasmids used in these studies.**

<b>plasmid</b>	<b>source</b>
<b>pSSA3-lacZ, URA3-based expression plasmid, GPD promoter</b>	[Liu 1999]
<b>pCH-FLAG-RatGR, HIS3-based expression plasmid</b>	[Liu 1999]
<b>pYRP-G2, 2 <math>\mu</math> URA3-based expression GRE-lacZ reporter</b>	[Liu 1999]
<b>p413TEF, HIS3-based expression plasmid, TEF promoter</b>	[Mumberg 1995]
<b>p413TEF-FLAG-SSE1, HIS3-based expression plasmid, TEF promoter</b>	[Abrams 2014]
<b>p413TEF-FLAG-SSE1<sub>nbd</sub>, HIS3-based expression plasmid, TEF promoter</b>	[Shaner 2004]
<b>p413TEF-FLAG-SSE1<sub>sbd</sub>, HIS3-based expression plasmid, TEF promoter</b>	this study
<b>p413TEF-FLAG-SSE1-RFA, HIS3-based expression plasmid, TEF promoter</b>	Julie Heffler
<b>p413TEF-FLAG-Hsc70cb, HIS3-based expression plasmid, TEF promoter</b>	this study
<b>pProEX-Htb-HIS<sub>6</sub>-SSE1, inducible bacterial expression plasmid</b>	this study
<b>pProEX-Htb-HIS<sub>6</sub>-SSE1<sub>sbd</sub>, inducible bacterial expression plasmid</b>	this study
<b>pProEX-Htb-HIS<sub>6</sub>-SSE-RFA, inducible bacterial expression plasmid</b>	this study
<b>pProEX-Hta-HIS<sub>6</sub>-Hsc70cb, inducible bacterial expression plasmid</b>	this study

Hsf1 activity was measured with strains harboring plasmid *pSSA3HSE-lacZ* as described (131, 132). For experiments testing CPY<sup>+</sup>-GFP degradation, strains were constructed using pRH2081 (generous gift from Dr. Randy Hampton, University of California, San Diego), a plasmid that carries *TDH3*-driven *CPY<sup>+</sup>-GFP* (133). The integrative plasmid was linearized using restriction endonuclease *Van91I* and transformed into indicated strains with Ura<sup>+</sup> selection.

To assess growth and complementation, cells were spotted on appropriate solid medium with a starting concentration of OD<sub>600</sub>=1.0 and serially diluted 1 in 10. Cultures were incubated at 15, 30, 34, 37, 39 °C, or in the presence of chemical compounds (formamide or trimethoprim) for 2-4 days at which point plates were photographed.

Cells were grown at 30 °C at a starting OD<sub>600</sub> of 0.05 with shaking while absorbance readings were detected every 15 minutes using a Synergy MX Microplate Reader (BioTek). Doubling time was calculated by plotting data points from a 16-hour growth curve. GraphPad Prism v.6 (GraphPad Software, La Jolla, CA) was used to determine the doubling time based on the log phase growth of each culture using an exponential growth equation.

### *Protein Purification*

Purified firefly luciferase (Sigma L-9506), citrate synthase (Sigma C-2360), and rhodanese (Sigma R1751) were obtained from Sigma Chemical Corp. (St. Louis, MO). Sse1 was purified from *Escherichia coli* BL21 (DE3) by metal affinity chromatography followed by size exclusion chromatography as described in (134). Hexa-histidine tagged Sse1 was purified from *E. coli* by chemical lysis (Bug Buster, Millipore) in buffer B (50 mM Tris pH 7.5, 200 mM NaCl, 2 mM MgCl<sub>2</sub>, 5 mM imidazole). The cell lysate was incubated with His-Pur Cobalt Resin (Thermo Scientific), washed with buffer B and C (50 mM Tris pH 7.5, 600 mM NaCl, 2 mM MgCl<sub>2</sub>, 10 mM imidazole), and eluted with Buffer E (50mM Tris pH 7.5, 700 mM NaCl, 2 mM MgCl<sub>2</sub>, 200 mM imidazole). Sse1-containing elution fractions were combined, buffer exchanged (25 mM Tris pH 7.5, 100 mM NaCl), and further

purified by size exclusion chromatography using Sephacryl S-100 (GE Healthcare). Purification of Hsc70cb was performed following the same protocol as for Sse1.

#### *Nucleotide Binding Assay*

Fluorescently labeled nucleotide, N<sup>6</sup>-(6-Amino)hexyl-ATP-5-FAM (ATP-FAM) (provided by Dr. Jason Gestwicki; Jena Bioscience, Jena, Germany), was incubated at a concentration of 20 nM with increasing amounts of Sse1 or Sse1<sub>sbd</sub> chaperone in buffer (25 mM Tris-HCl, pH7.5, 100 mM NaCl, 5 mM MgCl<sub>2</sub>, 50 mM KCl, 5% glycerol) for 30 minutes at room temperature as described (135). Fluorescence polarization was measured (excitation  $\lambda$ : 485 nm emission  $\lambda$ : 535 nm) using a SpectraMax M5 plate reader (Molecular Devices). Equilibrium binding constants were calculated using a saturation binding one-site equation via GraphPad Prism v.6 (GraphPad Software, La Jolla, CA). These experiments were conducted in the laboratory of Dr. Jason Gestwicki (University of California San Francisco) with use of their equipment and reagents.

#### *Nucleotide Exchange Assay*

The HSPA8 (Hsc70) protein was a generous gift from Dr. Betty Craig (University of Wisconsin, WI). HSPA8 (70  $\mu$ g) was loaded with 100  $\mu$ Ci of  $\alpha$ -<sup>32</sup>P-ATP in a total volume of 120  $\mu$ L of complex buffer (25 mM HEPES-KOH pH 7.5, 100 mM KCl, 11 mM MgOAc, and 25  $\mu$ M ATP) for 30 minutes at 4 °C, and HSPA8-<sup>32</sup>P-ATP complex was obtained by centrifugation through a Microspin G-25 column (GE Healthcare, Chicago, IL). Labeled HSPA8 (7.8  $\mu$ g) was incubated in the presence or absence of 5  $\mu$ g of NEF at 30 °C. At designated times, the HSPA8-NEF reactions were again passed over G-25 columns to separate from released nucleotide. Radiolabeled nucleotide that remained bound to HSPA8 was determined using a TRI-CARB 2900TR Liquid Scintillation Analyzer and normalized to counts obtained at time zero.

### *Protein Aggregation Assay*

Aggregation assays were conducted in a Synergy MX Microplate Reader. Rhodanese and citrate synthase were incubated in denaturing buffer (6 M guanidinium chloride, 5 mM dithiothreitol) at concentrations of 13.3 and 11.6  $\mu\text{M}$ , respectively for 1 hour at room temperature (136) (137) (138). Refolding buffer (25 mM Tris pH 7.5, 100 mM NaCl) or denaturing buffer (6 M guanidinium chloride, 5 mM dithiothreitol) were pre-equilibrated at 25 °C in a 96-well, half area, UV-transmissible plate (675801, Greiner Bio-One) for 5 min and baseline absorbance was determined. After equilibration, chemically denatured substrate was added to a final concentration of 150, 300, 600, or 900 nM into the refolding buffer or 900 nM into the denaturing buffer to a final volume of 180  $\mu\text{L}$ . The samples were mixed thoroughly and absorbance was measured at 320 nm at 30-second intervals for 30 minutes. Changes in absorbance were calculated after subtracting baseline absorbance at time zero, and all experiments with a given substrate were performed concurrently on a single microplate.

To compare chaperone capabilities of Sse1, Sse1<sub>sbd</sub>, or Hsc70cb, substrate aggregation was measured as described in (134) with the following modifications. Stock concentrations of firefly luciferase or citrate synthase were incubated in denaturing buffer for 1 hour at room temperature. In a 96 well, half area, UV-transmissible plate refolding buffer alone, varying concentrations of chaperone in refolding buffer, or denaturing buffer were pre-equilibrated at 25 °C for 5 minutes and baseline light scattering was determined. After equilibration, chemically denatured substrate was added to each sample at a final concentration of 200 nM into the refolding buffer to a final volume of 180  $\mu\text{L}$ . The samples were mixed vigorously for 5 seconds and aggregation was measured at 320 nm at 30-second intervals for 30 minutes. Changes in absorbance were calculated after subtracting baseline absorbance at time zero.

To assess fractionation of protein into soluble and insoluble aggregates, samples (175  $\mu\text{L}$ ) were taken from the endpoint of the substrate aggregation experiments and subject to centrifugation at 16,000  $\times g$  for 4 minutes. 170  $\mu\text{L}$  were recovered as the supernatant or soluble fraction. The lower 5

$\mu$ L fraction was considered the pellet or insoluble fraction and volume was normalized to 170  $\mu$ L with the addition of refolding buffer. 30  $\mu$ L of each fraction were separated by 12% SDS-PAGE and stained with Coomassie Blue. Band densities were calculated using Image Studio Software (Li-Cor Biosciences, Lincoln, NE).

### *Immunoblotting*

Cultures were grown overnight and secondary cultures started and allowed to grow to an OD<sub>600</sub> of 0.8 at which point cells were shifted to 37 °C or maintained at 30 °C for 6 hours. Cells were collected and processed for protein lysates. Sse1 protein levels were detected by immunoblot using anti-Sse1 antiserum (generous gift from Dr. Jeff Brodsky, University of Pittsburgh, PA) and anti-phosphoglycerate kinase (PGK; Invitrogen, Carlsbad, CA) was used as a loading control. Band analysis was performed using Image Studio Software and Sse1 levels were normalized to the levels of PGK. Hsp90 levels were assessed in cells grown at 30 °C by immunoblot using anti-Hsp90 (generous gift from Dr. Avrom Caplan, CUNY, NY) with anti-Sse1 and anti-PGK as internal controls. Band analysis was performed using Image Studio Software. Sse1 and Hsp90 levels were normalized to PGK levels.

### *Immunoprecipitations*

Sse1 proteins were expressed with an N-terminal FLAG-tag. Protein extracts were prepared from 30 mL of cultures grown at 30 °C or 37 °C for 6 hours. Protein lysates were incubated with 40  $\mu$ L of M2 resin (Sigma) in TEGN (20 mM Tris-HCl, pH 7.9, 0.5 mM EDTA, 10% glycerol, 50 mM NaCl) at 4 °C for two hours. After washing with 4 mL of buffer, the resin was incubated with 40  $\mu$ L of FLAG peptide for 25 minutes at room temperature to elute the FLAG-Sse1 complexes. Immunoprecipitated proteins were analyzed by SDS-PAGE and Coomassie Stain. Band analysis was performed using Image Studio Software and the co-immunoprecipitation efficiency of Hsp70 was calculated relative to the amount of Sse1 immunoprecipitated.



The GFP immunoprecipitation was performed using Sepharose beads conjugated with anti-GFP monoclonal antibody. Protein lysates from 35 mL of cells at log phase were obtained and incubated with anti-GFP (Thermo Fisher Scientific Inc., Waltham, Massachusetts) in buffer (TEGN, protease inhibitor, 0.1% Triton X-100). The protein lysate/antibody solution was incubated with protein A sepharose (Sigma-Aldrich, St. Louis, MO) followed by washing. Immunoprecipitated proteins were eluted in 40  $\mu$ L Laemmli sample buffer at 80° C. Samples were visualized by SDS-PAGE and Coomassie Stain.

#### *Glucocorticoid Receptor Activation*

The various Sse1 strains were transformed with plasmids *pCH-Flag-RatGR* and *pYRP-G2* expressing the glucocorticoid receptor protein and a *GRE-lacZ* transcriptional reporter, respectively (131). Cells grown to mid-logarithmic phase were treated with DMSO only (-DOC) or 10  $\mu$ M deoxycorticosterone in DMSO (+ DOC) for 1.5 hours.  $\beta$ -galactosidase activity was measured by adding 50  $\mu$ L of cell suspension at OD<sub>600</sub> 0.4 and 50  $\mu$ L of Beta-Glo reagent (Promega, Madison, WI) and incubating for 30 minutes at 30 °C followed by luminescence detection using a Synergy MX Microplate Reader.

#### *CPY<sup>+</sup>-GFP Degradation Assay*

To track the degradation of the CPY<sup>+</sup>-GFP protein *in vivo*, cells were grown to mid-logarithmic phase, treated with 100  $\mu$ g/mL cycloheximide, and 10 mL of culture were collected at 0, 1, and 2 hours. Denatured protein extracts were prepared using a glass bead lysis method with SUME buffer (1% SDS, 8M Urea, 10mM MOPS, pH 6.8, 10mM EDTA). The CPY<sup>+</sup>-GFP protein was detected by immunoblot using anti-GFP (Roche, Basel, Switzerland) and anti-PGK was used as an internal control. In parallel experiments, CPY<sup>+</sup>-GFP-expressing cells were collected immediately after treatment at 0, 45, and 90 minutes and visualized using an Olympus IX81-ZDC inverted microscope as described in (14).

The experiments to assess CPY<sup>+</sup>-GFP aggregates in the *SSE1-RFA* strain were conducted by growing the different strains in the absence or presence of 500  $\mu$ M trimethoprim for 6 hours or more. When the cells reached log phase, they were treated with cycloheximide and cells were analyzed via immunoblot or by microscopy at the times indicated.

#### *Protein similarity analysis*

Hsc70cb and Sse1 were compared to determine protein similarity using the NCBI protein blast software. For the Hsc70cb query, the protein sequence used was Hsc70Cb (isoform A) obtained from uniprot.org (<http://www.uniprot.org/uniprot/Q9VUC1>). The Sse1 (YPL106C) amino acid sequence was obtained from the Saccharomyces Genome Database using reference strain S288C (<http://www.yeastgenome.org/locus/S000006027/protein>).

#### *Statistics*

The data represented in the graphs is the mean of independent replicates and the error bars represent  $\pm$  standard deviation. Statistical analysis was performed using a student's t-test.

### **Chapter 3: Semi-automated microplate monitoring of protein polymerization and aggregation**

Note: This chapter was derived from work that is published in the Journal of Analytical Biochemistry. Garcia VM, Rowlett VW, Margolin W, Morano KA. Semi-automated microplate monitoring of protein polymerization and aggregation. Anal. Biochem. 2016 Sept. 508: 9-11. I acquired the data presented in this chapter. FtsZ polymerization experiments were performed by Veronica Rowlett, Ph.D., in collaboration with the laboratory of William Margolin, Ph.D. These data are thus excluded from this chapter. Permission to use previously published material was granted by Elsevier, owner of Analytical Biochemistry, through license number 4063260221106.

## Introduction

Static light scattering (SLS) techniques such as multi-angle (MALS) and right-angle (RALS) measure the light deflected from particles in solution that are larger than the wavelength of the light emitted. Such methods typically require expensive fluorimetry equipment, consume large amounts of purified protein, and may be unsuitable for high-throughput assays (136, 139). For example, a fluorimeter equipped with a stirrable, temperature-controlled cell holder is required for RALS analysis, and the cost of such equipment may be prohibitive for many laboratories. Furthermore, such devices are limited to single cell measurements, and the need to maintain solution homogeneity through mechanical stirring dictates mL-scale volumes per experiment. If proteins are tested at nano- or micromolar concentrations, significant amounts of purified or purchased proteins are required.

Described here is an alternative method for tracking the formation of aggregates of proteins that yields results comparable to SLS. This approach utilizes a microplate reader with temperature control, along with 96-well half area microplates that allow for multiple reactions to be analyzed simultaneously in a low reaction volume. While previous applications of microplate technology for following protein dynamics in high-throughput molecular screens have been described (66, 140, 141), I demonstrate here the sensitivity and range of this technique by measuring protein aggregation of three traditional chaperone substrates and aggregate prevention by a molecular chaperone. The method described here measures, in real-time, the increase in turbidity that occurs as high molecular weight protein complexes or aggregates form in an aqueous buffer. Our overall goal was to show that a method for sensitive, rapid and reproducible comparative monitoring of protein assembly dynamics in small volumes can be accessible to molecular biologists.

## Results

Various biological applications require the study of large protein complexes. For example, tracking the formation of aggregates allows the characterization of molecular chaperones. By monitoring the aggregation of model substrates in the presence of chaperones, we can understand the substrate specificity, molecular dynamics, and environmental requirements for chaperone function. Traditionally, methods like MALS or RALS are utilized to detect dynamics of aggregate formation and chaperone activity. A sample is placed in the path of emitted light, and these techniques directly measure light that is scattered at multiple designated angles for MALS or at a right angle from the light source in the case of RALS. While these methods can produce a lot of information about the given sample, such as the absolute molar mass or average molecular size of the molecules in the solution, the instruments required to conduct this type of analysis are expensive and not widely available. Initially, I characterized protein aggregation and chaperone activity using RALS but the requirement of large volumes of protein at high concentrations became prohibitive (equipment provided by the laboratory of Dr. Vasanthi Jayaraman, UTHealth). The alternative method I describe here can track the formation of aggregates by measuring absorbance. The reduction in light transmittance is detected as aggregates increase and grow in a solution (Figure 3-1.A). Aggregation is monitored in real time, using smaller protein volumes, and across multiple samples concurrently.

Chaperones detect unfolded proteins and prevent their aggregation by stabilizing unfolded polypeptides until native conformations are achieved (5). Chaperones differ in substrate specificity and their molecular interactions with clients, and various aggregation-prone model proteins including firefly luciferase, rhodanese, and citrate synthase have been used to elucidate biochemical features of chaperone function and specificity (107, 137, 142-144). Due to the irreversible side reactions that occur during unfolding, these, and other commonly employed substrates, rapidly aggregate when diluted from a denaturing solution into a non-denaturing buffer unless accompanied by molecular

chaperones (138, 145). Firefly luciferase was chemically denatured (denaturing buffer: 6 M guanidinium chloride, 5 mM dithiothreitol) and diluted into the refolding buffer (25 mM Tris pH 7.5, 100 mM NaCl) or denaturing buffer. The samples were mixed thoroughly while making sure to not introduce air bubbles and transmittance was measured at 320 nm at 30 second intervals for 45 minutes at 25 °C. Changes in transmittance were calculated after subtracting baseline transmittance at time zero. Figure 3-1.B demonstrates that denatured firefly luciferase remains denatured in the presence of guanidinium chloride and that aggregation can be detected in the refolding buffer. As an alternative approach, the samples that were monitored during the aggregation experiments were collected and centrifuged to isolate the soluble firefly luciferase and the insoluble substrate aggregates into the supernatant and pellet respectively (106). This technique served to confirm that the increase in absorbance that was detected for the firefly luciferase in refolding buffer was due to substrate aggregation. Notably, transmittance changes due to the aggregation of firefly luciferase correlated with high-speed fractionation of the substrate into soluble (supernatant) and insoluble fractions (pellet) (Figure 3-1.C). Also, the firefly luciferase diluted further into denaturing buffer did not track an increase in transmittance and remained soluble, likely as monomers, as indicated by the differential centrifugation.

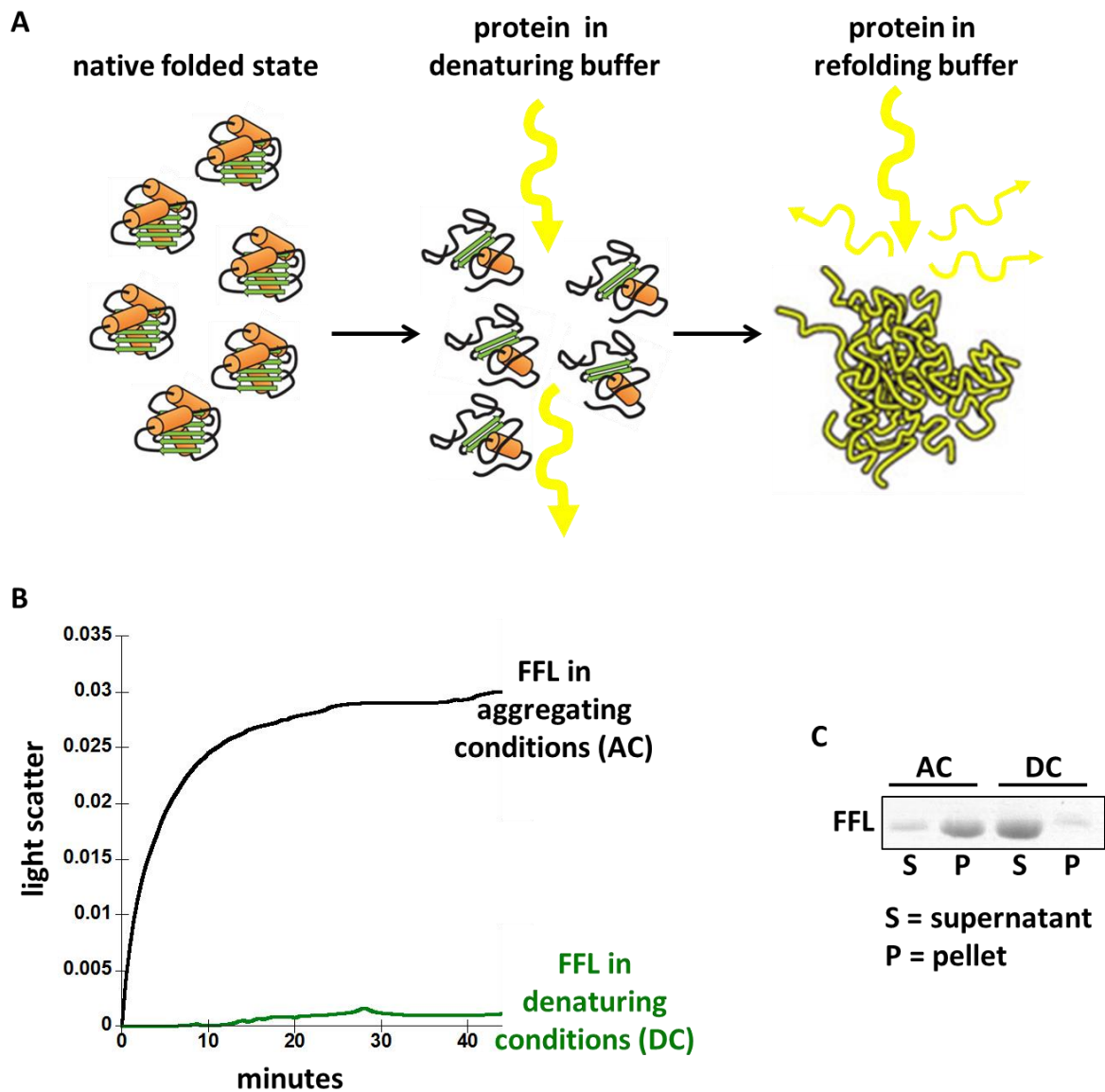


**Figure 3-1. Monitoring aggregation of firefly luciferase.** A. Aggregates are monitored through a decrease in light transmittance. B. Aggregation of 200 nM chemically denatured firefly luciferase (FFL) is monitored in denaturing buffer (DC) or refolding buffer (AC). Average data points are plotted (n=4) with a standard deviation  $\leq 0.003$ . C. One representative image of an SDS-PAGE gel and Coomassie stain visualizing the fractionation of soluble (S) or aggregated (P) FFL by centrifugation after 30 minutes.

The aggregation of chemically denatured rhodanese and citrate synthase was monitored at various concentrations (136-138). Refolding buffer or denaturing buffer were pre-equilibrated at 25°C in a 96-well, half area plate for 5 min and baseline transmittance was determined. After equilibration, denatured substrate was added to a final concentration of 150, 300, 600, or 900 nM into the refolding buffer or 900 nM into the denaturing buffer and transmittance was measured at 320 nm at 30 second intervals for 30 minutes. Changes in transmittance were calculated after subtracting baseline absorbance at time zero, and all experiments with a given substrate were performed concurrently on a single microplate. Denatured rhodanese aggregation was tracked by measuring absorbance at 320 nm (Figure 3-1. B). Our results indicate that this method successfully detects increasing aggregation over time, using concentrations of denatured rhodanese in line with those previously published (136, 144). Similarly, the results obtained using chemically denatured citrate synthase were similar to those previously published (106, 143). Aggregates formed by either substrate were detected at concentrations as low as 150 nM and the change in transmittance increased with greater substrate concentrations, consistent with increased light scattering due to the formation of aggregates (Figure 3-2. B).



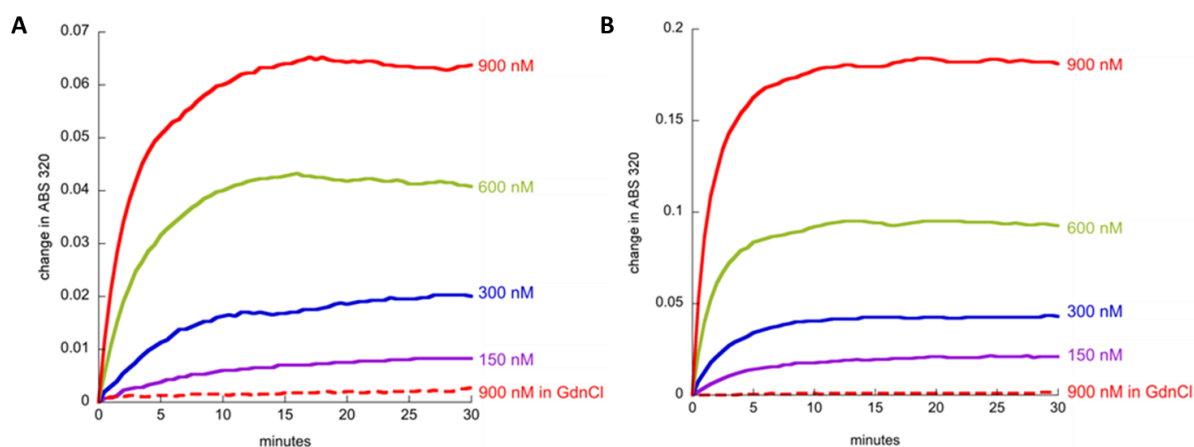


**Figure 3-2. Aggregation of model chaperone substrates rhodanese and citrate synthase.** A. Rhodanese was denatured in 6 M guanidinium chloride + 5 mM DTT for 45 minutes. Denatured rhodanese was diluted into 180  $\mu$ L of assay buffer (25 mM TRIS pH7.5 + 100 mM NaCl) and aggregation was measured at 25  $^{\circ}$ C by change in absorbance using a Biotek Synergy MX plate reader. Average data points are plotted (n=4) with a standard deviation  $\leq$  0.003. B. The aggregation of citrate synthase was measure using the same method as for rhodanese. Average data points are plotted (n=2) with a standard deviation  $\leq$  0.003.

I assessed whether this microplate reader assay would be adaptable to study the ability of molecular chaperones to modulate protein aggregation. Molecular chaperones help to maintain cellular proteomes by interacting with unfolded or partially folded proteins, preventing their aggregation and stabilizing polypeptides until native conformations are achieved (3). Citrate synthase is recognized as a substrate by the Hsp110 class of chaperones that stabilize the unfolded protein to prevent aggregation (142, 146). I analyzed the aggregation dynamics of citrate synthase in the presence of the yeast Hsp110 chaperone, Sse1. Hexa-histidine tagged Sse1 was purified from *Escherichia coli* and used for analysis of protein aggregates in the presence of a chaperone. The protein solutions must be equilibrated to the temperature and buffer conditions of the assay, as an abrupt shift in buffers or temperature can result in an artificial increase in absorbance. Each sample was equilibrated in refolding buffer with 0, 100, 200, 400, or 800 nM Sse1 or denaturing buffer in the absence of Sse1 at 25° C in a 96-well, half area plate for 5 min while absorbance was measured. After equilibration, chemically denatured citrate synthase was added to 200 nM, chosen as a minimal aggregating substrate concentration, into the refolding buffer or into the denaturing buffer, with and without Sse1, to a final volume of 180 µL. The samples were mixed thoroughly for 5 sec and absorbance was measured at 320 nm every 30 sec for 30 min at 25°C. Consistent with reported results, increasing Sse1 concentrations promote solubility of the aggregate-prone substrate (Figure 3-3. A). Notably, absorbance changes due to the aggregation of citrate synthase correlated with transfer of the substrate from a high-speed sedimentable fraction to a soluble state as assessed by SDS-PAGE of endpoint samples followed by Coomassie Blue staining (Figure 3-3. B).

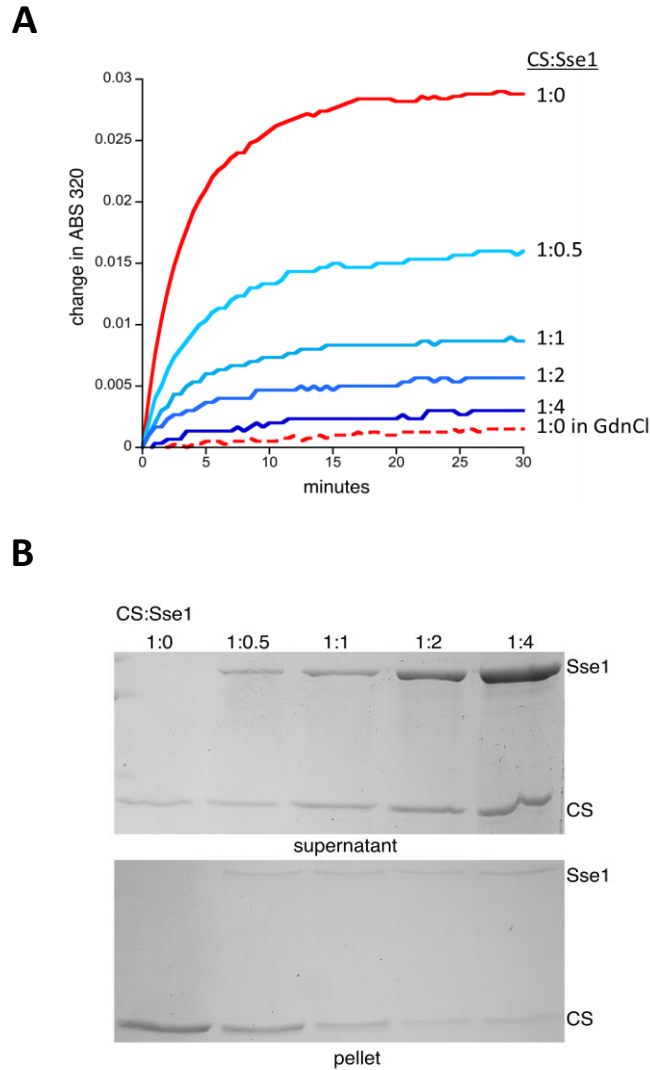


**Figure 3-3. Monitoring aggregate prevention of citrate synthase and protection by Sse1.** A. Citrate synthase (CS) was denatured same as described and diluted into assay buffer with increasing concentrations of chaperone. Average data points are plotted (n=3) with a standard deviation  $\leq 0.003$ . B. Samples were collected from the end point of experiment in (A) and the soluble and aggregated fractions of CS and Sse1 were separated into supernatant and pellet through differential centrifugation followed by analysis on SDS-PAGE and Coomassie stain.

## Discussion

I have described an accessible, low- to high-throughput alternative to SLS that provides similar results at levels of detection comparable to single-cell analysis. In this work, I have demonstrated the applicability of this method to study the aggregation of three different model substrates that are routinely used to characterize chaperone activity (firefly luciferase, citrate synthase, and rhodanese). The method I presented has some limitations when compared with traditional MALS or RALS. It should be noted that a few seconds of data are lost during insertion and calibration of the plate when using a plate reader, making this technique unsuitable for analysis of initial burst dynamics. However, kinetic analyses to determine aggregation parameters may be undertaken using standard calculations (147). Further, the method adaptation I describe cannot provide information about molecular weight or size of the aggregates. Nonetheless, the technique presented here is a simpler, quicker, and more efficient way to simultaneously compare the dynamics of high molecular weight protein assemblies across multiple samples and conditions. As microplate readers can be outfitted with both injection systems and ambient temperature controls, this approach can allow for concurrent analysis of multiple experimental variables.

#### **Chapter 4: Substrate binding by the yeast Hsp110 nucleotide exchange factor and molecular chaperone, Sse1, is not obligate for its biological activities**

Note: This chapter was derived from work performed by Veronica Margarita Garcia. The data discussed regarding the refolding and disaggregating capacity of Sse1 and Sse1<sub>sbd</sub> is the work of Nadinath Nillegoda, Ph.D. with recombinant Sse1 proteins supplied by Garcia, as a collaborative effort with the laboratory of Bernd Bukau, Ph.D. Because this work was not performed by Garcia, the data have been excluded.

## Introduction

Proteins must fold into a proper three-dimensional configuration, or native state, to execute their intended functions. Proteomic stressors such as exposure to harmful chemicals, oxidative stress, and aging can inhibit protein folding, disrupt protein homeostasis and result in cell death and human disease (3). Misfolded proteins or amyloid aggregates contribute to the development or progression of neurodegenerative disorders; Alzheimer's disease, Huntington's disease and Parkinson's disease are all fundamentally diseases of protein misfolding (116, 120). Cell survival during and after stress conditions is promoted by molecular chaperones that optimize protein folding by stabilizing folding intermediates until native conformations have been obtained. The highly conserved Hsp70 chaperone is integral to protein biogenesis, quality control, and degradation of terminally misfolded proteins (53). The Hsp70 protein folding cycle is ATP-dependent and is regulated by co-chaperones such as Hsp40s and nucleotide exchange factors (NEFs) that stimulate ATP hydrolysis and exchange, respectively (148, 149). The budding yeast *Saccharomyces cerevisiae* expresses three classes of cytosolic NEFs all with human orthologs: the Hsp110-type proteins Sse1/Sse2, the HSPBP1-type protein Fes1 and the BAG-1-type protein Snl1 (150). *SSE1* deletion results in slow growth and temperature sensitivity, whereas a combined deletion of *SSE1* and *SSE2* is lethal despite the presence of Fes1 and Snl1, suggesting a potentially unique role for the Hsp110 proteins (151, 152). The Hsp110 proteins are highly homologous to Hsp70 composed of an amino-terminal nucleotide binding domain (NBD) and a substrate binding domain (SBD) that is further subdivided into a  $\beta$ -sandwich domain and an  $\alpha$ -helical "lid" domain (59, 60, 104). Distinct from Hsp70, Sse1/2 bind ATP which stabilizes the NBD, but catalytic activity (ATP hydrolysis) is not required to functionally complement the null mutant *in vivo* or to accelerate Hsp70 nucleotide exchange *in vitro* (40, 44, 45, 47, 112).

While the NEF function of Hsp110/Sse is well established, possible biological roles for substrate binding by the SBD remain speculative. Crystal structures of the Hsp70-Sse1 complex depict

the Hsp70 SBD in close proximity to the Sse1  $\beta$ -domain, suggesting possible cooperative substrate binding (60, 104). The Hsp110 SBD is structurally similar, but not identical, to that of Hsp70, and it is suggested that it binds peptides much like Hsp70 through interactions with both  $\beta$ -sheets and the connecting loops within the  $\beta$ -domain (106-108). Hsp110s are highly efficient at blocking aggregation of misfolded substrates *in vitro* (defined as “holdase” activity) and Sse1 possesses a unique peptide binding preference for regions enriched in aromatic amino acids, relative to the yeast Hsp70, Ssa1 (30, 109). While contributions to substrate selection and targeting to Hsp70 by Hsp40 co-chaperones are established, it remains unclear if the holdase activity of Sse1 or other Hsp110 chaperones contributes to Hsp70-dependent functions *in vivo* (57). Deletion mutagenesis to remove the Sse1 SBD is complicated by the fact that carboxyl-terminal deletions render the protein unstable, and that the  $\alpha$ -helical domain is required for heterodimerization with Hsp70 (44, 60, 104). Site-specific mutagenesis targeting residues in the Sse1 substrate binding domain modeled on the peptide binding site of the bacterial Hsp70, DnaK, was likewise unsuccessful (60). Yeast cells lacking Sse1 are defective in folding of newly synthesized polypeptides and degradation of some misfolded proteins (40, 132, 153). However, overexpression of either Fes1 or a soluble, truncated mutant form of the normally ER-associated NEF Snl1, both of which lack demonstrated holdase activities, partially suppresses these phenotypes (39, 114). In contrast, other NEFs cannot substitute for Hsp110 in protein disaggregation reactions, suggesting that Hsp110 possesses specific properties that could be linked to its unique substrate binding domain (54, 110, 112, 154).

In this study, I generated an Sse1 variant that separates, for the first time, the nucleotide exchange and substrate binding functions of this chaperone. Multiple targeted single-residue substitutions in the  $\beta$ -sandwich region of the SBD were introduced to generate a novel mutant (Sse1<sub>sbd</sub>) that exhibits greatly reduced aggregation-preventing activity while retaining nucleotide binding and Hsp70 nucleotide exchange potency. Strikingly, Sse1<sub>sbd</sub> was competent to restore growth to cells lacking *SSE1* and/or *SSE2*, to promote disaggregase activity in a reconstituted *in vitro* system,

and to support Hsp70-dependent signal transduction and protein degradation while exhibiting minor defects in stress resistance and protein quality control. The data presented here suggest that the substrate binding function of Sse1, despite being conserved among the eukaryotic Hsp110 proteins, plays a minor role in maintaining protein homeostasis in the yeast system.

## Results

I generated a novel Sse1 substrate binding domain (SBD) mutant based on previous structural studies (60, 109) that indicated the region mutated could be within a putative peptide binding site (Figure 4-1.A). This putative substrate binding defective mutant (Sse1<sub>sbd</sub>) includes four specific amino acid substitutions (L433A, N434P, F439L, and M441A) within the L<sub>3,4</sub> region of the  $\beta$ -sandwich domain in Sse1. I first verified that the introduced mutations exclusively targeted substrate binding while maintaining proper nucleotide binding in the NBD. Recombinant proteins were purified from *E. coli* to conduct *in vitro* experiments (Figure 4-2). ATP binding was measured with fluorescently labeled nucleotide through fluorescence anisotropy. When compared to the wild-type protein, Sse1<sub>sbd</sub> bound FAM-ATP with approximately the same affinity ( $K_d$  of 12.1  $\mu$ M  $\pm$ 1.9 for Sse1<sub>sbd</sub>, vs. 8.6  $\mu$ M  $\pm$ 1.4 for wild-type Sse1, Figure 4-1.B). These values are consistent with previously reported affinities measured using a different fluorescently labeled nucleotide, MABA-ATP (2.1  $\mu$ M  $\pm$ 0.6) (47). It was also essential that the mutant protein could still function as a nucleotide exchange factor (NEF) for Hsp70. I measured the exchange of  $\alpha$ -<sup>32</sup>P-ATP loaded onto human Hsc70 (HSPA8) in the absence of NEF, or in the presence of Sse1 or Sse1<sub>sbd</sub>, and found no discernable difference in the accelerated exchange rates (Figure 4-1.C). Together these results demonstrate that Sse1<sub>sbd</sub> retains critical nucleotide-binding and NEF features of the Hsp110 chaperone.



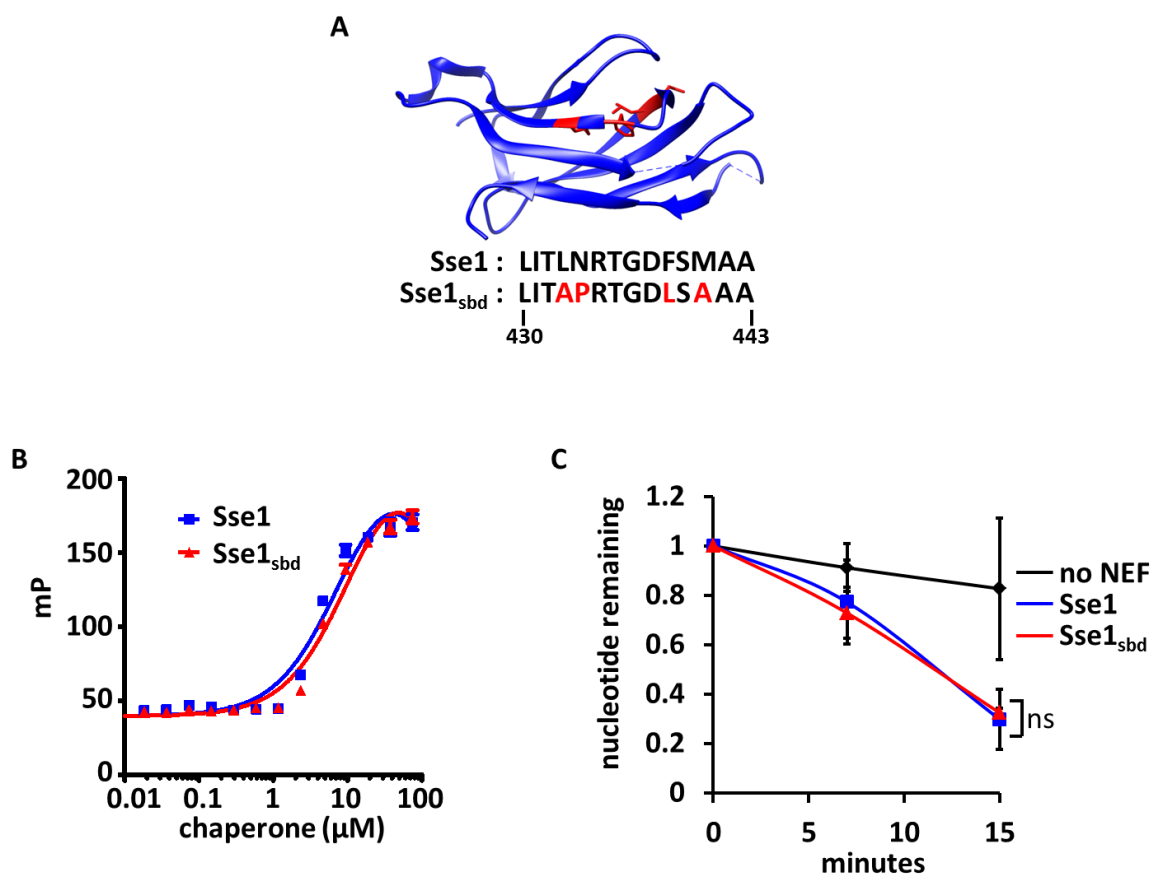


**Figure 4-1. Novel Sse1 substrate binding mutant retains Hsp70 nucleotide exchange capacity.** A. Crystal structure of the Sse1  $\beta$ -domain with amino acids selected for mutations highlighted in red (109). B. Fluorescence anisotropy was performed with increasing concentrations of chaperone (Sse1 or Sse1<sub>sbd</sub>) binding fluorescently labeled ATP-FAM. (n=3) C. Nucleotide exchange activity assays using HSPA8 (Hsp70) pre-bound to  $\alpha$ -<sup>32</sup>P-ATP in the presence or absence of Sse1 (n=2). Error bars in all panels indicate standard deviation.

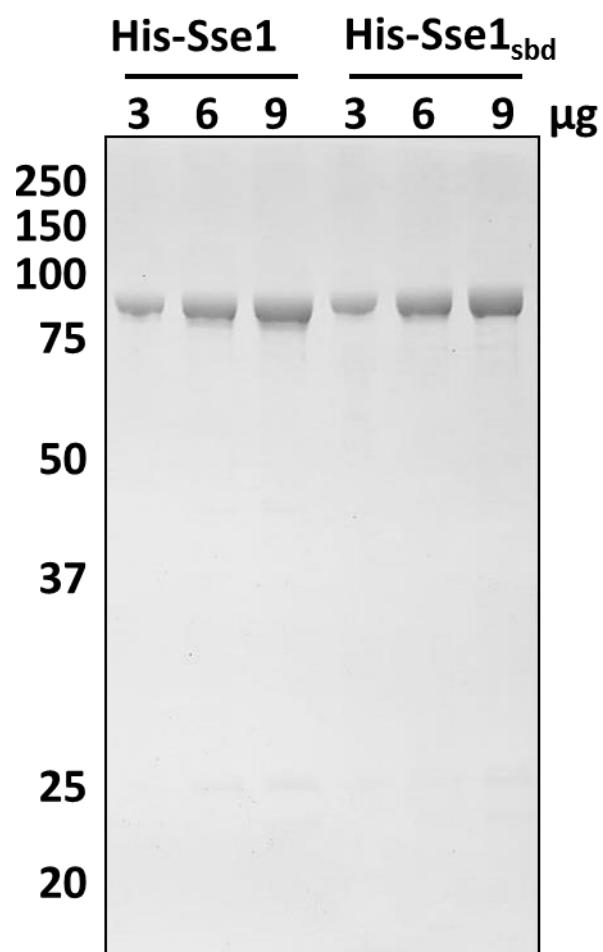


**Figure 4-2. Purification of recombinant Hexa-histidine tagged Sse1 proteins.** A. Recombinant His-Sse1 and His-Sse1<sub>sbd</sub> purified from *E. coli* visualized on an SDS-PAGE gel using Coomassie stain.

To assess whether substrate binding was impaired as predicted, I measured the ability of Sse1 and Sse1<sub>sbd</sub> to prevent the aggregation of chemically denatured firefly luciferase (FFL) using an established assay system (134). Whereas wild-type Sse1 effectively reduced FFL aggregation relative to that observed in the absence of chaperone, the Sse1<sub>sbd</sub> protein was significantly impaired in aggregate prevention (Figure 4-3.A). To verify that the spectrophotometric assays reflected substrate aggregation into insoluble material, end-point samples were analyzed by differential centrifugation followed by SDS-PAGE and densitometry quantitation (Figure 4-3.B). Sse1 maintained 72% of FFL in a soluble state after 30 min, whereas only 39% of FFL is soluble in the presence of Sse1<sub>sbd</sub> as the chaperone. Similar results were obtained with citrate synthase as the unfolded substrate (Figure 4-4.A-C). Increasing the ratio of Sse1 to FFL or CS allowed for better aggregate prevention, whereas increasing the ratio of Sse1<sub>sbd</sub> only mildly improved protection of the denatured substrate (Figure 4-3.C and Figure 4-4.D). These data indicate the novel Sse1<sub>sbd</sub> mutant is defective in its ability to passively chaperone unfolded proteins while NEF function and nucleotide binding remain intact.

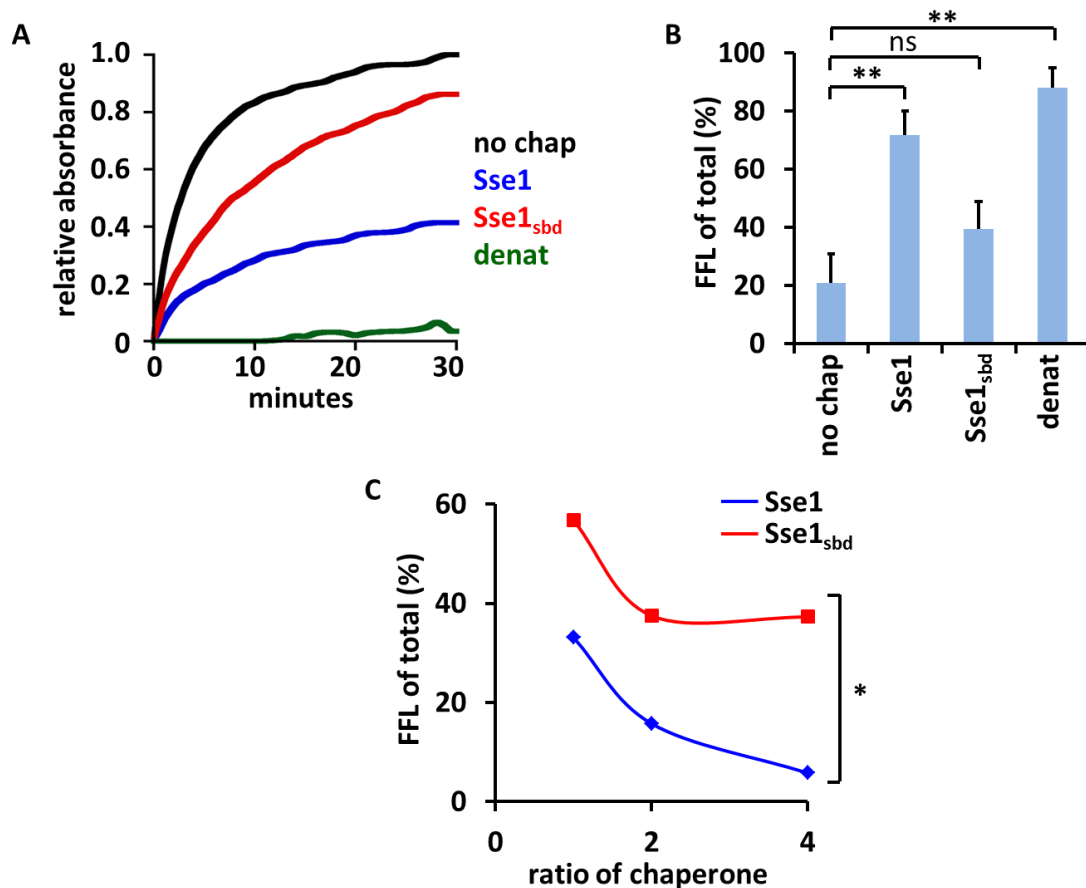


**Figure 4-3. Sse1 substrate binding domain mutant exhibits impaired chaperone holdase activity towards firefly luciferase (FFL).** A. Substrate aggregation experiments were conducted using chemically denatured firefly luciferase (FFL) (200 nM) diluted into refolding buffer without chaperone, with Sse1 (400 nM), or with Sse1<sub>sbd</sub> (400 nM). FFL diluted further into denaturing buffer was used as a control. B. Differential centrifugation analysis of FFL aggregation in the absence of chaperone or with Sse1 or Sse1<sub>sbd</sub> after a 30 min holdase assay. Samples were visualized by SDS-PAGE followed by Coomassie stain, and scanning densitometry quantitation was performed to determine FFL aggregation under each condition. Graph represents the average FFL that remained soluble in each sample  $\pm$  standard deviation (n=4) (p< 0.01). C. Analysis of holdase experiments using denatured FFL with varying ratios of chaperone were quantified using the endpoint degree of aggregation detected as in (B). Graph represents the average FFL that aggregated in each sample (n=2). Error bars represent  $\pm$  standard deviation (p< 0.05).

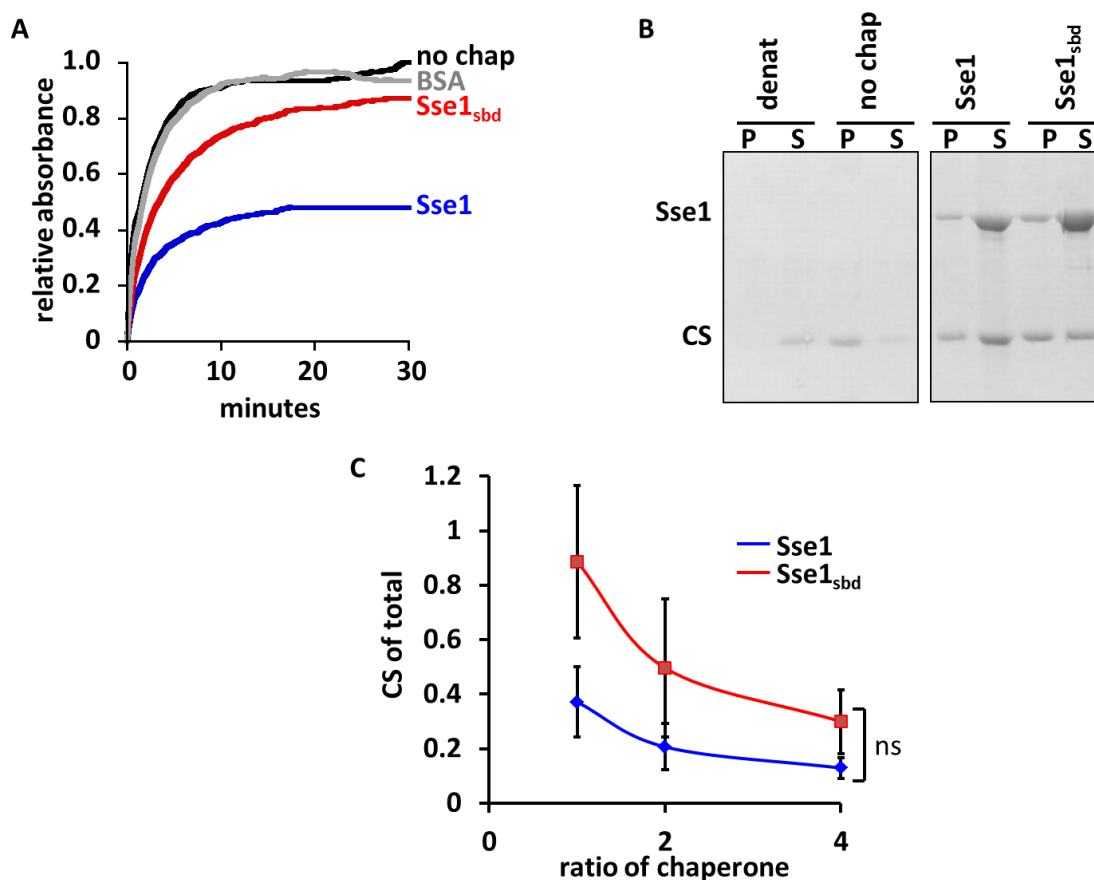


**Figure 4-4. Sse1 substrate binding domain mutant exhibits impaired chaperone holdase activity towards citrate synthase (CS).** A. Substrate aggregation experiments conducted using chemically denatured CS (200 nM) diluted into refolding buffer without chaperone, with Sse1 (200 nM), with Sse1sbd (200 nM), or with BSA (400 nM) as a non-chaperone control. B. Analysis of CS aggregation in the absence of chaperone in refolding or denaturing buffer or in the presence of different chaperones after 30 min in a holdase assay via differential centrifugation. Samples were analyzed via SDS-PAGE and Coomassie stain. C. Analysis of holdase experiments using denatured CS with varying ratios of chaperone using the endpoint amount of aggregation detected (n=2). Errors bars represent  $\pm$  standard deviation. Data is not statistically significant between Sse1 and Sse1<sub>sbd</sub>.

Hsp110 however, when compared to other NEFs, has been demonstrated to boost the aggregate solubilization activity of the Hsp70-based disaggregase machine (54, 110, 154, 155). Nillegoda therefore tested if the substrate binding function of Sse1 is required in this capacity. As a first step, he tested if substrate binding by Sse1 was important for re-folding of thermally denatured monomeric FFL. FFL was heat denatured in the presence of HSPA8 (Hsc70), DnaJB1 (Hsp40), and Hsp26 for 10 min at 42 °C (110). The samples were shifted to 30 °C and a nucleotide regeneration system was added. Refolding of FFL was measured in the presence of no NEF, Sse1, Sse1<sub>sbd</sub>, or HSPH2 (human Hsp110) as a control. It has been previously established that yeast and human Hsp110s are functionally interchangeable (110). Sse1 and Sse1<sub>sbd</sub> were observed to aid Hsp70/Hsp40 equally in successful refolding of FFL (data not shown). To test if the substrate binding function of Sse1 might be necessary for the more difficult task of disaggregating FFL, aggregates were formed by FFL heat denaturation (15 min, 45 °C) in the presence of Hsp26, and the aggregates were mixed with a cocktail of chaperones containing HSPA8, DnaJB1, and no NEF, Sse1, Sse1<sub>sbd</sub>, or HSPH2. Again, substrate binding deficient mutant Sse1<sub>sbd</sub> functioned with Hsp70/Hsp40 as effectively as the wild-type Sse1 or the HSPH2 (human Hsp110) control (data not shown). All three Hsp110 proteins were able to reactivate over 40% of the aggregated FFL within the two-hour time course. The data indicate that Sse1 holdase activity is not obligatory for effective refolding or disaggregase activity of at least the model substrate FFL.

Sse1 is a critical component of the protein quality control machineries. Indeed, *sse1Δ* cells demonstrate significant growth deficiencies including temperature sensitivity, and *sse1Δsse2Δ* cells are unviable (151). Furthermore, Sse1 and Sse2 are unique among known cytosolic NEFs for possessing substrate binding activity, raising the possibility that this activity is important *in vivo*. To test this hypothesis, I began by determining the expression of Sse1<sub>sbd</sub> to ensure that the introduced mutations did not affect its stability *in vivo*. At 30 °C and 37 °C, plasmid-borne Sse1, Sse1<sub>sbd</sub> and a previously described NEF-defective mutant carrying the G233D mutation (here designated Sse1<sub>nbd</sub>),

were expressed at similar levels, both slightly higher than endogenous Sse1 (Figure 4-5.A and B). I also wanted to ensure that Sse1<sub>sbd</sub> retained interaction with the yeast cytosolic Hsp70s (Ssa and Ssb) to function as a NEF *in vivo*. All Sse1 proteins were expressed with a FLAG-tag fused to the N-terminus and co-immunoprecipitations were performed (44). Sse1<sub>sbd</sub> was found to associate with the cytosolic Hsp70s, Ssa and Ssb, at both temperatures in a manner indistinguishable from wild-type Sse1 (Figure 4-5.C and D).

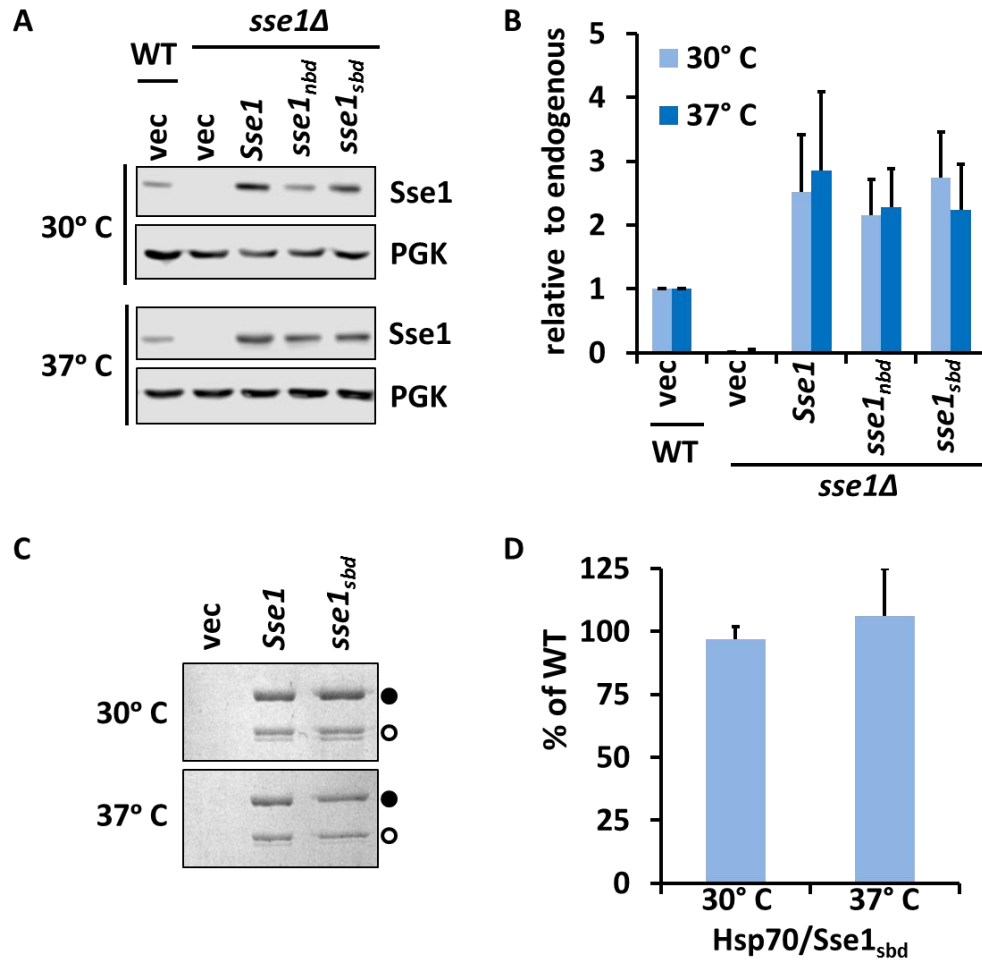


**Figure 4-5. *Sse1<sub>sbd</sub>* is stable and interacts with endogenous yeast Hsp70 proteins *in vivo*.** A. Protein lysates from cells expressing the indicated SSE1 alleles and cultured at 30 °C or 37 °C were analyzed by immunoblot to determine expression levels and stability (n=3). B. Quantitative analysis of the immunoblots in (A). Error bars represent  $\pm$  standard deviation. C. Co-immunoprecipitation experiments using FLAG-tagged Sse1 (labeled with a closed circle) variants were performed to assess interactions with endogenous Ssa and Ssb proteins (labeled with an open circle) (n=3). Samples were analyzed via Coomassie stain on an SDS-PAGE. D. Quantitative analysis of band densities in (C). Error bars represent  $\pm$  standard deviation.



Given that Sse1<sub>sbd</sub> displayed normal stability and retained Hsp70 interaction at both standard and heat shock temperatures, I next assessed the contribution of substrate binding to Sse1 functions *in vivo*. As previously mentioned, the *sse1<sub>nbd</sub>* allele contains the mutation G233D which renders it unable to bind nucleotide, interact with Hsp70, or act as a NEF (40, 44, 128). I compared the growth of *sse1Δ* cells expressing *SSE1*, *sse1<sub>nbd</sub>*, or *sse1<sub>sbd</sub>* under cold stress or heat stress. While *sse1<sub>sbd</sub>* fully complements *sse1Δ* cells grown in optimal conditions and under cold stress, the mutant allele could not confer normal growth under heat stress (Figure 4-6). This behavior contrasted with the inability of the *sse1<sub>nbd</sub>* allele to complement under any condition, suggesting that thermal stress may impose distinct requirements for Sse1 functions that include NEF and substrate holdase activities. To further probe this question, and to ask whether the presence of the closely related Sse2 protein masked growth defects of *sse1<sub>sbd</sub>* under non-heat shock conditions, I transformed *sse1Δsse2Δ* cells with *sse1<sub>sbd</sub>*- or *SSE1*-expressing plasmids using a plasmid shuffle technique (151). I again observed indistinguishable growth between the two alleles at 30°C, while *sse1<sub>sbd</sub>* was unable to maintain viability at 37°C (Figure 4-6.A and B). Consistent with the phenotypes seen under thermal stress, cells grown in the presence of formamide, which acts as a general protein denaturant, exhibited phenotypes consistent with heat stress (Figure 4-6.C). Cells expressing the *sse1<sub>nbd</sub>*, or *sse1<sub>sbd</sub>* were hypersensitive to formamide, and this phenotype was augmented with combined heat stress. These results suggest that despite being unnecessary for substrate refolding and disaggregation *in vitro*, or resistance to other forms of proteotoxic stress, the Sse1 SBD and its holdase activity are important for cell physiology and survival under prolonged thermal stress.

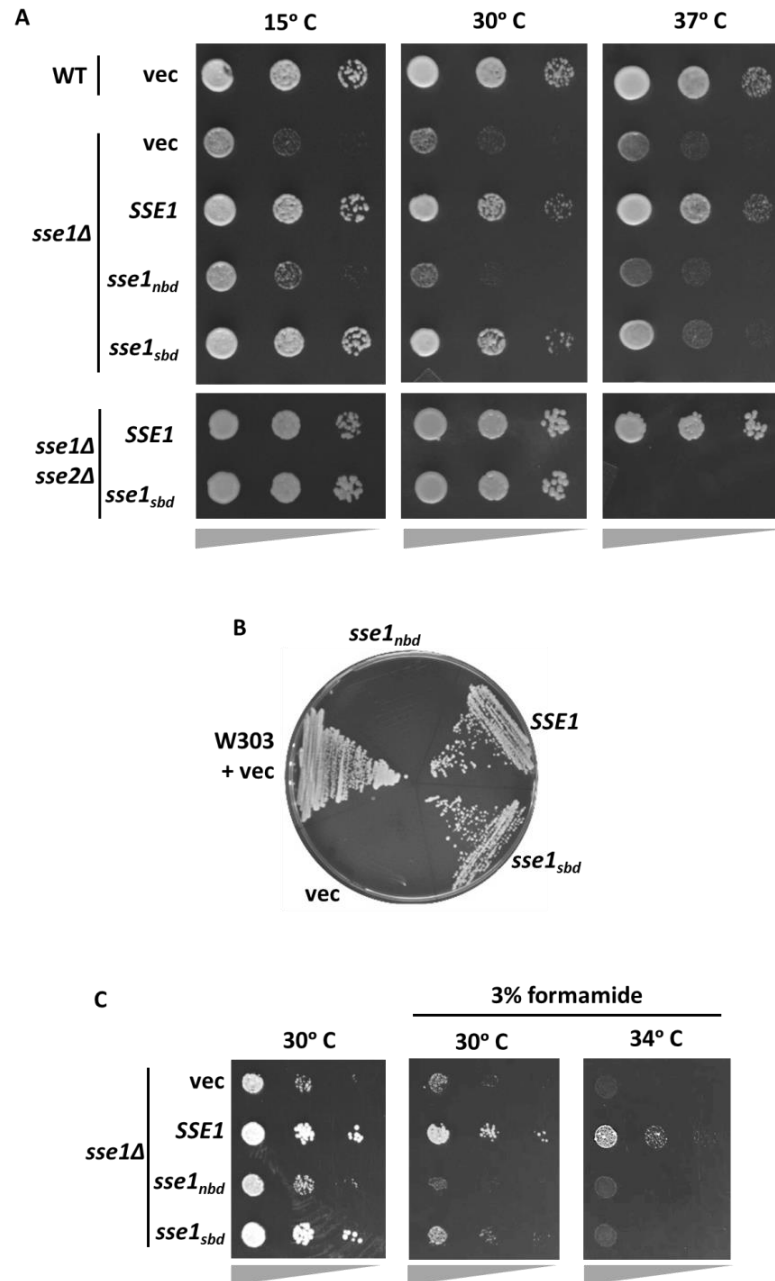


**Figure 4-6. *Sse1<sub>sbd</sub>* supports growth at normal but not heat shock temperatures.** A. Serial dilution plating of *sse1Δ* or *sse1Δsse2Δ* cells complemented with the indicated plasmid-expressed *SSE1* alleles and cultured at the indicated temperatures. Wedges below images represent relative cell density. B. Complementation of *sse1Δsse2Δ* with plasmid expressed *Sse1* alleles at 30 °C. C. Serial dilution plating of *sse1Δ* cells complemented with the indicated plasmid-expressed *Sse1* alleles cultured on formamide.

I envisioned two possible explanations to account for the results obtained from the growth analyses with *sse1<sub>sbd</sub>*. One is that Sse1 substrate binding is important only during heat stress due to physiological insults that occur exclusively under those conditions. The second possibility is that the Sse1 SBD is functioning at all times to maintain proteostasis. During normal growth conditions it minimally contributes to the chaperones network, but it takes on a more impactful role during heat stress and is required to endure the increased burden on protein quality control systems. To determine if a non-functional Sse1 SBD has any impact on the proteome while cells are grown under optimal conditions, I assessed the activation of the heat shock response (HSR) as a proxy for disruption of proteostasis using an established *HSE-lacZ* reporter (131, 132). To prevent possible variability from plasmid expression in these and subsequent experiments, I chose to directly integrate the *SSE1* mutants into the yeast chromosome at the endogenous locus. It is known that *sse1Δ* cells exhibit a two- to four-fold elevated HSR, consistent with chronic proteostatic imbalance (131). I confirmed that cells expressing the NEF-defective allele *sse1<sub>nbd</sub>* also demonstrated an activated HSR (Figure 4-7.A). Interestingly, cells expressing *sse1<sub>sbd</sub>* exhibited modest activation of the HSR (~1.8-fold) supporting the idea that the Sse1 SBD may play some role in proteome maintenance even during non-stress conditions. As a complementary approach, I assessed Hsp90 expression since it is exclusively a target of Hsf1 (156, 157) (10). Using immunoblot analysis, I determined that the *sse1Δ*, *sse1<sub>nbd</sub>*, *sse1<sub>sbd</sub>* cells exhibited a modest 1.5- to 3-fold increase in steady state Hsp90 levels in accordance with the HSR activation results (Figure 4-7.B). These data suggest that the holdase activity of Sse1 nominally contributes to proper functioning of the chaperone network under normal physiological conditions.

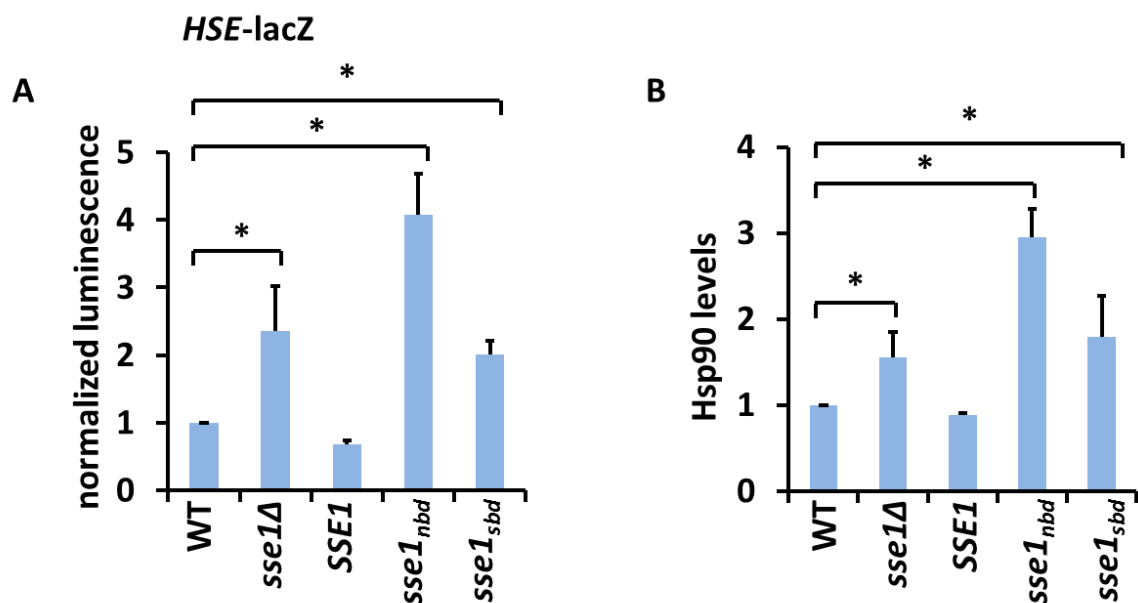


**Figure 4-7. Loss of Sse1 holdase activity results in mild proteotoxicity.** A.  $\beta$ -galactosidase activity assays from cells expressing the indicated *SSE1* alleles integrated at the endogenous locus and expressing the HSF reporter *pSSA3HSE-lacZ* grown under optimal conditions and in the absence of stress (n=3). B. Protein lysates from cells grown to mid-log phase under optimal conditions and in the absence of stress were analyzed for Hsp90 protein levels by SDS-PAGE and immunoblot. Scanning densitometry quantitation of Hsp90 levels from blots and normalized to a PGK immunoblot as a load control (n=3). Error bars represent  $\pm$  standard deviation ( $p < 0.05$ ).

In addition to general contributions to proteostasis, Sse1 supports signal transduction and functions of Hsp90 (114). For example, *sse1Δ* cells are especially sensitive to inhibitors that target Hsp90-facilitated receptor activation such as geldanamycin and macbecin (131). To assess if this biological role required Sse1 to functionally interact with unfolded substrates, I used the maturation and activation of the mammalian glucocorticoid receptor (GR) in yeast cells as a benchmark of Hsp90 activity.  $\beta$ -galactosidase activity was measured in cells co-expressing a glucocorticoid response element (GRE)-*lacZ* reporter and the different *SSE1* alleles after activation of the GR via the synthetic hormone deoxycorticosterone (DOC) (Figure 4-8). Wild-type cells exhibited a robust response to DOC treatment indicative of GR activation. Likewise, cells expressing *sse1<sub>sbd</sub>* were also able to activate the GR, whereas activation was abolished in *sse1Δ* and *sse1<sub>nbd</sub>* cells indicating that the Sse1 substrate binding function is not required to contribute to this Hsp90-dependent activity. This is evidence that the NEF function of Sse1 is primarily involved in Hsp90-mediated receptor activation.

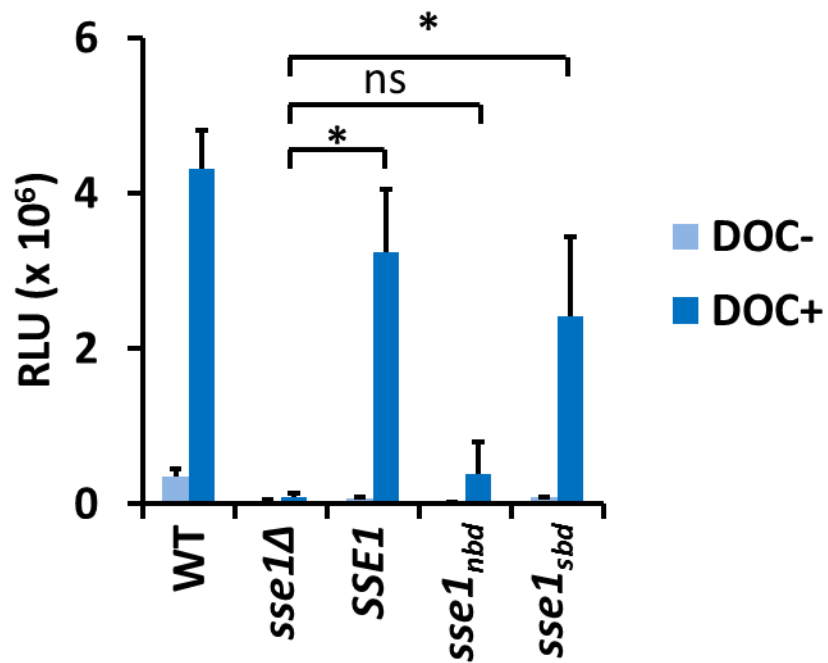


**Figure 4-8. SBD function is not required for Hsp90-dependent glucocorticoid activation via *Sse1*.** Cells were grown under optimal conditions and activation of the rat glucocorticoid receptor was measured via a *LacZ* reporter in the absence and presence of 10  $\mu$ M deoxycorticosterone (DOC). Luminescence was measured and the relative light units (RLU) detected were graphed as a mean (n=4) with error bars representing  $\pm$  standard deviation. \*=p<0.05 and ns indicates no statistical difference.

Another established cellular role for Sse1 is its participation in the triage decision for Hsp70-mediated protein folding versus degradation, wherein Sse1 is required for targeting terminally misfolded proteins to the proteasome for degradation. Specifically, Sse1 stimulates ubiquitination and degradation of the model misfolded protein CPY<sup>+</sup>-GFP, an engineered variant of the vacuolar protease carboxypeptidase Y that lacks the ER signal sequence and is permanently misfolded (132, 133). I utilized CPY<sup>+</sup>-GFP to assess if Sse1 substrate binding was important for targeting terminally misfolded proteins for degradation. After treating cells with cycloheximide, I tracked the clearance of CPY<sup>+</sup>-GFP in cells expressing *SSE1*, *sse1<sub>ndb</sub>*, or *sse1<sub>sbd</sub>* by immunoblot. In the presence of a fully functional Sse1 protein, CPY<sup>+</sup>-GFP levels decrease in cells after cycloheximide treatment as the misfolded protein is degraded (Figure 4-9). I found that *sse1<sub>ndb</sub>*-expressing cells matched *sse1Δ* cells in their inability to clear the terminally misfolded protein after two hours of cycloheximide chase. In contrast, *sse1<sub>sbd</sub>*-expressing cells fully cleared CPY<sup>+</sup>-GFP indicating that the Sse1 SBD function is not required for targeting terminally misfolded proteins for degradation. In addition to immunoblot analysis, I assessed the amount of CPY<sup>+</sup>-GFP aggregates forming in cells expressing the different Sse1 alleles and tracked their clearance over time using fluorescence microscopy. CPY<sup>+</sup>-GFP aggregate clearance correlated precisely with protein clearance (Figure 4-10.A and B). To test if Sse2 could be masking a substrate binding role for Sse1 in protein degradation, I used *SSE1sse2Δ* and *sse1<sub>sbd</sub>sse2Δ* strains (constructed by Unekwu Yakubu) and tracked the ability of these cells to clear the CPY<sup>+</sup>-GFP aggregates. Cells expressing the substrate binding deficient mutant cleared the aggregates at the same rate as *SSE1sse2Δ* cells (Figure 4-10.C and D). Although all the microscopy images were taken with equal exposures, the images of cells at 90 minutes have very bright backgrounds due to the overall decrease in cellular GFP signal. Together, these data strongly support the contention that Sse1 substrate binding is not required to support Hsp90 signaling activities or to promote the degradation of terminally misfolded cytosolic proteins.

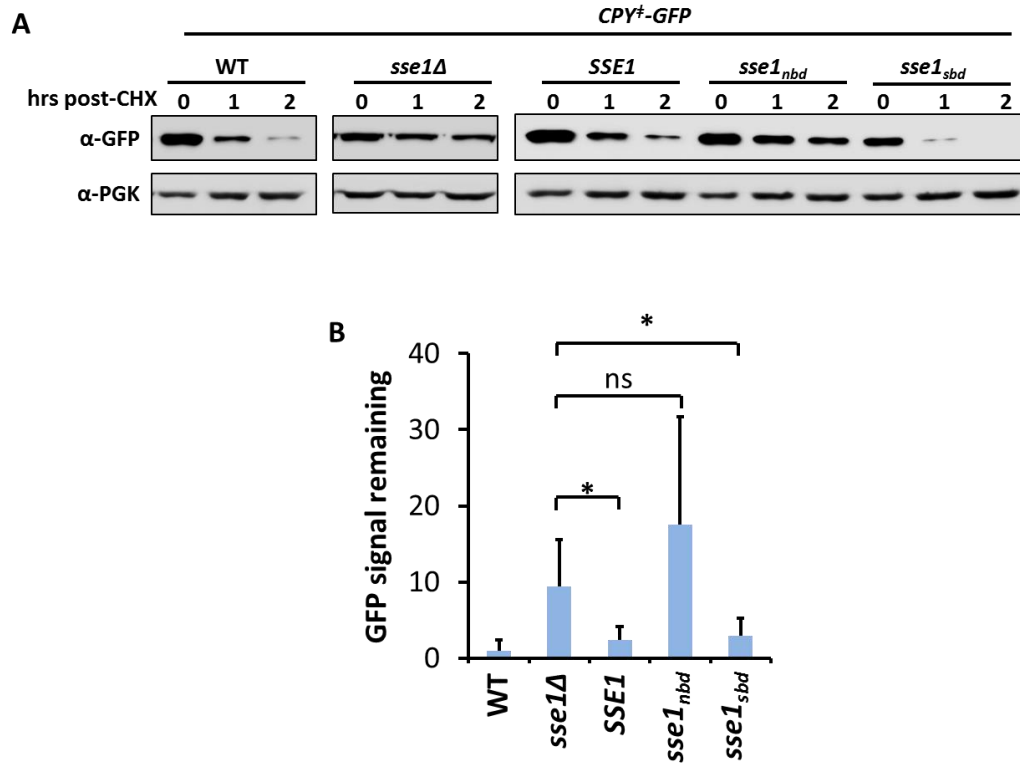


**Figure 4-9. Sse1 SBD function is not required for clearance of the misfolded CPY<sup>+</sup>-GFP reporter.** A. Immunoblot analysis of CPY<sup>+</sup>-GFP after a 2 hour cycloheximide treatment. Degradation of the CPY<sup>+</sup>-GFP was analyzed using anti-GFP antibody and PGK was used as a load control. B. Scanning densitometry quantitation was performed on anti-GFP blots and normalized to the PGK signal within each sample. The remaining normalized level of GFP signal was plotted after the 2 hour cycloheximide treatment (n=3).



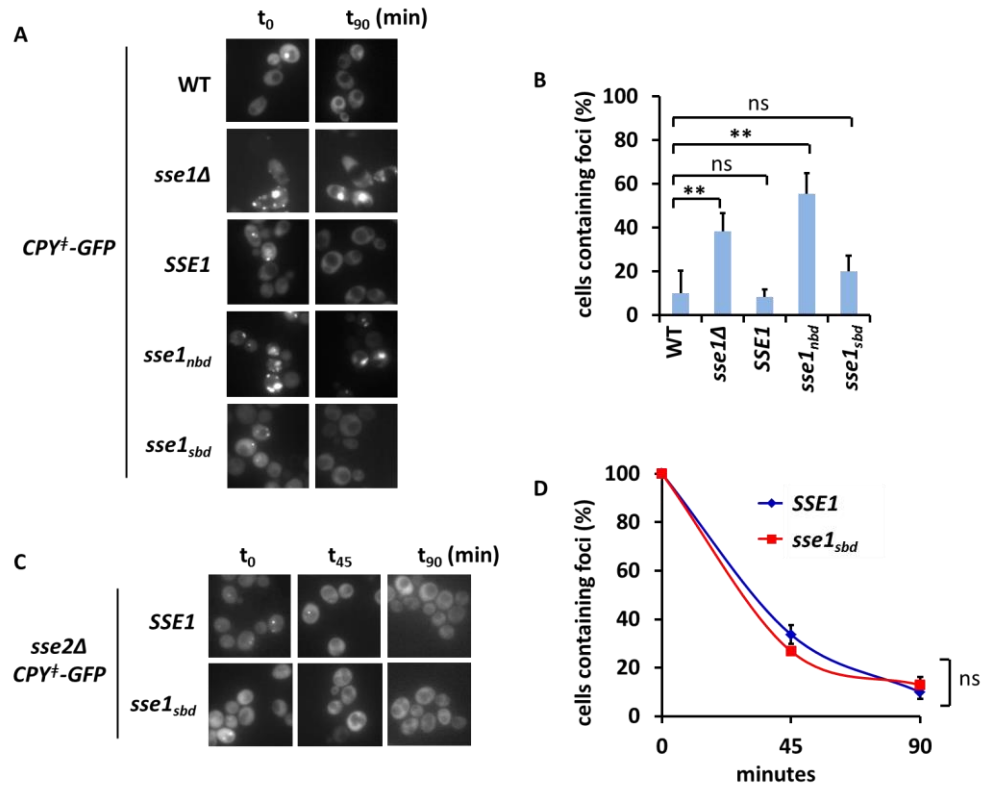


**Figure 4-10. Sse1 SBD function is not required for clearance of the CPY<sup>+</sup>-GFP aggregates.** A. Representative micrographs of the various *SSE1* strains at 0 and 90 min after cycloheximide treatment to track CPY<sup>+</sup>-GFP aggregate clearance in the cell population. B. Quantitation of the experiments shown in (A), percentage calculated as aggregate containing cells relative to time zero. Three independent experiments were conducted and at least 95 cells were counted for each strain under each time point. Error bars represent standard deviation and \*\*=p<.01. C. Representative micrographs of *SSE1sse2Δ* or *sse1<sub>sbd</sub>sse2Δ* strains tracking CPY<sup>+</sup>-GFP aggregate clearance at the indicated time points. D. Quantitation of the experiments shown in (D), percentage calculated as aggregate containing cells relative to time zero. Three independent experiments were conducted and at least 136 cells were counted for each strain under each time point. Error bars represent standard deviation, and ns indicates no statistical difference. All experiments were performed using cells expressing the indicated *SSE1* alleles integrated at the endogenous locus.

## Discussion

Among the three classes of cytosolic NEFs, Hsp110/Sse is the sole family demonstrated to possess holdase activity for unfolded proteins, yet no *in vivo* role has been exclusively attributed to this domain. To address this quandary, I generated a novel Sse1 allele that disrupts the ability of the chaperone to prevent aggregation, presumably via substrate binding and sequestration, while maintaining interaction with Hsp70 and NEF activity. Data from our laboratory and others strongly suggest that the yeast cytosolic Hsp110s, Sse1 and Sse2, play critical cellular roles in maintaining protein homeostasis during physiological and stress conditions (114, 131, 132). This interpretation is bolstered by the fact that *sse1Δsse2Δ* cells are unviable and while overexpression of the other yeast NEFs can only partially complement growth phenotypes at 30°C, the complete absence of Hsp110 proteins can only be fully remedied by expression of either *SSE1* or *SSE2* (114). In all cases studied to date, elimination of Hsp110/Sse NEF activity phenocopies the gene deletion, suggesting that indeed, the NEF function is a primary, if not dominant, role for this class of chaperone. Known Sse1 roles that might additionally be impacted by loss of Hsp110/Sse holdase activity were tested such as refolding and disaggregation *in vitro*, responses to different proteotoxic stresses, signaling through Hsp90, and targeting of terminally misfolded cytosolic proteins for degradation. Strikingly, there was no demonstrable role for Sse1 SBD function in the reconstituted luciferase refolding or disaggregation reactions, leading us to conclude that the holdase activity is dispensable for these activities. Likewise, Hsp90-dependent signaling and protein degradation were fully supported by the Sse1<sub>sbd</sub> mutant. This is in apparent contrast to a recent study by the Hendershot group that identified two secretory pathway proteins, immunoglobulin  $\gamma$ 1 heavy chain and NS-1  $\kappa$  light chain, that are preferentially bound by the ER homolog of Hsp110, Grp170, and when this interaction is eliminated processing of these substrates is disrupted (158). Although these findings suggest a biological role for Grp170 substrate binding, these same regions within the substrates are both aggregation-promoting and

recognized by the ER Hsp40 co-chaperones ERdj4 and ERdj5, precluding a clear interpretation. Additionally, models have been proposed wherein Hsp110 chaperones are competent to promote the folding of unfolded substrates when assisted by Hsp40 co-chaperones in an ATP-dependent folding cycle, an activity that would presumably rely on the SBD (111). However, the ability of catalytically inactive *SSE1* mutant alleles to fully support known Sse1-dependent activities challenges the biological relevance of the observation by Mattoo et al. in which Hsp110 was able to fold denatured substrates in the absence of Hsp70 (39, 128).

It is possible that the Hsp110/Sse SBD plays a (minor and perhaps redundant) role in protein folding events that is magnified under certain stress conditions. For example, *Sse1<sub>sbd</sub>* was unable to serve as the sole Hsp110 allele under extended growth at 37°C or in the presence of formamide, the latter a phenotype that I and others have demonstrated to be functionally analogous to thermal stress (159, 160). It cannot be excluded, however, that these phenotypes are ultimately more tightly linked with cell wall integrity than protein homeostasis, an idea reinforced by the clear suppression of *sse1* mutant phenotypes with 1M sorbitol, an osmotic stabilizing agent (161).

It may be relevant to consider that the *Sse1<sub>sbd</sub>* mutant is not completely defective in substrate binding, retaining between 20-50% of its aggregation prevention potential in a substrate-specific manner. It is possible that a complete abrogation of substrate interaction is necessary to reveal more dramatic phenotypes in the different Sse1 functions tested. However, I attempted to generate a more severe holdase-defective mutant through additional targeted amino acid substitutions based on the work of Liu and colleagues, without success (109). Importantly, I observed nearly identical outcomes in multiple *in vitro* and *in vivo* assays that are highly dependent on Sse1 and sensitive to perturbations in its status. Tellingly, the recently described role for Hsp110/Sse as a critical component of the eukaryotic disaggregase machine provided a prime opportunity to answer the open question of whether substrate holding by this family of proteins contributed to the remarkable ability of the Hsp110•Hsp70•Hsp40 complex to extract and refold aggregated proteins. Our findings support the

growing contention that Hsp110 NEF activity, not holdase activity, is the key accelerator of disaggregation in this context (54). However, as the Sse1<sub>sbd</sub> mutant is not completely without substrate binding capacity, I cannot yet formally exclude a role for substrate binding by Hsp110 chaperones in disaggregation. The passive holdase activity of Hsp110/Sse has previously been shown to promote the refolding of luciferase by yeast cytosol, likely by stabilizing the unfolded polypeptide and preventing its aggregation. This activity may also be compared to subtle interactions under certain conditions with the Sup35 prion in yeast that appear to be independent of Sse1 NEF function (162, 163). In both these latter scenarios the Sse1 holdase function is likely operating independently of Hsp70.

It may be of interest to further probe potential contributions of Hsp110/Sse1 holdase activity in aggregate prevention for specific aggregation-prone substrates. For example, Hsp105 in human cells is known to modulate cystic fibrosis transmembrane conductance regulator (CFTR) folding and processing (164). Hsp110 suppresses the aggregation and associated toxicity of the mutant proteins that lead to amyotrophic lateral sclerosis and Alzheimer's disease respectively, when expressed in *C. elegans* and mice (123, 127). Hsp110 has also been found to be an important modulator of neuronal degeneration caused by the expression of toxic polyglutamine proteins that model Huntington's disease in the fly (125, 126). Strikingly, Hsp110 can also ameliorate toxicity caused by the G85R variant of SOD1, a contributor to amyotrophic lateral sclerosis (ALS), significantly extending survival of SOD1G85R-YFP transgenic mice when overexpressed in motor neurons (165, 166). The specific mechanisms by which Hsp110 prevents aggregation and disease progression in these model systems are unknown. Given the increasing significance of Hsp110 chaperones in modulation of proteotoxic aggregation, it will be important to more precisely define the features that contribute to such activities as a precursor to therapeutically manipulating the chaperone network to combat progression of protein-misfolding disorders.

## **Chapter 5: A carboxyl-terminus regulated fluorescence affinity tag affects Sse1 functions**

## Introduction

In parallel to the substrate binding function of *SSE1* study discussed in chapter 4, I attempted to find additional mutants of Sse1 that were substrate-binding defective. This was of particular importance as the Sse1<sub>sbd</sub> mutant was only partially defective in substrate interactions (retained 20-50% of substrate binding). In particular, I hoped to identify mutants that completely abolished substrate interactions. In collaboration with Julie Heffler, an undergraduate student in the Morano laboratory, we attempted to use manganese and Taq polymerase-induced mutagenesis to isolate SBD mutants (130). The error-prone PCR mutagenesis screen was conducted by modulating Taq activity through MgCl<sub>2</sub> levels and nucleotide concentrations thus inducing transcription errors during PCR amplification of the Sse1 SBD  $\beta$ -domain. The mutant  $\beta$ -domain DNA fragments amplified were transformed into yeast cells along with a linearized vector and the DNA for the NBD and  $\alpha$ -domain of Sse1. Transformants were screened for wild-type growth at 30 °C and a slow growth phenotype at 37 °C. Heffler identified ten *SSE1* mutants that demonstrated the desired growth phenotypes and the candidates were analyzed for expression and protein stability at the two temperatures. Unfortunately, none of the candidates were stable at the elevated temperature indicating that the growth defect observed at 37 °C was due to the absence of the Sse1 protein under that condition. Additionally, we characterized multiple SBD site-directed mutants that were based on Hsp70 and Hsp110 literature (103, 109, 167, 168). I built *SSE1* alleles with the following mutations: *SSE1-SBD4*<sup>V467T</sup>, *SSE1-SBD5*<sup>S440L</sup>, *SSE1-SBD6*<sup>P426L</sup>, and *SSE1-SBD9*<sup>Y404I,W406LL433A,N434P,F439L,M441A</sup>. The mutagenesis screen and the targeted mutants did not yield in any Sse1 proteins that displayed the phenotypes of a non-functional SBD while retaining stability and expression *in vivo* as well as Hsp70 interaction.

Because these methods were unsuccessful in producing viable mutants, I utilized a previously developed strategy to modify Sse1 via a tunable, destabilized domain which acts a dominant degron in the absence of a small molecule ligand. A publication from the Goldberg laboratory used a

regulated fluorescent affinity (RFA) tag to control degradation of essential proteins in the parasite *Plasmodium falciparum* (169). The RFA tag provides an avenue to knock down protein levels due to the inherent instability of the dihydrofolate reductase (DHFR) degradation domain (DDD) it contains. The synthetic folate analog trimethoprim (TMP) binds the same site that folate binds within DHFR, so the compound can be used *in vivo* to stabilize the DDD and prevent its degradation (170, 171). Therefore, the RFA tag is unstable and degradation prone in the absence of a bound ligand but can be stabilized when a ligand such as TMP is available. The researchers observed that the RFA was not degraded when fused to *PfHsp110* even in the absence of TMP, indicating some level of protection by the molecular chaperone in *P. falciparum*. Their data suggested that the RFA tag fused to the C-terminus of *PfHsp110* was bound by the chaperone's SBD to protect the unstable domain and prevent its degradation (169).

Based on these findings, the RFA tag was used as a tool to study the substrate binding capabilities of Sse1. I proposed that the misfolded DDD in the absence of TMP would be recognized by the Sse1 acting as a physical occlusion in the SBD of the chaperone. The RFA tag could be manipulated through the absence or presence of TMP as an occluded or liberated Sse1 SBD, respectively. In this study, the *SSE1-RFA* strain was often characterized along with *sse1<sub>sbd</sub>* as I expected that the two proteins were inhibited in the ability to interact with substrate and would therefore show similar phenotypes. While the sensitivity to proteomic stressors was similar, the cells expressing *SSE1-RFA* were distinctively defective in degradation and aggregate clearance of a misfolded cytosolic protein. Furthermore, the observed degradation defects in the *SSE1-RFA* strain were not rescued in the presence of TMP. The data presented here suggest that the defects of the *SSE1-RFA* strain demonstrates might be due to the presence of a tag on the C-terminus of Sse1 and not because the tag contains a DDD within. To address this, I compared the *SSE1-RFA* strain to a strain which expressed an Sse1 protein with a C-terminus GFP fusion (*SSE1-GFP*). Cells expressing *SSE1-GFP* also

demonstrated reduced thermal tolerance at 37 °C. These data suggest that a blocked C-terminus interferes with specific Sse1 activities, possibly its roles in degradation.

## Results

Given the work recently published by Muralidharan et. al., Sse1-RFA was used to characterize the substrate binding function of Sse1 (130, 169). The RFA tag was hypothesized to interfere with the ability of the Sse1 SBD to recognize or bind an unfolded polypeptide (Figure 5-1). This tag could serve as a regulated Sse1 protein which could have an occluded SBD in the absence of trimethoprim (TMP) and a liberated SBD in the presence of TMP which stabilizes the DDD within the tag. The *SSE1-RFA* genetic construct was built by Julie Heffler, and she characterized *SSE1-RFA* cells for growth, assessed the stability of Sse1-RFA in the presence and absence of TMP, and assessed the ability of the protein to interact with Ssa and Ssb *in vivo* (130).



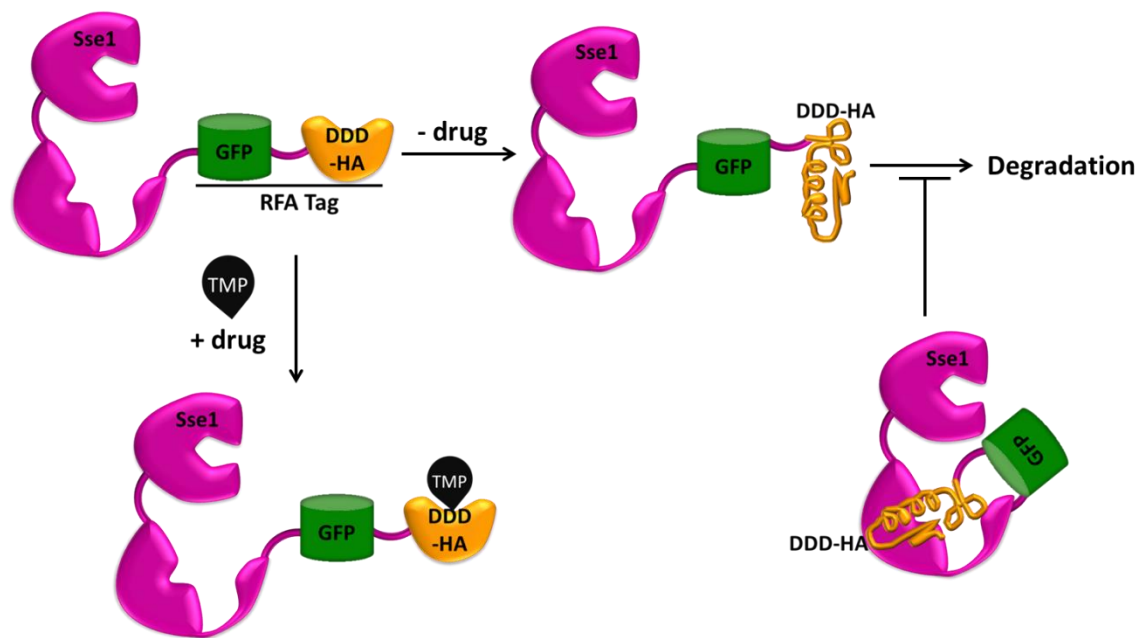


**Figure 5-1. Model of Sse1 fused to a carboxyl-terminus regulated fluorescence affinity (RFA) tag.**

The RFA tag contains a GFP domain followed by a DHFR degradation domain (DDD) with an HA-tag on the C-terminus. The degradation domain is inherently unstable and misfolded but can be stabilized in the presence of the ligand, trimethoprim (TMP). When RFA is fused to Sse1, the unstable DDD is recognized by the SBD of the chaperone to prevent degradation.

To verify the functionality of *SSE1-RFA*, I wanted to assess complementation of the *sse1Δ* strain growth phenotypes (130). Plasmid-borne *SSE1* alleles were expressed in *sse1Δ* cells and growth was compared under optimal conditions, during cold stress, and heat stress (Figure 5-2.A). *SSE1-RFA* cells show phenotypes very similar to those observed for the *sse1<sub>sbd</sub>* cells. Under optimal conditions (30 °C) and cold stress (15 °C), both alleles complement the *sse1Δ* slow growth phenotypes and grow significantly better than the non-functional *sse1<sub>nbd</sub>* cells. These data demonstrate that the *SSE1-RFA* allele is a functional copy of *SSE1* under these conditions. When cells are grown under heat stress (37 °C) *SSE1-RFA* cannot complement the slow growth phenotype of the *sse1Δ* cells. The phenotypes observed for *SSE1-RFA* cells reproduce the phenotypes expected for a non-functional Sse1 substrate binding domain mutant such as the *Sse1<sub>sbd</sub>* (Figure 4-5). Previous work by Julie Heffler demonstrated that *SSE1-RFA* cells are rescued from heat sensitivity when grown under the presence of TMP (cite Julie's thesis). I grew cells at 37 °C with TMP, and obtained comparable results (Figure 5-2.A). The phenotypic rescuing by TMP suggested that the RFA tag was functioning as predicted (Figure 5-1). Finally, similar to the phenotype of *sse1<sub>sbd</sub>* cells, the *SSE1-RFA* allele cannot complement the lethality of *sse1Δ sse2Δ* cells at 37 °C (Figure 5-2.B). These data also indicate that the Sse1-RFA protein is functional under most conditions except under heat stress. In addition to heat stress, *sse1Δ* cells complemented with the different *SSE1* alleles were also grown in the presence of formamide, a general protein denaturing agent (Figure 5-3). The phenotypes observed for *SSE1-RFA* cells were similar to those of the *sse1<sub>sbd</sub>* mutant. These data suggest that Sse1-RFA could be functioning in a similar fashion to the substrate binding domain mutant *Sse1<sub>sbd</sub>*.

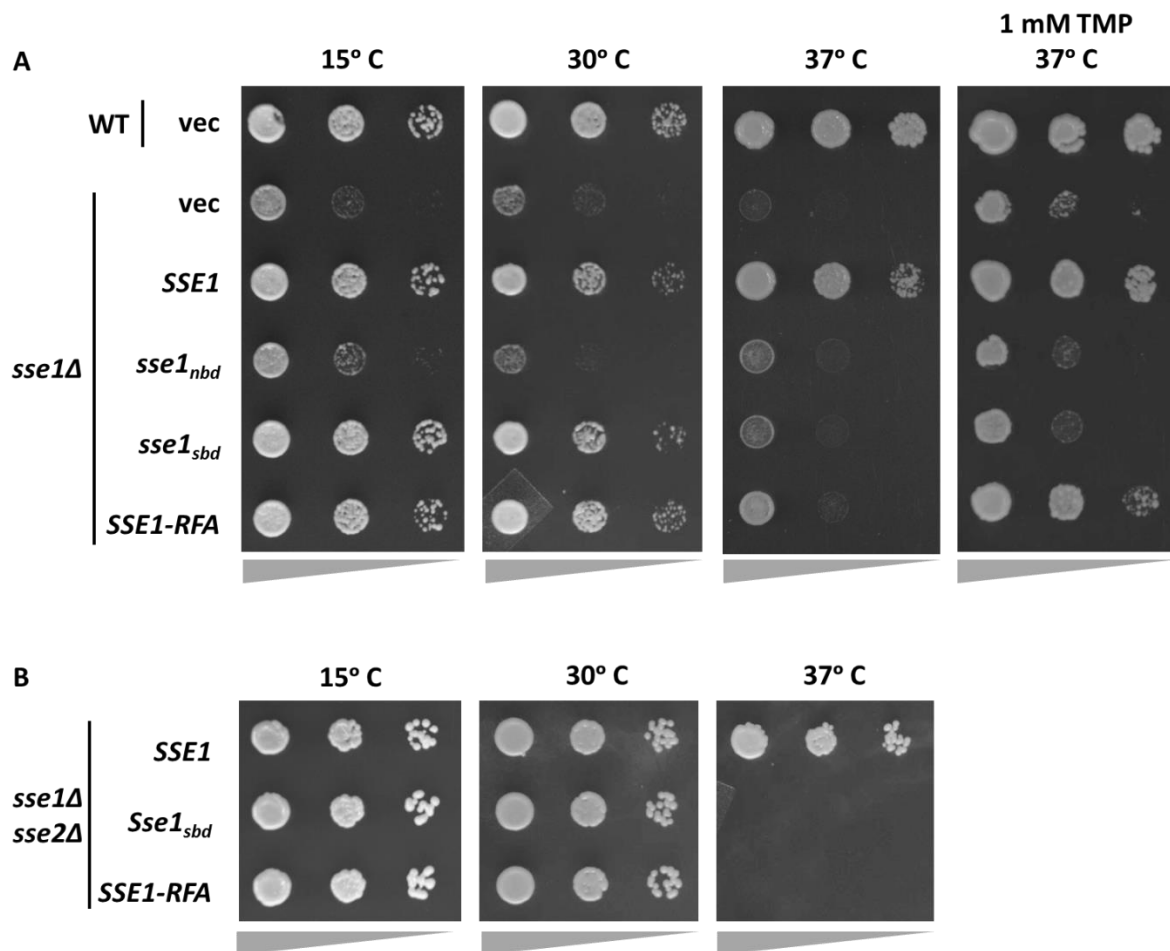


**Figure 5-2. Sse1-RFA phenocopies the sensitivity to heat stress of the Sse1 substrate binding mutant.** A. Serial dilution plating of *sse1Δ* cells complemented with the indicated plasmid-expressed *SSE1* alleles and cultured at the indicated temperatures and in the presence of TMP. Wedges below images represent relative cell density. B. Complementation of *sse1Δsse2Δ* with plasmid expressed *SSE1* alleles.

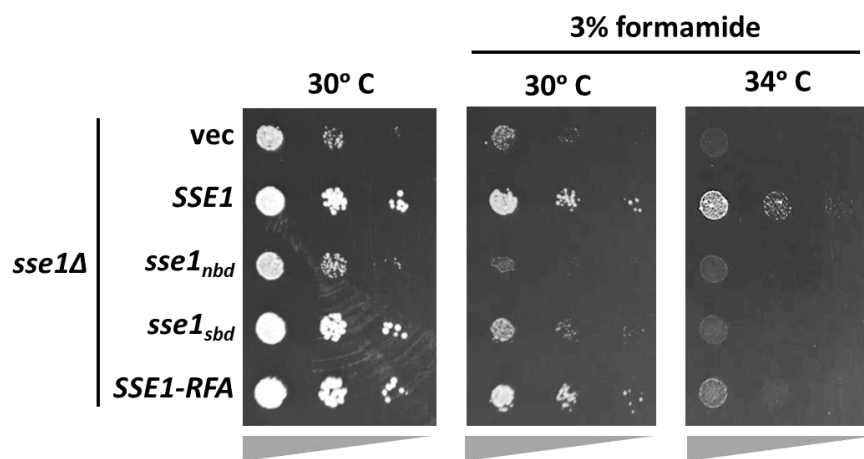


**Figure 5-3. Similar to a substrate binding mutant, Sse1-RFA is sensitive to formamide.** Serial dilution plating of *sse1Δ* cells complemented with the indicated plasmid-expressed Sse1 alleles cultured on formamide at the indicated temperatures.

I assessed if cells expressing the *SSE1-RFA* cells would behave like *sse1<sub>sbd</sub>* cells in a series of experiments that I performed characterizing the substrate binding mutant (Chapter 4). Evaluating these functions would require proper regulation of the *SSE1* variants, so *SSE1-RFA* was integrated into the yeast genome via allelic exchange. To ensure that *SSE1-RFA* cells were growing like the parental strain (WT) as well as the *SSE1* integrant, I calculated doubling times of the different *SSE1* strains under optimal conditions as a measurement of growth rate. As expected, WT, *SSE1*, *sse1<sub>sbd</sub>*, and *SSE1-RFA* strains had similar doubling times of approximately 126 minutes. The *sse1Δ* and *sse1<sub>nbd</sub>* strains grew more slowly and had doubling times of 261 or 178 minutes respectively (Figure 5-4.A). It is established that *sse1Δ* cells exhibit a two- to four-fold elevated HSR, consistent with a proteostatic imbalance (131). First, I wanted to assess the state of heat shock response (HSR) regulation as a marker for general proteotoxicity. *sse1Δ* cells and those expressing the NEF-defective allele *sse1<sub>nbd</sub>* demonstrated an activated HSR (Figure 5-4.B). Interestingly, *SSE1-RFA* cells had a lower activation (not significant) of the HSR (~1.2 fold) compared to *sse1<sub>sbd</sub>* cells (~1.8-fold). Hsp90 is exclusively a target of Hsf1, the master transcription regulator of the heat HSR (10, 156, 157). In parallel with the HSR activation experiments, I measured Hsp90 protein levels (Figure 5-4.C). Corresponding with the HSR activation results, the immunoblot analysis determined that the *sse1Δ*, *sse1<sub>nbd</sub>*, *sse1<sub>sbd</sub>* cells exhibited a modest 1.5- to 3-fold increase in steady state Hsp90 levels. *SSE1-RFA* cells displayed Hsp90 levels between those of WT and the *sse1<sub>sbd</sub>* cells, much like the results for the HSR activation experiment. These data suggest that Sse1 holdase activity contributes minimally to proper functioning of the chaperone network and proteostasis under normal physiological conditions and lack of this function results in a slight proteomic imbalance. *SSE1-RFA* cells were better able to maintain proteostasis than *sse1<sub>sbd</sub>* cells, and these somewhat dissimilar phenotypes suggest that the defects of the Sse1-RFA mutant are different from that of Sse1<sub>sbd</sub>. Interestingly, cells that express *sse1<sub>nbd</sub>* cells demonstrate a higher derepression of the HSR in both the HSR-LacZ experiments as well as the analysis of Hsp90 levels, but the strain does not have a growth defect as severe as the *sse1Δ* cells. This suggests that the

presence of a NEF defective Sse1 protein in the cell functions as a dominant negative and has a proteotoxic effect. This observation was noted but was not further addressed experimentally.

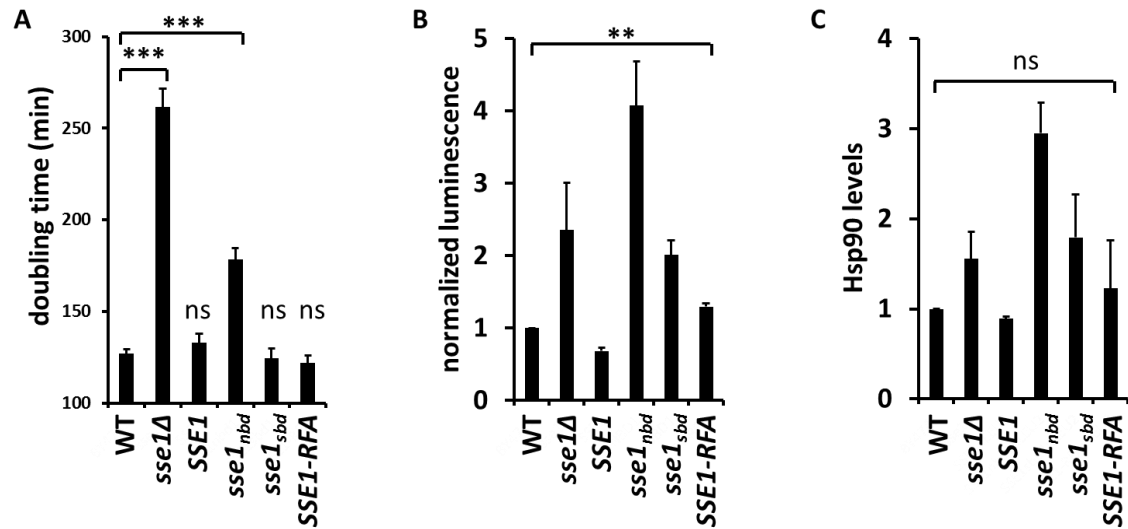


**Figure 5-4. Sse1-RFA cells grow like wild-type cells and demonstrate a negligible HSR activation.** A. Doubling time in minutes for the WT (BY4741), *sse1Δ*, and the various *SSE1* genomic integrants (n=4). B.  $\beta$ -galactosidase activity assays from cells expressing the indicated *SSE1* alleles integrated at the endogenous locus and expressing the HSF reporter *pSSA3HSE-lacZ* (n=3). Data was normalized to WT (parent strain). C. Protein lysates from cells grown to mid-log phase were analyzed for Hsp90 protein levels by SDS-PAGE and immunoblot. Scanning densitometry quantitation of Hsp90 levels from blots and normalized to a PGK immunoblot as a load control (n=3). Error bars represent  $\pm$  standard deviation. \*= $p < 0.05$ , \*\*= $p < 0.01$ , \*\*\*= $p < 0.005$ , and ns indicates not statistically different.

As discussed in Chapter 4, Sse1 promotes signal transduction and functions of Hsp90 (114, 131). I used the activation of the mammalian glucocorticoid receptor (GR) in yeast cells as a benchmark of Hsp90 activity, to evaluate if the Sse1-RFA mutant had deficiencies in this biological role of Sse1.  $\beta$ -galactosidase activity was measured in cells co-expressing a glucocorticoid response element (GRE)-*lacZ* reporter and the different *SSE1* alleles after activation of the GR via treatment with the synthetic hormone deoxycorticosterone (DOC) (Figure 5-5). WT, *SSE1*, *sse1<sub>sbd</sub>*, and *SSE1-RFA* cells exhibited a robust response to DOC treatment indicative of GR activation, whereas activation was abolished in *sse1 $\Delta$*  and *sse1<sub>nbd</sub>* cells implying that the NEF activity of Sse1 primarily drives maturation of the GR via Hsp90.



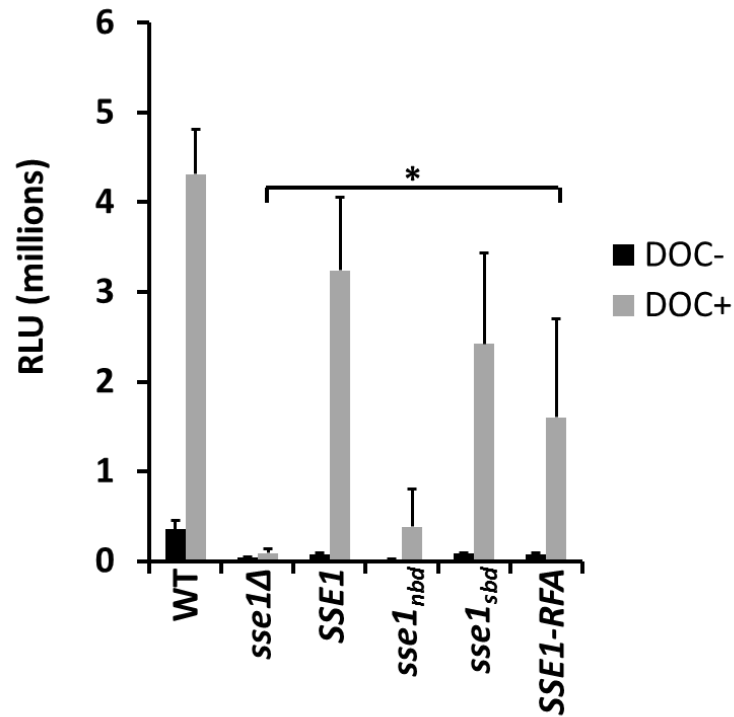


**Figure 5-5. Sse1-RFA is capable of activating the Hsp90-dependent glucocorticoid receptor via Sse1.**

Cells were grown under optimal conditions and activation of the rat glucocorticoid receptor was measured via a *LacZ* reporter in the absence and presence of 10  $\mu$ M deoxycorticosterone (DOC). Luminescence was measured and the relative light units (RLU) detected were graphed as a mean (n=4) with error bars representing  $\pm$  standard deviation. \*=p<0.05.

Lastly, *SSE1-RFA* cells were tested for ability to execute the Sse1 established role of targeting terminally misfolded proteins for degradation. I assessed this role *in vivo* by using CPY<sup>+</sup>-GFP which is an engineered, terminally misfolded protein from the vacuolar protease carboxypeptidase Y that lacks the ER signal sequence (131, 132). Cells were treated with cycloheximide to pause translation, and CPY<sup>+</sup>-GFP clearance was assessed via immunoblot (Figure 5-6.A). CPY<sup>+</sup>-GFP was stabilized in *sse1Δ* cells expressing the vector, *sse1<sub>nbd</sub>*, and *SSE1-RFA*, whereas cells expressing *SSE1* or *sse1<sub>sbd</sub>* were able to degrade the model substrate. Additionally, I tracked clearance of CPY<sup>+</sup>-GFP aggregates in cells containing the variant *SSE1* alleles as genomic integrations following cycloheximide treatment (Figure 5-6.B and C). Microscopic visualization demonstrated that *SSE1-RFA* cells have phenotypes resembling those of *sse1Δ* and *sse1<sub>nbd</sub>* cells as they were unable to clear the CPY<sup>+</sup>-GFP aggregates. Additionally, the micrograph image of *SSE1-RFA* cells that are not expressing CPY<sup>+</sup>-GFP demonstrates that Sse1-RFA is a soluble protein and remains appropriately distributed throughout the cytosol (Figure 5-6.B). Data from these experiments indicate that Sse1-RFA, in contrast to Sse1<sub>sbd</sub>, is not able to target this misfolded protein for degradation. The inability of Sse1-RFA to clear CPY<sup>+</sup>-GFP from cells might be due to an inhibition of the substrate binding function through the occlusion of the substrate binding domain. Given that the *sse1<sub>sbd</sub>* cells were not defective degrading CPY<sup>+</sup>-GFP or in clearing its aggregates, there was also the possibility that the phenotypes observed for *SSE1-RFA* were not due to defective substrate binding function but something else being affected by the presence of the RFA tag.

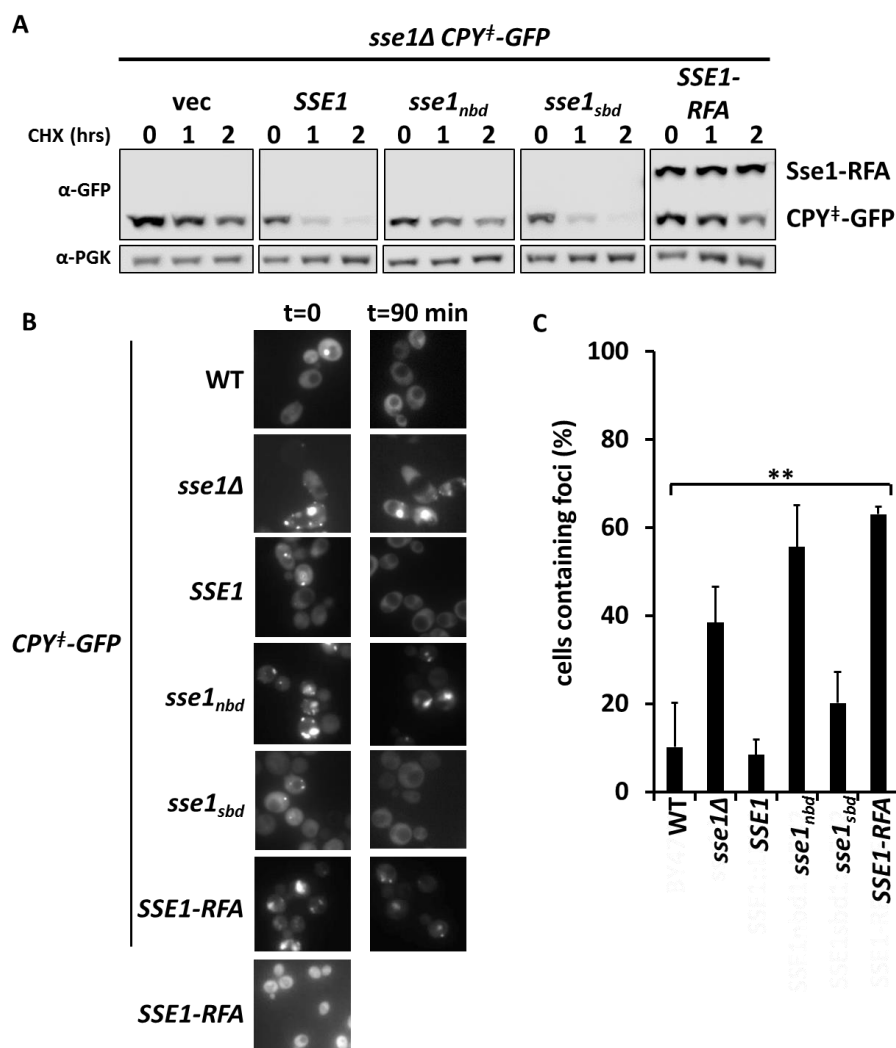


**Figure 5-6. Sse1-RFA is non-functional in clearing the misfolded CPY<sup>+</sup>-GFP substrate.** A. Degradation of CPY<sup>+</sup>-GFP was analyzed in *sse1Δ* cells expressing the plasmid-borne *SSE1* variants. Immunoblot analysis of CPY<sup>+</sup>-GFP degradation was performed at 0, 1, or 2 hours after cycloheximide treatment was using anti-GFP antibody and PGK was used a load control. B. Representative micrographs of the various *SSE1* strains at 0 and 90 min after cycloheximide treatment to track CPY<sup>+</sup>-GFP aggregate clearance in the cell population. C. Quantitation of the experiments shown in (B), percentage calculated as aggregate containing cells relative to time zero. Three independent experiments were conducted and at least 95 cells were counted for each strain under each time point. Error bars represent standard deviation and \*\*= $p < .01$ .

To test these possibilities, I repeated the experiments using the CPY<sup>+</sup>-GFP reporter in the presence or absence of TMP. Given that TMP can rescue the growth defect of the SSE1-RFA strain under heat conditions (Figure 5-2) (130), I expected that TMP would improve CPY<sup>+</sup>-GFP degradation. Surprisingly, TMP did not have an effect on Sse1-RFA function. Immunoblot analysis to assess the degradation of the protein showed that CPY<sup>+</sup>-GFP was stabilized in *SSE1-RFA* cells whether or not TMP was present (Figure 5-7.A). Additionally, tracking the clearance of CPY<sup>+</sup>-GFP via microscopy also demonstrated a TMP independent accumulation of aggregates (Figure 5-7.B).

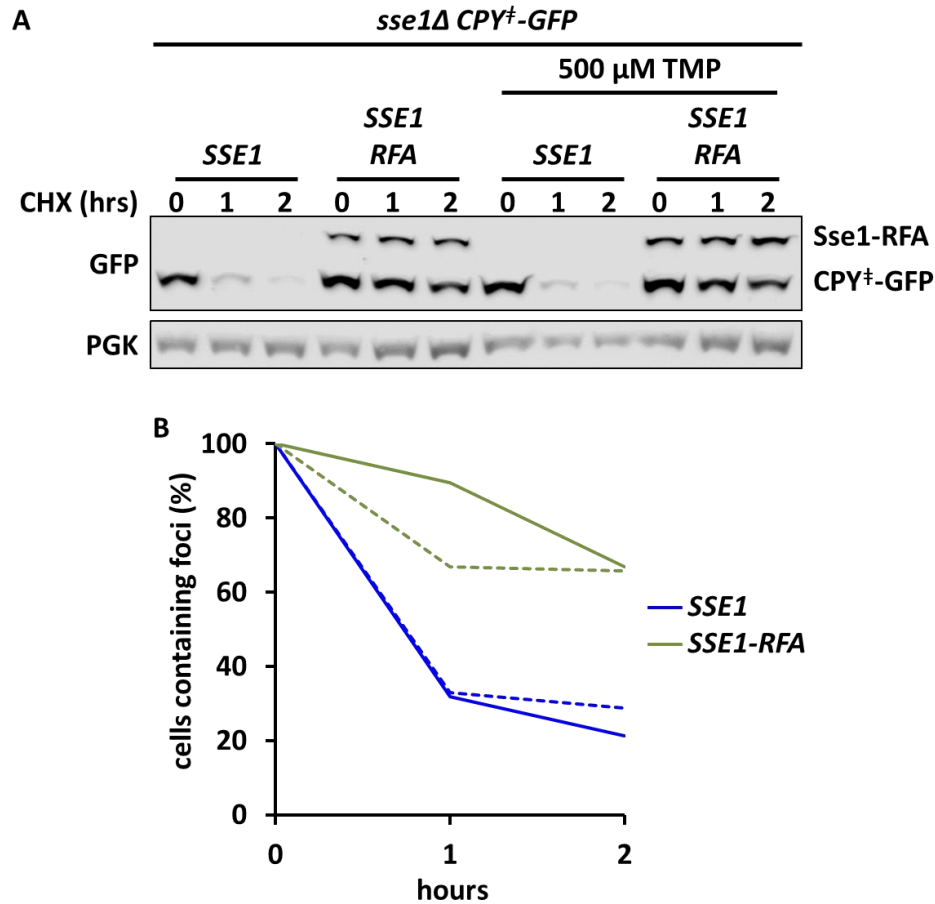


**Figure 5-7. TMP does not rescue the clearance defect of *SSE1-RFA* cells.** A. Degradation of CPY<sup>+</sup>-GFP was analyzed in *sse1Δ* cells expressing the plasmid-borne *SSE1* variants in the presence or absence of TMP. Analysis was performed at 0, 1, or 2 hours after cycloheximide treatment was using anti-GFP antibody and anti-PGK as a load control. B. Cells were grown in the absence (solid lines) or presence (dotted lines) of 500  $\mu$ M TMP. At least 90 cells per sample were visualized and cells containing foci of total were counted at 0, 1, or 2 hours after cycloheximide treatment. Percentage calculated as aggregate containing cells relative to time zero.

Given the data obtained from the HSR activation and the CPY<sup>+</sup>-GFP substrate clearance experiments, it was important to consider that Sse1-RFA was not behaving like the substrate binding domain mutant, Sse1<sub>sbd</sub>. Furthermore, the inability of TMP to rescue the CPY<sup>+</sup>-GFP clearance defect suggested that something other than SBD occlusion might be occurring with the Sse1-RFA protein. Therefore, I hypothesized that Sse1-RFA was showing phenotypic defects due to the placement of the RFA tag which could be interfering with other Sse1 activities. Experiments similar to those previously conducted using the *Pf*Hsp110 were used to characterize the Sse1-RFA (169). I used proteins with an N-terminus FLAG-tag expressed in *sse1Δ* yeast cells to measure the availability, or exposure, of the different domains of Sse1-RFA. The RFA tag is comprised of a GFP domain, the DDD, and an HA-tag at the C-terminus (Figure 5-1). If the DDD was bound by the substrate binding domain of Sse1, the GFP domain would be less available to bind antibodies in its native state during an immunoprecipitation (IP) based on the previous characterization of an Hsp110-RFA fusion (169). To ensure that the proteins, F-Sse1, F-Sse1-RFA, and F-RFA, were expressed and properly folded, I began by conducting an immunoprecipitation using FLAG antibody resin (Figure 5-8.A). As expected, the FLAG-tag effectively immunoprecipitated all of the proteins as it is located at the N-terminus and is likely not affected by SBD function or the presence of a tag at the C-terminus. Concurrent with what was previously published, the FLAG-IP results reproduced data demonstrating that Sse1-RFA can interact with the yeast cytosolic Hsp70 proteins suggesting that the NEF activity of the protein is intact (130). A second IP was performed using Sepharose beads conjugated with anti-GFP monoclonal antibody (Figure 5-8.B). If the RFA tag is bound by the SBD of Sse1, the GFP domain of Sse1-RFA would be less available compared to that of the RFA tag alone. The GFP domain appeared to be available in the Sse1-RFA fusion as well as the RFA alone. While these data do not guarantee that the DDD is not bound by the Sse1 SBD, it does provide evidence that the GFP domain in the Sse1-RFA fusion is unobstructed in the native state.

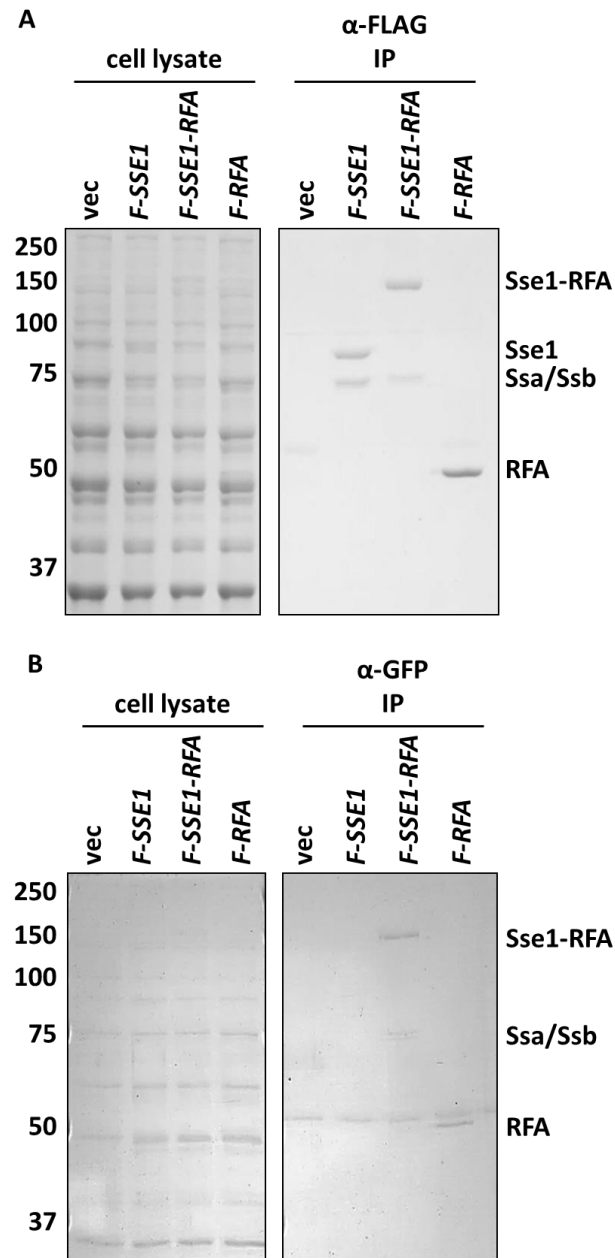


**Figure 5-8. The Sse1-RFA domains are accessible *in vivo*.** A. Immunoprecipitation experiments using FLAG-tagged proteins were performed using anti-FLAG conjugated resin. Samples were analyzed via Coomassie stain on an SDS-PAGE. B. anti-GFP IP was performed using Sepharose beads conjugated with anti-GFP monoclonal antibody. Samples were analyzed via SDS-PAGE and Coomassie stain.

The results of the IP experiments provided evidence that the phenotypes observed for *SSE1-RFA* cells were likely due to the presence of a tag on the C-terminus of the protein and not to the tag being recognized as unstable and bound by the Sse1 SBD. I used GFP as a large alternative tag fused to the C-terminus of Sse1 to test this conclusion (molecular weight: RFA 46 kDa, GFP: 27 kDa). *SSE1-GFP* cells grow like WT cells under optimal conditions but have a growth defect under heat stress (Figure 5-9. A). Sse1 protein levels of the different strains were assessed by immunoblot and growth was compared for the different *SSE1* variants (Figure 5-9.B). The observed thermal sensitivity of the *SSE1-GFP* strain phenocopies that of the *SSE1-RFA* strain. This indicates that the presence of a fused tag on the C-terminus of Sse1 renders it unable to function optimally during heat stress. The sensitivity to elevated temperatures exhibited by the Sse1-RFA and Sse1-GFP mutants indicate that heat stress tolerance might require Sse1 interactions that are conferred by the extreme C-terminus of the chaperone.



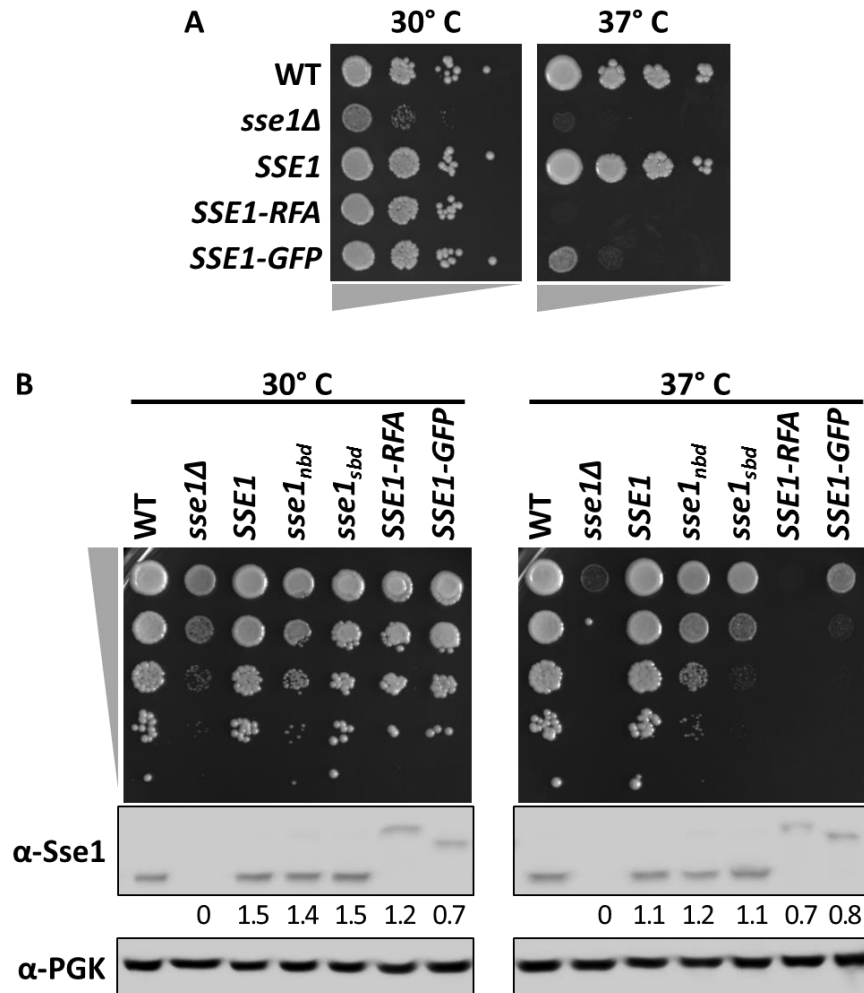


**Figure 5-9. A GFP tag on the C-terminus of *SSE1* results in growth phenotypes similar to the *SSE1-RFA* strain.** A. Serial dilution plating of cells expressing the various *SSE1* alleles integrated in the yeast genome, including *SSE1-RFA* and *SSE1-GFP*, and cultured at the indicated temperatures. Wedges below images represent relative cell density. B. *SSE1* strains were serially diluted and cultured under different temperature conditions. Protein lysates from cells were analyzed by immunoblots performed in parallel to the growth on solid media to determine protein expression levels. The numbers below the anti-Sse1 immunoblot indicate the Sse1 protein level relative to the WT for each temperature. PGK was used a load control and to normalize quantification.

## Discussion

Initially, Sse1-RFA was proposed as an alternative method to study the substrate binding domain functions of SSE1. In the initial phases of the study, *SSE1-RFA* cells phenocopied the *sse1<sub>sbd</sub>* strain (Figure 5-2). It was stable in yeast and maintained interactions with the cytosolic Hsp70s at 30° C and 37° C (130) (Figure 5-8.A and B) It was particularly striking that *SSE1-RFA* cells demonstrated a comparable sensitivity to heat, complete tolerance for cold stress, and complementation of the non-viable *sse1Δsse2Δ*. Furthermore, the heat sensitivity was rescued by the presence of TMP as was previously demonstrated (130). In addition to the growth assessments under optimal and stress conditions, the *SSE1-RFA* strain displayed phenotypes that were slightly more defective than the *SSE1* strain but less impacted than the *sse1<sub>sbd</sub>* strain in the assessments for the HSR regulation and the activation of the glucocorticoid receptor (Figure 5-4 and 5-5). Taking these data together with the work that was published using the *PfHsp110-RFA*, I posited that Sse1-RFA was a protein that was defective in binding substrate due to the occlusion of the chaperone SBD by the DDD within the RFA tag. I tested the ability of Sse1-RFA to function as a holdase *in vitro* using the aggregation assay discussed in chapter 3. Although the data were preliminary (protein purity was low and only one protein preparation was tested), they suggest that Sse1-RFA can bind unfolded citrate synthase similarly to Sse1 (data not shown).

Surprisingly, during testing each Sse1 variant in its ability to degrade CPY<sup>+</sup>-GFP, the *SSE1-RFA* strain provided phenotypes that were very different from those observed in the *sse1<sub>sbd</sub>* strain. These results could be for two different reasons. One reason could be that the Sse1-RFA had a higher degree of inhibition in binding substrate than the Sse1<sub>sbd</sub> that has up to a 50% reduction in its ability to interact with unfolded substrates compared to Sse1 (Figures 4-2 and 4-3). If the Sse1-RFA SBD is occluded by the RFA tag, it could be a complete inactivation of substrate binding by the pool of Sse1-RFA in the cell given each chaperone is fused to a tag. The high degree of substrate binding inhibition

in Sse1-RFA could result in the complete loss in ability to degrade CPY<sup>+</sup>-GFP or clear aggregates (Figure 5-6). The data presented in Figure 5-7 suggest that this rationale is incorrect because the presence of TMP, which stabilizes the DDD within the RFA tag, does not rescue the CPY<sup>+</sup>-GFP degradation or aggregate clearance phenotype in *SSE1-RFA* cells. Moreover, the immunoprecipitation experiments did not indicate that the RFA is bound or occluded by the chaperone (Figure 5-8). There is still more characterizing that needs to be completed in order to determine the availability of each domain in the native Sse1-RFA.

If Sse1-RFA does not have a higher degree of inhibition in binding substrate than the Sse1<sub>sbd</sub>, the other possibility is that the presence of the tag on C-terminus is preventing certain Sse1 functions. This second possibility is supported by the data presented (Figure 5-7 and Figure 5-9). Cells expressing Sse1 fused with a C-terminal GFP (strain *SSE1-GFP*) also demonstrate sensitivity to heat. To make a definitive conclusion regarding the effect a C-terminus tag has on Sse1 function, Sse1-RFA and Sse1-GFP need to further characterized and compared. Moreover, Sse1 is known to work cooperatively with the ubiquitin proteasome system when triaging terminally misfolded proteins for degradation (132, 133, 153). It is possible that the degradation defects seen for the *SSE1-RFA* strain might be due to the presence of the C-terminal tag which somehow inhibits those functions. Ultimately, characterization of Sse1-RFA and other C-terminus obstructions would further our understanding of Sse1 involvement in roles like targeting misfolded proteins for degradation.

## Chapter 6: Characterization of the *Drosophila melanogaster* Hsp110 (Hsc70cb)

## Introduction

In the cellular environment, proteins frequently encounter stress conditions that can cause misfolding and aggregation. Additionally, genetic mutations can occur within cells that produce irregular proteins which also form aggregates. Cellular protein inclusions caused by misfolded proteins lead to cytotoxicity and disease (5). To reduce the potential effects of protein damage, a network of molecular chaperones is deployed to protect the proteome by helping proteins fold or clearing them from the cell. In animals, the inability of chaperones to counteract excessive protein misfolding can lead to amyloid fibrillar aggregates that deposit around brain neurons contributing to the development or progression of neurodegeneration: Alzheimer's disease, Huntington's disease and Parkinson's disease are all fundamentally diseases of protein misfolding (116, 117). A complete understanding of the mechanisms of protein quality control is required to allow treatment of these devastating pathological states.

*Drosophila melanogaster* is an excellent multicellular organism in which to study the molecular basis of protein misfolding disorders. While flies cannot precisely reproduce the symptoms associated with human neurodegenerative disorders, consequences of expressing the human mutant protein that is characteristic of the disease can be visualized as phenotypes in a tissue specific manner, usually the fly eye (172). Using *Drosophila* in this type of model can help in two ways. The model can be used to gain an understanding of the molecular mechanisms that drive the pathology, and also to find strategies to repress phenotypes of the mutant, disease-prone protein. Hsc70cb, the fly Hsp110, was uncovered through an RNAi screen to be one of the most potent suppressors of polyglutamine Htt aggregation in *Drosophila* cells (125). Using established fly models of Huntington's disease with controlled Hsp110 levels, confirmed that this chaperone could affect the formation of aggregates as well as the progression of neuronal degradation (125, 126). Furthermore, Hsp110 associates with polyglutamine proteins *in vivo*, and *in vitro* studies indicate that this interaction is

conferred through the SDB  $\beta$  domain of the chaperone(124). These studies provide motivation for understanding how Hsp110 chaperones might interact with disease-prone proteins that contain polyglutamine tract expansions.

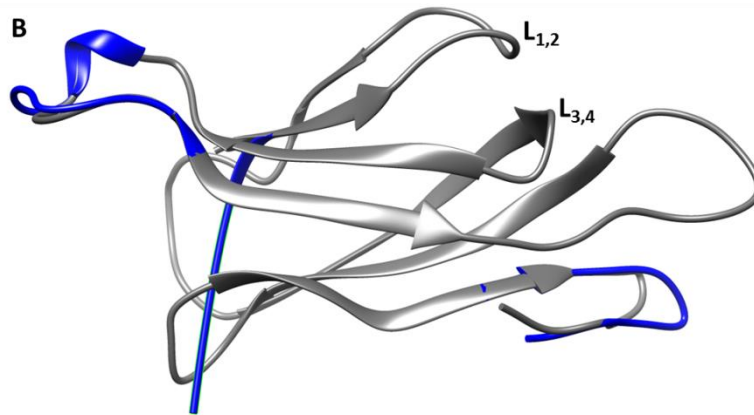
In this study, I sought to characterize the *D. melanogaster* Hsp110 protein, Hsc70cb, and develop mutants that were defective in binding substrate. Hsc70cb demonstrated holdase function in the established *in vitro* aggregation assay (Chapter 3) which can be used to characterize substrate binding mutants. Characterization of the wild-type Hsc70cb and a mutant collection could be utilized to study the role that Hsp110 proteins play in modulating the disease progression in animal models of neurodegenerative disorders.

## Results

Hsp110 chaperones are a highly conserved family of proteins that exists in eukaryotes (40, 152). There are two Hsp110 homologs in yeast, one in flies, and three in humans (Figure 6) (65, 173, 174). Since flies only possess one gene that produces an Hsp110 protein, Hsc70cb, it makes this a good animal model in which to study Hsp110 function as effects from homologs can be minimized. The knowledge gained from studying the Sse1 substrate binding function can be utilized to characterize the Hsc70cb given their high degree of conservation. The two proteins share 57% similarity and highly comparable substrate binding domains.

**A**

species	Hsp110 proteins
yeast	Sse1 Sse2
fly	Hsc70cb
human	Hsp105 Apg1 Apg2

**B**

**Figure 6-1. Characterizing the substrate binding domain in yeast, fly and human biology.** A. Hsp110 homologs across various species B. Hsc70cb SBD structure (gray) was modeled based on the Sse1 crystal structure (blue) using Protein Homology/Analogy Recognition Engine V 2.0 (PHYRE 2) with a confidence of 99.2% (59, 175).

To evaluate if the proteins shared functional homology with each other, *Hsc70cb* was expressed from a plasmid in *sse1Δ* cells and growth was assessed under optimal conditions and under heat stress. The *Hsc70cb* expressing strain shows the same slow growth phenotypes of the *sse1Δ* cells at either temperature indicating that the fly protein cannot functionally complement deletion of the yeast Hsp110 (Figure 6-2.A). These results could be due to poor expression or stability of the Hsc70cb protein or because the *D. melanogaster* protein was not contributing to the yeast chaperone network. To answer this question, FLAG-tagged Sse1 or Hsc70cb proteins were expressed in *sse1Δ* cells and a FLAG immunoprecipitation was used to assess the ability of each Hsp110 protein to interact with the yeast cytosolic Hsp70 (Ssa/Ssb) proteins (Figure 6-2.B). Whereas Hsp70 co-immunoprecipitated with 66% of Sse1, Hsp70 only co-immunoprecipitated with 18% of Hsc70cb (Figure 6-2.C). The slow growth phenotype observed for the *sse1Δ* cells complemented with *Hsc70cb* was likely due to the inability of the fly protein to interact with the yeast Hsp70 proteins. These results indicate that the Hsc70cb cannot functionally complement the deletion of the yeast Hsp110 proteins.



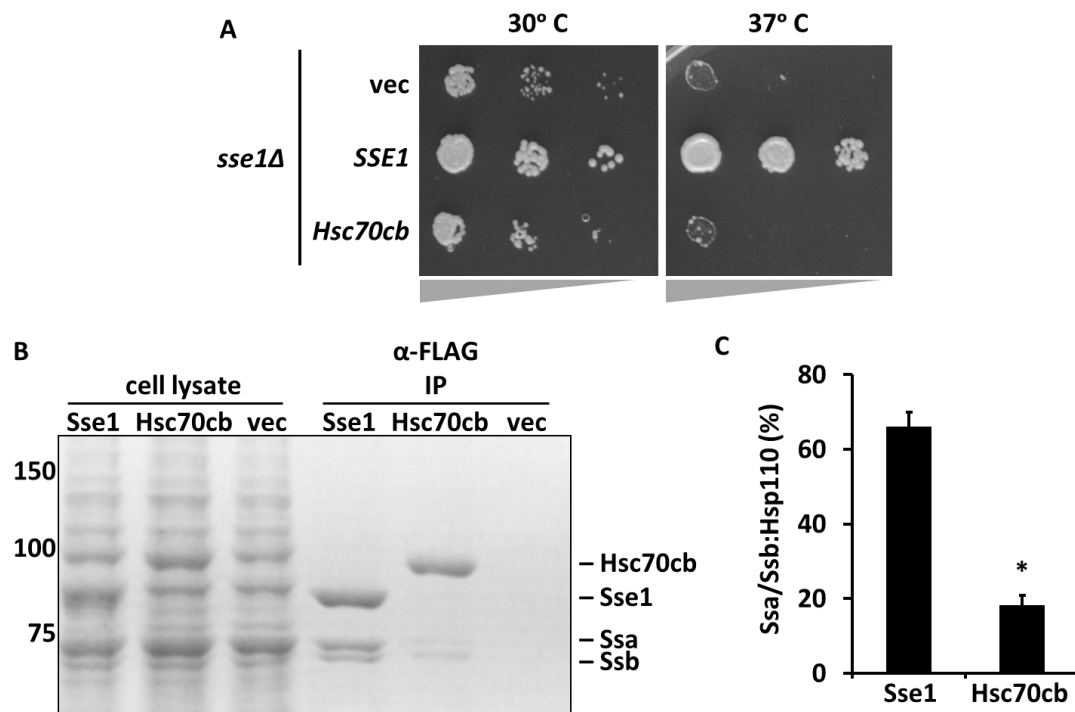


**Figure 6-2. Hsp70cb does not complement an *sse1Δ* or interact with the yeast Hsp70s.** A. Serial dilution plating of *sse1Δ* cells complemented with the *SSE1* or *Hsc70cb* alleles expressed from a *p413TEF* vector and cultured at the indicated temperatures. Wedges below images represent relative cell density. B. Co-immunoprecipitation experiments using FLAG-tagged Hsp110 proteins were performed to assess interactions with the yeast Ssa and Ssb proteins. Samples were analyzed via Coomassie stain on an SDS-PAGE. C. Quantitative analysis of band densities in (B). Error bars indicate  $\pm$  standard deviation and  $*=p<0.05$ .

Hsc70cb was tested for its ability to function as a nucleotide exchange factor using recombinant protein purified from *E. coli* (Figure 6-3.A) (Figure 6-4). Human Hsc70 (HSPA8) had a high level of nucleotide exchange in the presence of Hsc70cb. In fact the fly Hsp110 protein was a more robust NEF when compared with Sse1. After ensuring that the purified Hsc70cb was NEF-functional, the holdase activity of Hsc70cb could be assessed. Due to their high degree of conservation, I expected that Hsc70cb would possess substrate binding function similar to other Hsp110 chaperones, including those of yeast and mammals (30, 106, 107, 111). I measured its ability to prevent the aggregation of chemically denatured firefly luciferase (FFL) using an established assay system (134). Hsc70cb prevented the aggregation of FFL to a level that was comparable to SSE1 establishing that Hsc70cb maintains the holdase function that is characteristic of Hsp110 chaperones.

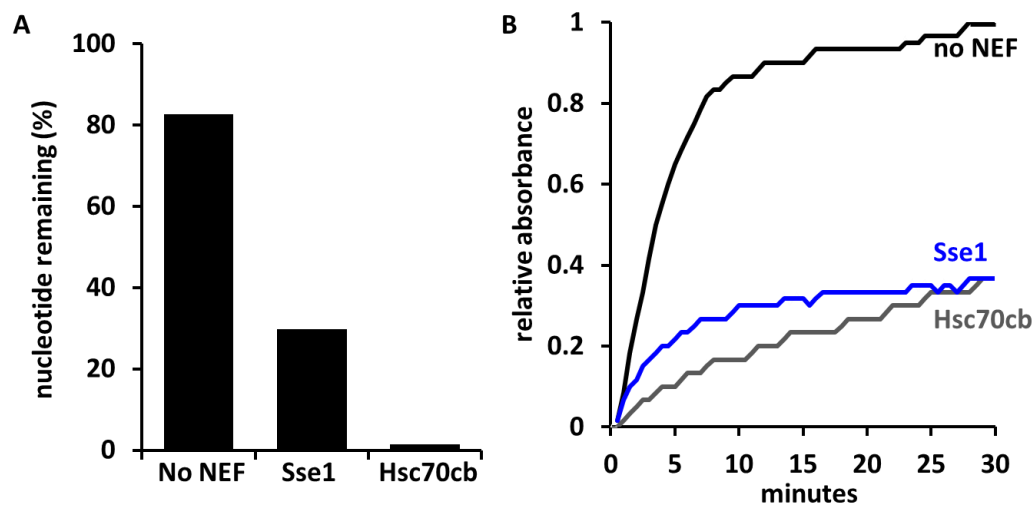


**Figure 6-3. Substrate holding function is conserved in Hsp70cb.** A. Nucleotide exchange activity assays using HSPA8 (Hsp70) pre-bound to  $\alpha$ -<sup>32</sup>P-ATP in the absence of NEF, or in the presence of Hsc70cb or Sse1 for 15 min. B. Substrate aggregation experiments conducted using chemically denatured CS (200 nM) diluted into refolding buffer without chaperone, with Hsc70cb (400 nM), or with Sse1 (400 nM).

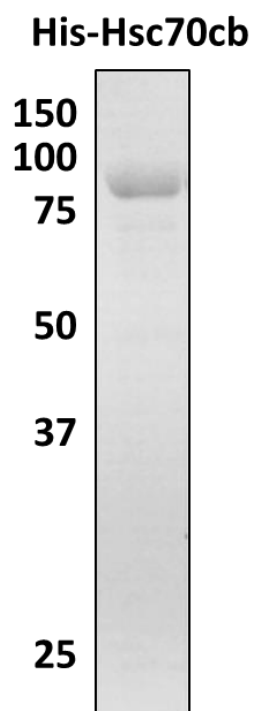


**Figure 6-4. Recombinant protein purification of Hexa-histidine tagged Hsc70cb.** A. SDS-PAGE of 3  $\mu$ g of recombinant His<sub>6</sub>-Hsc70cb purified from *E. coli* visualized by Coomassie stain.

## Discussion

Initially, I proposed screening Hsc70cb SBD mutants by expressing the fly proteins in *sse1Δ* yeast cells. Given that the substrate binding defective mutants cannot complement the heat sensitivity phenotype in this strain, this could be a quick and useful read-out to screen mutants. Hsc70cb cannot complement an *Sse1* deletion and cannot interact with the yeast cytosolic *Ssa/Ssb*; therefore it is not possible to conduct this screen or study how Hsc70cb substrate interaction might contribute to a chaperone network *in vivo* using yeast cells their chaperone networks. The Hsc70cb chaperone will have to be characterized mechanistically *in vitro* and functionally characterized in the fruit fly. To study the substrate binding function of Hsc70cb, I propose several mutants that target the SBD of the protein (Figure 6-4). Hsc70cb<sub>sbd</sub> is a mutant that is analogous to the *Sse1*<sub>sbd</sub> characterized in Chapter 5. Hsc70cb<sub>sbd9</sub> has two additional residue substitutions at positions V401 and W403 that target the putative binding site located within SBD- $\beta$  stand  $\beta_1$  and L<sub>1,2</sub> (Figure 6-1.B) (109). While the *Sse1*-RFA mutant still needs to further characterized to determine its substrate binding capacity (Chapter 5), the fact that it demonstrated deficiencies in the clearance of misfolded protein make this a suitable candidate to test in the polyglutamine Htt fly model. Once the defect is mechanistically defined for the C-terminus tag, this information can be used to study Hsc70cb. The proposed mutants with internal deletions are based on the known *Sse1* crystal structures as well as literature that has characterized Hsp110 substrate binding *in vivo* (107) (124) (60) (104) (109). The mutants proposed here can be tested for holdase function using the aggregation assay I established (Chapter 3 and Figure 6-3.B). Developing mutants of Hsc70cb which are defective in specific functions and comparing those mutants to wild-type or NEF defective proteins will help further our understanding of the role that Hsp110 is playing in modulating the progression of the Huntington model of disease.

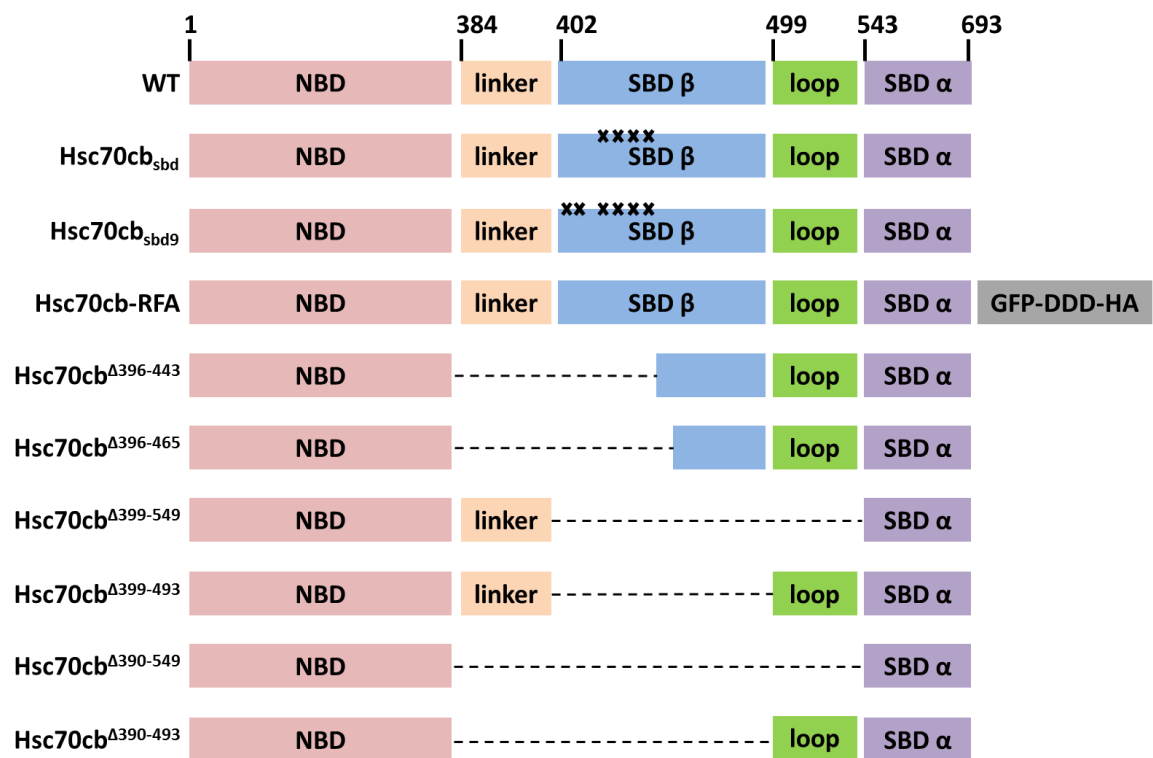


**Figure 6-4. Proposed mutants to characterize the substrate binding function of Hsc70cb while retaining the NEF function.** These Hsc70cb mutants target the SBD-β domain of the protein with either targeted residue substitutions (depicted as a black x) or internal deletions (depicted as a dotted line).

Recently, the Hsp70, Hsp40, and Hsp110 chaperone machine has been established as a powerful metazoan disaggregase machine with the capacity to resolubilize proteins (54, 110, 111, 155). Hsp110 proteins possess distinct molecular activities which include driving the nucleotide-dependent Hsp70 as well as its independent substrate binding domain. These characteristics make it a worthy chaperone to study in regard to neurodegenerative disorders and their causative cytotoxic proteins. In a screen conducted by Dr. Sheng Zhang, he discovered that Hsp110 alleviates the degenerative effects of aggregate formation by mutant Htt in *D. melanogaster* (125). Despite being implicated in this and other amyloid disease models, Hsp110 has not been characterized for its physiological role or how it may be contributing to protein quality control. It remains unknown how the two distinct functions of Hsp110 contribute to neuronal protection. The knowledge gained from this project can be applied to test whether the NEF or SBD function of Hsp110 is important in modifying the progression of polyglutamine Htt based degeneration in the fly.

## **Chapter 7: Discussion**



## Summary

In this thesis, I present an analysis of the functions conferred by the substrate binding domain of Hsp110 chaperones. In chapter 3, a novel technique is described which is used to characterize the molecular dynamics of large protein complexes such as protein aggregates. I illustrate how a microplate reader can be used to obtain signals comparable to right angle light scattering, which typically requires a fluorimeter with a stirrable, temperature-controlled cell holder. The method presented uses less protein and reagents, with the advantage of being able to test multiple conditions in parallel. This account is an alternative method that can detect formation of rhodanese and citrate synthase aggregates as well as the differential prevention of aggregate formation by the molecular chaperone Sse1 with the same sensitivity as traditional methods of light scattering. Chapter 4 builds on this technological development to characterize the substrate chaperoning capacity of Sse1, the yeast Hsp110, through biochemical analysis. Furthermore, the work presented defines, for the first time, the contribution of Sse1 substrate binding to the maintenance of cellular proteostasis. The work presented in chapter 5 characterized a fusion protein of Sse1 which contained a regulated fluorescence affinity tag. I anticipated that this protein fusion would render the substrate binding domain of Sse1 non-functional, however several lines of evidence presented in the chapter suggest that the SBD may remain competent while the carboxyl-terminal fusion interferes with a role for Sse1 in targeting substrates for degradation. Further characterization will have to be completed to determine if the fusion protein is in fact inhibited for SBD function or an alternative Sse1 role or interaction. Finally, Chapter 6 established that the fruit fly Hsc70cb behaves like a canonical Hsp110 with regard to interaction with Hsp70 and its ability to induce nucleotide exchange from the chaperone. Additionally the data presented demonstrated that Hsc70cb can function as a holdase to chaperone unfolded polypeptides. This creates a platform upon which Hsp110 functions can be probed in a model for polyglutamine-mediated neurodegeneration in flies.

## Hsp110 as a nucleotide exchange factor and a substrate chaperone

Among the eukaryotic NEFs, which include the mitochondrial GrpE, and the cytosolic HspBP1, and BAG families, the Hsp110 classes distinctively possess a substrate binding domain and therefore are unique in their ability to interact with unfolded polypeptides. The nucleotide exchange function of Hsp110 proteins has been extensively characterized (44, 45, 105, 152). The potent NEF activity of these proteins is widely accepted as the driving force behind many Hsp70-mediated functions. Previous work has characterized the substrate binding function of Hsp110 chaperones. Prior to this study, it was known that Sse1 as well as mammalian Hsp110 can bind unfolded polypeptides *in vitro* and this function is carried out by the substrate binding domain (30). The specific interaction was localized to the SBD  $\beta$  by deletion mutagenesis (60, 106, 107, 109). Prior to this study a mutant of any Hsp110 protein that inhibited substrate interactions while retaining the NEF function had not been identified therefore the substrate binding function was never characterized *in vivo*. C-terminal truncations produce unstable proteins that cannot interact with Hsp70 to induce nucleotide exchange because this interaction is partially mediated by the SBD  $\alpha$  of Hsp110 (45, 60). Separating these two Hsp110 roles was integral to understanding the role each function was playing. Furthermore, by separating the NEF and SBD activities it was possible to study how each contributes to chaperone complexes.

Based on work published by other labs, I created a mutant that targeted the putative peptide binding site of Sse1 (60). The mutant contained four amino acid substitutions within the Sse1 SBD  $\beta$ . For the first time a stable and NEF functional protein was available to characterize Sse1 holdase function independent of its other roles. The SBD defective mutant, Sse1<sub>sbd</sub>, was tested for its ability to complement the established slow growth phenotype of *sse1 $\Delta$*  cells. Sse1<sub>sbd</sub> was not able to rescue the growth sensitivity under specific proteomic stressors such as heat and formamide. Moreover, the Sse1<sub>sbd</sub> protein was able to rescue nonviable *sse1 $\Delta$ sse2 $\Delta$*  cells but was insufficient to rescue those cells

at elevated temperatures likely due to the absence of Sse2, In cells that expressed SSE2, with an intact NEF and SBD, some Hsp110 activity was providing additional support to the chaperone network. This was striking evidence that substrate binding by Sse proteins is required under specific stresses.

### **Hsp110 contribution to Hsp70 functions**

This study assessed the contributions of NEF and SBD activity of Hsp110 in Hsp70-mediated chaperone functions. In the absence of Sse1 function the HSR is activated even if cells are grown under optimal conditions likely because of general protein misfolding that is occurring (131, 132). Interestingly, when cells were grown under optimal conditions, the NEF-defective Sse1 strain demonstrated high activation of the HSR indicating that those cells were under proteomic stress due to the non-functional *SSE1* allele they were expressing. I tested the activation of the HSR in cells that carried an Sse1 with proper NEF activity but deficient in substrate interactions (chapter 4). Cells expressing the substrate binding deficient *sse1<sub>sbd</sub>* also demonstrated an activation of the HSR, but it was not as robust. These results are evidence that the Sse1 SBD partially contributes to proteome maintenance but not to the extent that NEF function contributes. Another recognized Sse1 role is its requirement in complex with Hsp70 and Hsp90 to promote maturation of protein clients. During cell wall stress, the cooperative Hsp110-Hsp70-Hsp90 complex is required for the maturation of the Slr2 kinase which signals through the cell integrity pathway and activates the transcription factors SBF and Rlm1 (161). In the same way, maturation of the glucocorticoid receptor (GR) requires Hsp110-Hsp70-Hsp90 complex (114). A mature GR can activate the transcription of genes with GR elements (GRE) in the promoter. I used the GR with GRE-*lacZ* system to assess the extent to which the Sse1 NEF or SBD activities supplemented this Hsp70-Hsp90 mediated role. I hypothesized that Sse1, through its holdase function, along with Hsp70 would maintain substrate in a competent state for Hsp90 activities, but the data indicate that the Sse1 NEF activity played the predominant role in GR

maturation. In conclusion, the Hsp70-mediated Sse1 roles we tested showed that the SBD functions contributes minimally to the tasks of the chaperone complex. Although I observed striking phenotypes in the growth of cells expressing the SBD defective mutant under proteomic stress, this could be due to a slight decrease in efficiency across multiple Sse1 or Hsp70 complex roles. It could be that the slight deficiency across multiple functions compounds to produce a prominent growth inhibition when the proteome is challenged.

In collaboration with Nadinath Nillegoda and the Bukau laboratory in Heidelberg, Germany, we tested how the Sse1 SBD might contribute to the disaggregating and refolding function of the Hsp70-Hsp40-Hsp110 machine. These *in vitro* experiments demonstrated that the Sse1 SBD is not required for this function. It seems that the nucleotide exchange capacity of Sse1 is sufficient to drive the protein folding machine. Previously published data are contradictory regarding whether or not the Hsp110 can disaggregate proteins *in vitro* collaboratively with Hsp40 and in the absence of Hsp70. Matoo et. al. have published reports that human Hsp110 (HSP105 and Apg2) can act with Hsp40 in the absence of Hsp70 to effectively refold denatured proteins and solubilize aggregates (111). This activity would surely require substrate binding by the Hsp110 chaperone. Contradicting this model, other published studies indicate that Hsp110 cannot function to disaggregate or refold proteins in the absence of Hsp70 (110, 155). They propose that it is through the Hsp110 NEF function that the Hsp70-Hsp40-Hsp110 complex tackles protein aggregates. If Hsp110 can function as a disaggregase independent of Hsp70, it is reasonable to predict that the SBD function would be required to interact with aggregated substrates. Along these lines, I did not explore the role that Sse1 might be playing in repairing damaged proteins that are unfolded or worse, have segregated into aggregates. Analysis of disaggregation and refolding conducted *in vivo* would address this question. There is still much to learn about the function of Hsp110 disaggregase activity and if the SBD function plays any role.

The extent to which the substrate binding function of Sse1 is contributing to *de novo* protein folding remains unexplored in other Hsp70 roles. Yeast possesses two distinct cytosolic yeast Hsp70

systems. Whereas the SSA proteins are primarily involved in the rescue of stress denatured proteins and helping cells tolerate stress, Ssb1/Ssb2 (SSB) play a major role in folding nascent polypeptides and are dedicated to assisting protein biogenesis due to their localization to the ribosome (176). Once SSB has released the ribosomal complex and is still substrate-bound, it interacts with Sse1 to induce nucleotide cycling and peptide folding (83, 84). *sse1Δ* cells demonstrate growth sensitivity in the presence of translation inhibitors hygromycin and cycloheximide (176). Additionally, *sse1Δ* cells display high degree of overall protein aggregation which is increased further upon the deletion of the nascent-polypeptide associated complex (NAC) which is functionally connected to SSB-mediated protein folding (177). The NEF Snl1, a Bag-1 protein that is tethered to the endoplasmic reticulum (ER) membrane, interacts with SSB in complex with the ribosome potentially to promote the nucleotide exchange in SSB (82). Fes1, another abundant cytosolic NEF does not interact with SSB and only forms a complex with Ssa proteins, (82, 132). The distinct post-ribosomal interactions of Sse1 suggest a role in which this NEF contributes to folding or delivery of SSB substrates. It remains to be explored whether Sse1 binds unfolded nascent chains while also interacting with SSB to induce nucleotide cycling during *de novo* folding. The study discussed in this thesis tested the role of Sse1, focusing on the substrate interaction function, in assisting the maturation of glucocorticoid receptor via Hsp90. Sse1 has been implicated in in the processing or maturation of other yeast clients. For example, Sse1 can aid in the translocation of the yeast mating pheromone  $\text{pp}\alpha\text{F}$ , in maintaining the v-Src tyrosine kinase properly folded, and maturation of the Slk2 kinase via an Hsp70-Hsp90 interaction (44, 142, 161). While the experiments testing the ability of *sse1<sub>sbd</sub>* or *SSE1-RFA* strains to activate the glucocorticoid receptor did not demonstrate a striking defect, I cannot rule out that the SBD or C-terminus of Sse1 plays a role in maturation of other protein clients.

Evidence suggests that Sse1 plays a major role in modulating the ubiquitination of Hsp70 substrates that are irreparable. Sse1 is required for proper ubiquitination of misfolded cytoplasmic substrates such as truncated Gnd1 (tGnd1), the mutant vacuolar protease CPY (CPY<sup>†</sup>), unstable DHFR

mutants, and the artificially ubiquitinated substrate Ub<sub>V76</sub>-Ura3 (133, 153). Sse1 is known to associate with the von Hippel-Lindau (VHL) tumor-suppressor protein, when expressed in yeast, to promote its degradation in association with Hsp70 (178). Moreover, Sse1 modulates the activity of the E3 ubiquitin ligases, Ubr1 and San1, *in vivo* (133,153) . I assessed the role that Sse1 plays in targeting misfolded proteins for proteolysis by testing the Sse1<sub>nbd</sub>, Sse1<sub>sbd</sub>, and the Sse1-RFA mutants in their ability to degrade CPY<sup>+</sup>-GFP. The Sse1<sub>sbd</sub> mutant displayed proper clearance of the misfolded substrate, whereas Sse1<sub>nbd</sub> and Sse1-RFA could not fulfill this Sse1 function. The results for the Sse1<sub>nbd</sub> strain are expected as this mutant has limited interaction with Hsp70 and therefore cannot participate in a chaperone complex. It was surprising that Sse1-RFA cells demonstrated a defect so distinct from the Sse1<sub>sbd</sub> strain. One explanation could be that the RFA moiety that is fused to Sse1 might interfere with allowing a ubiquitin ligase to access the permanently damaged protein substrate. It is important to note that Fes1 has also been implicated in promoting the degradation of the unstable DHFR mutants, but it plays no role in targeting CPY<sup>+</sup> or Ub<sub>V76</sub>-Ura3 for proteolysis (132, 153). This is evidence that there are functional and substrate distinctions between an Hsp70-Fes1 and an Hsp70-Sse1 complex although these remain undefined. As I have mentioned previously, the substrate binding and interactions have been characterized using model substrates, but it remains unknown which native proteins are Sse1/Hsp110 substrates *in vivo*. The studies cited here and those that will follow are important in defining the subset of proteins within the proteome of eukaryotes that are Hsp110 dependent. Understanding this will further our ability to comprehend the mechanisms by which chaperone networks prevent human disease.

### **The metazoan disaggregase**

After stress, cells need to solubilize and reactivate aggregated proteins. Functional proteins need to be refolded into their native state while terminally damaged proteins need to be cleared from

the cell. Prokaryotes and non-metazoan eukaryotes have a well characterized dissaggregation system which involves a powerful Hsp100 AAA+ ATPase, represented by Hsp104 in yeast (1, 13, 179). Hsp104 recovers proteins from aggregates as it threads polypeptides through the ring formed by the hexamer and delivers these to Hsp70 (26). In concert with Hsp70 and Hsp40, Hsp104 acts a machine that can break polypeptide loose from protein aggregates (1, 180).

Metazoans lack an Hsp100 protein that functions as a dedicated dissagregase which raised doubts about the ability of metazoan cells to clear aggregates. Recent work has established that a metazoan dissagregase composed of Hsp70-Hsp40-Hsp110 can disassemble aggregates and refold proteins (54, 110, 111, 155). Hsp40 targets Hsp70 to damaged substrates and Hsp110 functions as the preferred NEF to trigger aggregate dissolution (53, 110). Hsp110 is represented in mammals as three homologs, Hsp105 $\alpha$ , Apg-1, and Apg-2 and is one of three classes of cytosolic NEFs which include the HspBP1-type and the Bag-type. In parallel to the studies cited, which characterized the dissagregase machine *in vitro*, Hsp105 $\alpha$  knockout mouse cells were impaired in reactivating aggregated heat-denatured luciferase (181). Likewise, a study in *C. elegans* also showed defects in aggregate clearance when Hsp110 was depleted (110). These data indicate that Hsp110 proteins have a distinctive function that other NEFs in metazoans cannot accomplish.

Taking into account that the Hsp100 proteins in bacteria and fungi act in concert with Hsp70 and Hsp40 to create a machine which can “pull” aggregates apart to produce free polypeptides, it is possible that the substrate binding function of Hsp110 chaperones is required to propel this machine. The study presented in chapter 6 forms the basis for this next line of investigation. Using the *D. melanogaster* Hsp110 (Hsc70cb) chaperone mutant collection I proposed, a member of my laboratory, Unekwu Yakubu, is currently addressing this question. Finding mutants of Hsp110 that can isolate the NEF and the SBD functions is imperative to understand the molecular mechanism by which this chaperone modulates aggregates. These mutants can be tested *in vitro* using the aggregation assay described in chapter 3 with a polyglutamine protein substrate or by developing a

dissaggregation and refolding assay. Beyond the biochemical characterization, the Hsc70cb mutants can be used to investigate the role of Hsp110 substrate interactions in the previously characterized fruit fly model polyglutamine-based neurodegeneration (125).

### **Implications of Hsp110 in molecular progression of neurodegeneration**

Cellular proteostasis collapses when cells experience chronic proteotoxic stress and can lead to an accumulation of misfolded proteins. With the progression of age, cells also accumulate mutations that can produce toxic protein species (21, 28). Protein misfolding and aggregation have serious consequences for human disease ranging from many neurodegenerative diseases to diabetes (182). Neurodegeneration in disorders like Alzheimer's (AD), Parkinson's (PD), Huntington's (HD) disease, and Amyotrophic Lateral Sclerosis (ALS) are characterized by protein aggregates or plaques that form in and around neurons (120). *In vitro* and *in vivo* studies have demonstrated that molecular chaperones, particularly Hsp110, can modulate protein aggregation and can lessen the effect of the toxic protein species that cause cellular degeneration (28). Hsp110 proteins have been effective in preventing toxicity caused by hyperphosphorylated tau, polyglutamine proteins, and mutant SOD1 in mice, flies, and nematodes respectively (123-127). Hsp110 association with polyglutamine proteins and SOD1 mutants has been demonstrated in animal models (124) (127). The proteins that cause neurodegenerative disorders are not necessarily similar other than their common  $\beta$ -sheet rich regions that lead to aggregation and form stable amyloid fibrils (120). As mentioned in the previous section, humans do not possess the traditional Hsp100 disaggregase, but there is evidence that the Hsp70-Hsp40-Hsp110 complex can fulfill this role in metazoans.

These discoveries are recent and much is still unknown about the molecular mechanism that Hsp110 alone or in concert with Hsp70 is playing to modulate the effects of these toxic proteins. For example, Hsp110 is able to delay the onset of neurodegeneration by preventing the formation of



plaques, but it remains unclear how this occurs. Does Hsp110 help to fold amyloid-prone proteins to prevent the formation of amyloid plaques? Does Hsp110 act to hold amyloidogenic proteins in a soluble state until other chaperones can perform protein triage? Does Hsp110 promote the degradation of the amyloidogenic proteins directly? If the molecular mechanisms by which this is achieved can be understood, that specific chaperoning activity can be targeted to slow disease progression. Currently no treatments exist which can cure or reverse the impacts of neurodegenerative diseases. An incomplete understanding of molecular chaperones and the mechanisms by which specific substrate damage can be cleared or prevented to reverse proteome damage has resulted in limited therapeutic options.

#### **Hsp110 holdase as a clinical tool**

Finally, HSPs are currently being investigated for their benefits as vaccine adjuvants and are used to deliver antibodies, peptides, and antigens (183). Recent reports have indicated that Hsp110 is an excellent candidate to use when trying to deliver vaccine immunogens. It is particularly the ability of Hsp110 to bind substrate tightly and to chaperone vulnerable proteins that made it useful. Hsp110 can form a chaperone complex with large protein substrates, so researches are exploiting this chaperone function to deliver highly immunogenic cancer vaccines which can suppress tumors (184). For example, the intracellular domain (ICD) of HER-2/neu, an antigen relevant to breast cancer, was used in a complex with Hsp110 to elicit a specific immune response to the ICD without having secondary effects due to the presence of chaperone (185). These therapeutic application of the Hsp110 substrate binding capability have been successful and are currently being utilized in clinical trials (186). In conclusion, Sse1/Hsp110 are worthy candidates to explore eukaryotic proteome maintenance for their capacity of modulate disease as well as their potential use to chaperone substrates that need to be delivered as therapies.

## Bibliography

1. Lee, J., J. H. Kim, A. B. Biter, B. Sielaff, S. Lee, and F. T. Tsai. 2013. Heat shock protein (Hsp) 70 is an activator of the Hsp104 motor. *Proc Natl Acad Sci U S A* 110: 8513-8518.
2. Drummond, D. A., and C. O. Wilke. 2009. The evolutionary consequences of erroneous protein synthesis. *Nat Rev Genet* 10: 715-724.
3. Hartl, F. U., A. Bracher, and M. Hayer-Hartl. 2011. Molecular chaperones in protein folding and proteostasis. *Nature* 475: 324-332.
4. Dill, K. A., and J. L. MacCallum. 2012. The protein-folding problem, 50 years on. *Science* 338: 1042-1046.
5. Hartl, F. U., and M. Hayer-Hartl. 2009. Converging concepts of protein folding in vitro and in vivo. *Nat Struct Mol Biol* 16: 574-581.
6. Frydman, J. 2001. Folding of newly translated proteins in vivo: the role of molecular chaperones. *Annual review of biochemistry* 70: 603-647.
7. Warner, J. R. 1999. The economics of ribosome biosynthesis in yeast. *Trends in biochemical sciences* 24: 437-440.
8. von der Haar, T. 2008. A quantitative estimation of the global translational activity in logarithmically growing yeast cells. *BMC Syst Biol* 2: 87.
9. Pechmann, S., F. Willmund, and J. Frydman. 2013. The ribosome as a hub for protein quality control. *Mol Cell* 49: 411-421.
10. Solis, E. J., J. P. Pandey, X. Zheng, D. X. Jin, P. B. Gupta, E. M. Airoidi, D. Pincus, and V. Denic. 2016. Defining the Essential Function of Yeast Hsf1 Reveals a Compact Transcriptional Program for Maintaining Eukaryotic Proteostasis. *Mol Cell* 63: 60-71.
11. Duttler, S., S. Pechmann, and J. Frydman. 2013. Principles of cotranslational ubiquitination and quality control at the ribosome. *Mol Cell* 50: 379-393.

12. Zietkiewicz, S., J. Krzewska, and K. Liberek. 2004. Successive and synergistic action of the Hsp70 and Hsp100 chaperones in protein disaggregation. *J Biol Chem* 279: 44376-44383.
13. Parsell, D. A., A. S. Kowal, M. A. Singer, and S. Lindquist. 1994. Protein disaggregation mediated by heat-shock protein Hsp104. *Nature* 372: 475-478.
14. Abrams, J. L., and K. A. Morano. 2013. Coupled assays for monitoring protein refolding in *Saccharomyces cerevisiae*. *J Vis Exp*: e50432.
15. Dokladny, K., M. N. Zuhl, M. Mandell, D. Bhattacharya, S. Schneider, V. Deretic, and P. L. Moseley. 2013. Regulatory coordination between two major intracellular homeostatic systems: heat shock response and autophagy. *J Biol Chem* 288: 14959-14972.
16. Park, S. H., N. Bolender, F. Eisele, Z. Kostova, J. Takeuchi, P. Coffino, and D. H. Wolf. 2007. The cytoplasmic Hsp70 chaperone machinery subjects misfolded and endoplasmic reticulum import-incompetent proteins to degradation via the ubiquitin-proteasome system. *Molecular biology of the cell* 18: 153-165.
17. Esser, C., S. Alberti, and J. Hohfeld. 2004. Cooperation of molecular chaperones with the ubiquitin/proteasome system. *Biochimica et biophysica acta* 1695: 171-188.
18. Buchberger, A., B. Bukau, and T. Sommer. 2010. Protein quality control in the cytosol and the endoplasmic reticulum: brothers in arms. *Mol Cell* 40: 238-252.
19. Lanneau, D., G. Wettstein, P. Bonniaud, and C. Garrido. 2010. Heat shock proteins: cell protection through protein triage. *ScientificWorldJournal* 10: 1543-1552.
20. Kim, Y. E., M. S. Hipp, A. Bracher, M. Hayer-Hartl, and F. U. Hartl. 2013. Molecular chaperone functions in protein folding and proteostasis. *Annual review of biochemistry* 82: 323-355.
21. Balch, W. E., R. I. Morimoto, A. Dillin, and J. W. Kelly. 2008. Adapting proteostasis for disease intervention. *Science* 319: 916-919.

22. Amoros, M., and F. Estruch. 2001. Hsf1p and Msn2/4p cooperate in the expression of *Saccharomyces cerevisiae* genes HSP26 and HSP104 in a gene- and stress type-dependent manner. *Molecular microbiology* 39: 1523-1532.
23. Heldens, L., S. M. Hensen, C. Onnekink, S. T. van Genesen, R. P. Dirks, and N. H. Lubsen. 2011. An atypical unfolded protein response in heat shocked cells. *PloS one* 6: e23512.
24. Zheng, X., J. Krakowiak, N. Patel, A. Beyzavi, J. Ezike, A. S. Khalil, and D. Pincus. 2016. Dynamic control of Hsf1 during heat shock by a chaperone switch and phosphorylation. *Elife* 5.
25. Ankar, J., and L. Sistonen. 2011. Regulation of HSF1 function in the heat stress response: implications in aging and disease. *Annual review of biochemistry* 80: 1089-1115.
26. Hodson, S., J. J. Marshall, and S. G. Burston. 2012. Mapping the road to recovery: the ClpB/Hsp104 molecular chaperone. *Journal of structural biology* 179: 161-171.
27. Yu, A., Y. Shibata, B. Shah, B. Calamini, D. C. Lo, and R. I. Morimoto. 2014. Protein aggregation can inhibit clathrin-mediated endocytosis by chaperone competition. *Proc Natl Acad Sci U S A* 111: E1481-1490.
28. Morimoto, R. I. 2008. Proteotoxic stress and inducible chaperone networks in neurodegenerative disease and aging. *Genes Dev* 22: 1427-1438.
29. Roman, E., C. Moreno, and D. Young. 1994. Mapping of Hsp70-binding sites on protein antigens. *European journal of biochemistry / FEBS* 222: 65-73.
30. Goeckeler, J. L., A. P. Petruso, J. Aguirre, C. C. Clement, G. Chiosis, and J. L. Brodsky. 2008. The yeast Hsp110, Sse1p, exhibits high-affinity peptide binding. *FEBS letters* 582: 2393-2396.
31. Chappell, T. G., B. B. Konforti, S. L. Schmid, and J. E. Rothman. 1987. The ATPase core of a clathrin uncoating protein. *J Biol Chem* 262: 746-751.
32. Gragerov, A., L. Zeng, X. Zhao, W. Burkholder, and M. E. Gottesman. 1994. Specificity of DnaK-peptide binding. *Journal of molecular biology* 235: 848-854.

33. Davis, J. E., C. Voisine, and E. A. Craig. 1999. Intragenic suppressors of Hsp70 mutants: interplay between the ATPase- and peptide-binding domains. *Proc Natl Acad Sci U S A* 96: 9269-9276.
34. Zhuravleva, A., E. M. Clerico, and L. M. Gierasch. 2012. An interdomain energetic tug-of-war creates the allosterically active state in Hsp70 molecular chaperones. *Cell* 151: 1296-1307.
35. Yang, J., M. Nune, Y. Zong, L. Zhou, and Q. Liu. 2015. Close and Allosteric Opening of the Polypeptide-Binding Site in a Human Hsp70 Chaperone BiP. *Structure* 23: 2191-2203.
36. Zhuravleva, A., and L. M. Gierasch. 2015. Substrate-binding domain conformational dynamics mediate Hsp70 allostery. *Proc Natl Acad Sci U S A* 112: E2865-2873.
37. Zhang, P., J. I. Leu, M. E. Murphy, D. L. George, and R. Marmorstein. 2014. Crystal structure of the stress-inducible human heat shock protein 70 substrate-binding domain in complex with peptide substrate. *PloS one* 9: e103518.
38. Gassler, C. S., T. Wiederkehr, D. Brehmer, B. Bukau, and M. P. Mayer. 2001. Bag-1M accelerates nucleotide release for human Hsc70 and Hsp70 and can act concentration-dependent as positive and negative cofactor. *J Biol Chem* 276: 32538-32544.
39. Raviol, H., H. Sadlish, F. Rodriguez, M. P. Mayer, and B. Bukau. 2006. Chaperone network in the yeast cytosol: Hsp110 is revealed as an Hsp70 nucleotide exchange factor. *Embo J* 25: 2510-2518.
40. Dragovic, Z., S. A. Broadley, Y. Shomura, A. Bracher, and F. U. Hartl. 2006. Molecular chaperones of the Hsp110 family act as nucleotide exchange factors of Hsp70s. *EMBO J* 25: 2519-2528.
41. Mayer, M. P., T. Laufen, K. Paal, J. S. McCarty, and B. Bukau. 1999. Investigation of the interaction between DnaK and DnaJ by surface plasmon resonance spectroscopy. *Journal of molecular biology* 289: 1131-1144.

42. Craig, E. A., P. Huang, R. Aron, and A. Andrew. 2006. The diverse roles of J-proteins, the obligate Hsp70 co-chaperone. *Reviews of physiology, biochemistry and pharmacology* 156: 1-21.
43. Alderson, T. R., J. H. Kim, and J. L. Markley. 2016. Dynamical Structures of Hsp70 and Hsp70-Hsp40 Complexes. *Structure* 24: 1014-1030.
44. Shaner, L., H. Wegele, J. Buchner, and K. A. Morano. 2005. The yeast Hsp110 Sse1 functionally interacts with the Hsp70 chaperones Ssa and Ssb. *J Biol Chem* 280: 41262-41269.
45. Shaner, L., R. Sousa, and K. A. Morano. 2006. Characterization of Hsp70 binding and nucleotide exchange by the yeast Hsp110 chaperone Sse1. *Biochemistry* 45: 15075-15084.
46. Cyr, D. M. 2008. Swapping nucleotides, tuning Hsp70. *Cell* 133: 945-947.
47. Andreasson, C., J. Fiaux, H. Rampelt, S. Druffel-Augustin, and B. Bukau. 2008. Insights into the structural dynamics of the Hsp110-Hsp70 interaction reveal the mechanism for nucleotide exchange activity. *Proc Natl Acad Sci U S A* 105: 16519-16524.
48. Kityk, R., J. Kopp, I. Sinning, and M. P. Mayer. 2012. Structure and dynamics of the ATP-bound open conformation of Hsp70 chaperones. *Mol Cell* 48: 863-874.
49. Hennessy, F., W. S. Nicoll, R. Zimmermann, M. E. Cheetham, and G. L. Blatch. 2005. Not all J domains are created equal: implications for the specificity of Hsp40-Hsp70 interactions. *Protein Sci* 14: 1697-1709.
50. Tsai, J., and M. G. Douglas. 1996. A conserved HPD sequence of the J-domain is necessary for YDJ1 stimulation of Hsp70 ATPase activity at a site distinct from substrate binding. *J Biol Chem* 271: 9347-9354.
51. Jiang, J., E. G. Maes, A. B. Taylor, L. Wang, A. P. Hinck, E. M. Lafer, and R. Sousa. 2007. Structural basis of J cochaperone binding and regulation of Hsp70. *Mol Cell* 28: 422-433.
52. Cyr, D. M. 1995. Cooperation of the molecular chaperone Ydj1 with specific Hsp70 homologs to suppress protein aggregation. *FEBS letters* 359: 129-132.

53. Kampinga, H. H., and E. A. Craig. 2010. The HSP70 chaperone machinery: J proteins as drivers of functional specificity. *Nat Rev Mol Cell Biol* 11: 579-592.
54. Nillegoda, N. B., J. Kirstein, A. Szlachcic, M. Berynsky, A. Stank, F. Stengel, K. Arnsburg, X. Gao, A. Scior, R. Aebersold, D. L. Guilbride, R. C. Wade, R. I. Morimoto, M. P. Mayer, and B. Bukau. 2015. Crucial HSP70 co-chaperone complex unlocks metazoan protein disaggregation. *Nature* 524: 247-251.
55. Wall, D., M. Zylicz, and C. Georgopoulos. 1995. The conserved G/F motif of the DnaJ chaperone is necessary for the activation of the substrate binding properties of the DnaK chaperone. *J Biol Chem* 270: 2139-2144.
56. Li, J., X. Qian, and B. Sha. 2003. The crystal structure of the yeast Hsp40 Ydj1 complexed with its peptide substrate. *Structure* 11: 1475-1483.
57. Johnson, J. L., and E. A. Craig. 2001. An essential role for the substrate-binding region of Hsp40s in *Saccharomyces cerevisiae*. *J Cell Biol* 152: 851-856.
58. Ha, J. H., and D. B. McKay. 1994. ATPase kinetics of recombinant bovine 70 kDa heat shock cognate protein and its amino-terminal ATPase domain. *Biochemistry* 33: 14625-14635.
59. Liu, Q., and W. A. Hendrickson. 2007. Insights into Hsp70 chaperone activity from a crystal structure of the yeast Hsp110 Sse1. *Cell* 131: 106-120.
60. Polier, S., Z. Dragovic, F. U. Hartl, and A. Bracher. 2008. Structural basis for the cooperation of Hsp70 and Hsp110 chaperones in protein folding. *Cell* 133: 1068-1079.
61. Wu, C. C., V. Naveen, C. H. Chien, Y. W. Chang, and C. D. Hsiao. 2012. Crystal structure of DnaK protein complexed with nucleotide exchange factor GrpE in DnaK chaperone system: insight into intermolecular communication. *J Biol Chem* 287: 21461-21470.
62. Sharp, A., R. I. Cutress, P. W. Johnson, G. Packham, and P. A. Townsend. 2009. Short peptides derived from the BAG-1 C-terminus inhibit the interaction between BAG-1 and HSC70 and decrease breast cancer cell growth. *FEBS letters* 583: 3405-3411.

63. Shomura, Y., Z. Dragovic, H. C. Chang, N. Tzvetkov, J. C. Young, J. L. Brodsky, V. Guerriero, F. U. Hartl, and A. Bracher. 2005. Regulation of Hsp70 function by HspBP1: structural analysis reveals an alternate mechanism for Hsp70 nucleotide exchange. *Mol Cell* 17: 367-379.
64. Liu, Y., L. M. Gierasch, and I. Bahar. 2010. Role of Hsp70 ATPase domain intrinsic dynamics and sequence evolution in enabling its functional interactions with NEFs. *PLoS Comput Biol* 6.
65. Verghese, J., J. Abrams, Y. Wang, and K. A. Morano. 2012. Biology of the heat shock response and protein chaperones: budding yeast (*Saccharomyces cerevisiae*) as a model system. *Microbiol Mol Biol Rev* 76: 115-158.
66. Nelson, R. J., M. F. Heschl, and E. A. Craig. 1992. Isolation and characterization of extragenic suppressors of mutations in the SSA hsp70 genes of *Saccharomyces cerevisiae*. *Genetics* 131: 277-285.
67. Becker, J., W. Walter, W. Yan, and E. A. Craig. 1996. Functional interaction of cytosolic hsp70 and a DnaJ-related protein, Ydj1p, in protein translocation in vivo. *Mol Cell Biol* 16: 4378-4386.
68. Gasch, A. P., P. T. Spellman, C. M. Kao, O. Carmel-Harel, M. B. Eisen, G. Storz, D. Botstein, and P. O. Brown. 2000. Genomic expression programs in the response of yeast cells to environmental changes. *Molecular biology of the cell* 11: 4241-4257.
69. Lopez, N., J. Halladay, W. Walter, and E. A. Craig. 1999. SSB, encoding a ribosome-associated chaperone, is coordinately regulated with ribosomal protein genes. *Journal of bacteriology* 181: 3136-3143.
70. Walsh, P., D. Bursac, Y. C. Law, D. Cyr, and T. Lithgow. 2004. The J-protein family: modulating protein assembly, disassembly and translocation. *EMBO reports* 5: 567-571.
71. Mukai, H., T. Kuno, H. Tanaka, D. Hirata, T. Miyakawa, and C. Tanaka. 1993. Isolation and characterization of SSE1 and SSE2, new members of the yeast HSP70 multigene family. *Gene* 132: 57-66.



72. Kabani, M., J. M. Beckerich, and J. L. Brodsky. 2002. Nucleotide exchange factor for the yeast Hsp70 molecular chaperone Ssa1p. *Mol Cell Biol* 22: 4677-4689.
73. Kabani, M., C. McLellan, D. A. Raynes, V. Guerriero, and J. L. Brodsky. 2002. HspBP1, a homologue of the yeast Fes1 and Sls1 proteins, is an Hsc70 nucleotide exchange factor. *FEBS letters* 531: 339-342.
74. Sonderrmann, H., A. K. Ho, L. L. Listenberger, K. Siegers, I. Moarefi, S. R. Wentz, F. U. Hartl, and J. C. Young. 2002. Prediction of novel Bag-1 homologs based on structure/function analysis identifies Snl1p as an Hsp70 co-chaperone in *Saccharomyces cerevisiae*. *J Biol Chem* 277: 33220-33227.
75. Ho, A. K., G. A. Racznik, E. B. Ives, and S. R. Wentz. 1998. The integral membrane protein snl1p is genetically linked to yeast nuclear pore complex function. *Molecular biology of the cell* 9: 355-373.
76. Sahi, C., J. Kominek, T. Ziegelhoffer, H. Y. Yu, M. Baranowski, J. Marszalek, and E. A. Craig. 2013. Sequential duplications of an ancient member of the DnaJ-family expanded the functional chaperone network in the eukaryotic cytosol. *Mol Biol Evol* 30: 985-998.
77. Schmitt, M., W. Neupert, and T. Langer. 1996. The molecular chaperone Hsp78 confers compartment-specific thermotolerance to mitochondria. *J Cell Biol* 134: 1375-1386.
78. Huang, P., M. Gautschi, W. Walter, S. Rospert, and E. A. Craig. 2005. The Hsp70 Ssz1 modulates the function of the ribosome-associated J-protein Zuo1. *Nat Struct Mol Biol* 12: 497-504.
79. Leidig, C., G. Bange, J. Kopp, S. Amlacher, A. Aravind, S. Wickles, G. Witte, E. Hurt, R. Beckmann, and I. Sinning. 2013. Structural characterization of a eukaryotic chaperone--the ribosome-associated complex. *Nat Struct Mol Biol* 20: 23-28.

80. Peisker, K., D. Braun, T. Wolfle, J. Hentschel, U. Funfschilling, G. Fischer, A. Sickmann, and S. Rospert. 2008. Ribosome-associated complex binds to ribosomes in close proximity of Rpl31 at the exit of the polypeptide tunnel in yeast. *Molecular biology of the cell* 19: 5279-5288.
81. Preissler, S., and E. Deuerling. 2012. Ribosome-associated chaperones as key players in proteostasis. *Trends in biochemical sciences* 37: 274-283.
82. Verghese, J., and K. A. Morano. 2012. A lysine-rich region within fungal BAG domain-containing proteins mediates a novel association with ribosomes. *Eukaryotic cell* 11: 1003-1011.
83. Willmund, F., M. del Alamo, S. Pechmann, T. Chen, V. Albanese, E. B. Dammer, J. Peng, and J. Frydman. 2013. The cotranslational function of ribosome-associated Hsp70 in eukaryotic protein homeostasis. *Cell* 152: 196-209.
84. Yam, A. Y., V. Albanese, H. T. Lin, and J. Frydman. 2005. Hsp110 cooperates with different cytosolic HSP70 systems in a pathway for de novo folding. *J Biol Chem* 280: 41252-41261.
85. Karbstein, K. 2010. Chaperoning ribosome assembly. *J Cell Biol* 189: 11-12.
86. McClellan, A. J., and J. L. Brodsky. 2000. Mutation of the ATP-binding pocket of SSA1 indicates that a functional interaction between Ssa1p and Ydj1p is required for post-translational translocation into the yeast endoplasmic reticulum. *Genetics* 156: 501-512.
87. Deshaies, R. J., B. D. Koch, M. Werner-Washburne, E. A. Craig, and R. Schekman. 1988. A subfamily of stress proteins facilitates translocation of secretory and mitochondrial precursor polypeptides. *Nature* 332: 800-805.
88. Shulga, N., P. Roberts, Z. Gu, L. Spitz, M. M. Tabb, M. Nomura, and D. S. Goldfarb. 1996. In vivo nuclear transport kinetics in *Saccharomyces cerevisiae*: a role for heat shock protein 70 during targeting and translocation. *J Cell Biol* 135: 329-339.

89. Silberstein, S., G. Schlenstedt, P. A. Silver, and R. Gilmore. 1998. A role for the DnaJ homologue Scj1p in protein folding in the yeast endoplasmic reticulum. *J Cell Biol* 143: 921-933.
90. Johnson, N., K. Powis, and S. High. 2013. Post-translational translocation into the endoplasmic reticulum. *Biochimica et biophysica acta* 1833: 2403-2409.
91. Tyson, J. R., and C. J. Stirling. 2000. LHS1 and SIL1 provide a luminal function that is essential for protein translocation into the endoplasmic reticulum. *Embo J* 19: 6440-6452.
92. Nishikawa, S. I., S. W. Fewell, Y. Kato, J. L. Brodsky, and T. Endo. 2001. Molecular chaperones in the yeast endoplasmic reticulum maintain the solubility of proteins for retrotranslocation and degradation. *J Cell Biol* 153: 1061-1070.
93. Saris, N., H. Holkeri, R. A. Craven, C. J. Stirling, and M. Makarow. 1997. The Hsp70 homologue Lhs1p is involved in a novel function of the yeast endoplasmic reticulum, refolding and stabilization of heat-denatured protein aggregates. *J Cell Biol* 137: 813-824.
94. Buck, T. M., L. Plavchak, A. Roy, B. F. Donnelly, O. B. Kashlan, T. R. Kleyman, A. R. Subramanya, and J. L. Brodsky. 2013. The Lhs1/GRP170 chaperones facilitate the endoplasmic reticulum-associated degradation of the epithelial sodium channel. *J Biol Chem* 288: 18366-18380.
95. Schneider, H. C., B. Westermann, W. Neupert, and M. Brunner. 1996. The nucleotide exchange factor MGE exerts a key function in the ATP-dependent cycle of mt-Hsp70-Tim44 interaction driving mitochondrial protein import. *EMBO J* 15: 5796-5803.
96. Schmidt, S., A. Strub, K. Rottgers, N. Zufall, and W. Voos. 2001. The two mitochondrial heat shock proteins 70, Ssc1 and Ssq1, compete for the cochaperone Mge1. *Journal of molecular biology* 313: 13-26.
97. Kang, P. J., J. Ostermann, J. Shilling, W. Neupert, E. A. Craig, and N. Pfanner. 1990. Requirement for hsp70 in the mitochondrial matrix for translocation and folding of precursor proteins. *Nature* 348: 137-143.

98. Mokranjac, D., and W. Neupert. 2009. Thirty years of protein translocation into mitochondria: unexpectedly complex and still puzzling. *Biochimica et biophysica acta* 1793: 33-41.
99. Baumann, F., I. Milisav, W. Neupert, and J. M. Herrmann. 2000. Ecm10, a novel hsp70 homolog in the mitochondrial matrix of the yeast *Saccharomyces cerevisiae*. *FEBS letters* 487: 307-312.
100. Pareek, G., M. Samaddar, and P. D'Silva. 2011. Primary sequence that determines the functional overlap between mitochondrial heat shock protein 70 Ssc1 and Ssc3 of *Saccharomyces cerevisiae*. *J Biol Chem* 286: 19001-19013.
101. Schilke, B., J. Forster, J. Davis, P. James, W. Walter, S. Laloraya, J. Johnson, B. Miao, and E. Craig. 1996. The cold sensitivity of a mutant of *Saccharomyces cerevisiae* lacking a mitochondrial heat shock protein 70 is suppressed by loss of mitochondrial DNA. *J Cell Biol* 134: 603-613.
102. Lutz, T., B. Westermann, W. Neupert, and J. M. Herrmann. 2001. The mitochondrial proteins Ssq1 and Jac1 are required for the assembly of iron sulfur clusters in mitochondria. *Journal of molecular biology* 307: 815-825.
103. Zhu, X., X. Zhao, W. F. Burkholder, A. Gragerov, C. M. Ogata, M. E. Gottesman, and W. A. Hendrickson. 1996. Structural analysis of substrate binding by the molecular chaperone DnaK. *Science* 272: 1606-1614.
104. Schuermann, J. P., J. Jiang, J. Cuellar, O. Llorca, L. Wang, L. E. Gimenez, S. Jin, A. B. Taylor, B. Demeler, K. A. Morano, P. J. Hart, J. M. Valpuesta, E. M. Lafer, and R. Sousa. 2008. Structure of the Hsp110:Hsc70 nucleotide exchange machine. *Mol Cell* 31: 232-243.
105. Andreasson, C., J. Fiaux, H. Rampelt, M. P. Mayer, and B. Bukau. 2008. Hsp110 is a nucleotide-activated exchange factor for Hsp70. *J Biol Chem* 283: 8877-8884.
106. Oh, H. J., X. Chen, and J. R. Subjeck. 1997. Hsp110 protects heat-denatured proteins and confers cellular thermoresistance. *J Biol Chem* 272: 31636-31640.

107. Oh, H. J., D. Easton, M. Murawski, Y. Kaneko, and J. R. Subjeck. 1999. The chaperoning activity of hsp110. Identification of functional domains by use of targeted deletions. *J Biol Chem* 274: 15712-15718.
108. Polier, S., F. U. Hartl, and A. Bracher. 2010. Interaction of the Hsp110 molecular chaperones from *S. cerevisiae* with substrate protein. *Journal of molecular biology* 401: 696-707.
109. Xu, X., E. B. Sarbeng, C. Vorvis, D. P. Kumar, L. Zhou, and Q. Liu. 2012. Unique peptide substrate binding properties of 110-kDa heat-shock protein (Hsp110) determine its distinct chaperone activity. *J Biol Chem* 287: 5661-5672.
110. Rampelt, H., J. Kirstein-Miles, N. B. Nillegoda, K. Chi, S. R. Scholz, R. I. Morimoto, and B. Bukau. 2012. Metazoan Hsp70 machines use Hsp110 to power protein disaggregation. *Embo J* 31: 4221-4235.
111. Mattoo, R. U., S. K. Sharma, S. Priya, A. Finka, and P. Goloubinoff. 2013. Hsp110 is a bona fide chaperone using ATP to unfold stable misfolded polypeptides and reciprocally collaborate with Hsp70 to solubilize protein aggregates. *J Biol Chem* 288: 21399-21411.
112. Nillegoda, N. B., and B. Bukau. 2015. Metazoan Hsp70-based protein disaggregases: emergence and mechanisms. *Front Mol Biosci* 2: 57.
113. Brownridge, P., C. Lawless, A. B. Payapilly, K. Lanthaler, S. W. Holman, V. M. Harman, C. M. Grant, R. J. Beynon, and S. J. Hubbard. 2013. Quantitative analysis of chaperone network throughput in budding yeast. *Proteomics* 13: 1276-1291.
114. Mandal, A. K., P. A. Gibney, N. B. Nillegoda, M. A. Theodoraki, A. J. Caplan, and K. A. Morano. 2010. Hsp110 chaperones control client fate determination in the hsp70-Hsp90 chaperone system. *Molecular biology of the cell* 21: 1439-1448.
115. Gibney, P. A. 2009. The Eukaryotic Cellular Stress Response: Biochemical and Genetic Analyses in *Saccharomyces cerevisiae*. In *Microbiology and Molecular Genetics*. The University of Texas MD Anderson Cancer Center Graduate School of Biomedical Sciences. 228.

116. Broadley, S. A., and F. U. Hartl. 2009. The role of molecular chaperones in human misfolding diseases. *FEBS letters* 583: 2647-2653.
117. Valastyan, J. S., and S. Lindquist. 2014. Mechanisms of protein-folding diseases at a glance. *Dis Model Mech* 7: 9-14.
118. Kumar, V., N. Sami, T. Kashav, A. Islam, F. Ahmad, and M. I. Hassan. 2016. Protein aggregation and neurodegenerative diseases: From theory to therapy. *Eur J Med Chem* 124: 1105-1120.
119. Ross, C. A., and M. A. Poirier. 2004. Protein aggregation and neurodegenerative disease. *Nat Med* 10 Suppl: S10-17.
120. Soto, C. 2003. Unfolding the role of protein misfolding in neurodegenerative diseases. *Nat Rev Neurosci* 4: 49-60.
121. Nolan, M., K. Talbot, and O. Ansorge. 2016. Pathogenesis of FUS-associated ALS and FTD: insights from rodent models. *Acta Neuropathol Commun* 4: 99.
122. Parakh, S., and J. D. Atkin. 2016. Protein folding alterations in amyotrophic lateral sclerosis. *Brain research* 1648: 633-649.
123. Eroglu, B., D. Moskophidis, and N. F. Mivechi. 2010. Loss of Hsp110 leads to age-dependent tau hyperphosphorylation and early accumulation of insoluble amyloid beta. *Mol Cell Biol* 30: 4626-4643.
124. Ishihara, K., N. Yamagishi, Y. Saito, H. Adachi, Y. Kobayashi, G. Sobue, K. Ohtsuka, and T. Hatayama. 2003. Hsp105alpha suppresses the aggregation of truncated androgen receptor with expanded CAG repeats and cell toxicity. *J Biol Chem* 278: 25143-25150.
125. Zhang, S., R. Binari, R. Zhou, and N. Perrimon. 2010. A genomewide RNA interference screen for modifiers of aggregates formation by mutant Huntingtin in *Drosophila*. *Genetics* 184: 1165-1179.

126. Kuo, Y., S. Ren, U. Lao, B. A. Edgar, and T. Wang. 2013. Suppression of polyglutamine protein toxicity by co-expression of a heat-shock protein 40 and a heat-shock protein 110. *Cell Death Dis* 4: e833.
127. Wang, J., G. W. Farr, D. H. Hall, F. Li, K. Furtak, L. Dreier, and A. L. Horwich. 2009. An ALS-linked mutant SOD1 produces a locomotor defect associated with aggregation and synaptic dysfunction when expressed in neurons of *Caenorhabditis elegans*. *PLoS Genet* 5: e1000350.
128. Shaner, L., A. Trott, J. L. Goeckeler, J. L. Brodsky, and K. A. Morano. 2004. The function of the yeast molecular chaperone Sse1 is mechanistically distinct from the closely related hsp70 family. *J Biol Chem* 279: 21992-22001.
129. Mumberg, D., R. Muller, and M. Funk. 1995. Yeast vectors for the controlled expression of heterologous proteins in different genetic backgrounds. *Gene* 156: 119-122.
130. Heffler, J. 2014. Substrate Binding by Sse1 (Hsp110) is important for thermotolerance in *S. cerevisiae*. The University of Houston. 32.
131. Liu, X. D., K. A. Morano, and D. J. Thiele. 1999. The yeast Hsp110 family member, Sse1, is an Hsp90 cochaperone. *J Biol Chem* 274: 26654-26660.
132. Abrams, J. L., J. Verghese, P. A. Gibney, and K. A. Morano. 2014. Hierarchical functional specificity of cytosolic heat shock protein 70 (Hsp70) nucleotide exchange factors in yeast. *J Biol Chem* 289: 13155-13167.
133. Heck, J. W., S. K. Cheung, and R. Y. Hampton. 2010. Cytoplasmic protein quality control degradation mediated by parallel actions of the E3 ubiquitin ligases Ubr1 and San1. *Proc Natl Acad Sci U S A* 107: 1106-1111.
134. Garcia, V. M., V. W. Rowlett, W. Margolin, and K. A. Morano. 2016. Semi-automated microplate monitoring of protein polymerization and aggregation. *Anal Biochem* 508: 9-11.

135. Rauch, J. N., and J. E. Gestwicki. 2014. Binding of human nucleotide exchange factors to heat shock protein 70 (Hsp70) generates functionally distinct complexes in vitro. *J Biol Chem* 289: 1402-1414.
136. Lu, Z., and D. M. Cyr. 1998. The conserved carboxyl terminus and zinc finger-like domain of the co-chaperone Ydj1 assist Hsp70 in protein folding. *J Biol Chem* 273: 5970-5978.
137. Zhi, W., S. J. Landry, L. M. Gierasch, and P. A. Srere. 1992. Renaturation of citrate synthase: influence of denaturant and folding assistants. *Protein Sci* 1: 522-529.
138. Gorovits, B. M., W. A. McGee, and P. M. Horowitz. 1998. Rhodanese folding is controlled by the partitioning of its folding intermediates. *Biochimica et biophysica acta* 1382: 120-128.
139. Buchner, J., H. Grallert, and U. Jakob. 1998. Analysis of chaperone function using citrate synthase as nonnative substrate protein. *Methods Enzymol* 290: 323-338.
140. Kelley, C., Y. Zhang, A. Parhi, M. Kaul, D. S. Pilch, and E. J. LaVoie. 2012. 3-Phenyl substituted 6,7-dimethoxyisoquinoline derivatives as FtsZ-targeting antibacterial agents. *Bioorg Med Chem* 20: 7012-7029.
141. Lopes, N. M., H. P. Miller, N. D. Young, and B. K. Bhuyan. 1997. Assessment of microtubule stabilizers by semiautomated in vitro microtubule protein polymerization and mitotic block assays. *Cancer Chemother Pharmacol* 41: 37-47.
142. Goeckeler, J. L., A. Stephens, P. Lee, A. J. Caplan, and J. L. Brodsky. 2002. Overexpression of yeast Hsp110 homolog Sse1p suppresses ydj1-151 thermosensitivity and restores Hsp90-dependent activity. *Molecular biology of the cell* 13: 2760-2770.
143. Johnson, B. D., A. Chadli, S. J. Felts, I. Bouhouche, M. G. Catelli, and D. O. Toft. 2000. Hsp90 chaperone activity requires the full-length protein and interaction among its multiple domains. *J Biol Chem* 275: 32499-32507.



144. Silberg, J. J., K. G. Hoff, and L. E. Vickery. 1998. The Hsc66-Hsc20 chaperone system in *Escherichia coli*: chaperone activity and interactions with the DnaK-DnaJ-grpE system. *Journal of bacteriology* 180: 6617-6624.
145. Buchner, J., M. Schmidt, M. Fuchs, R. Jaenicke, R. Rudolph, F. X. Schmid, and T. Kiefhaber. 1991. GroE facilitates refolding of citrate synthase by suppressing aggregation. *Biochemistry* 30: 1586-1591.
146. Matsumori, M., H. Itoh, I. Toyoshima, A. Komatsuda, K. Sawada, J. Fukuda, T. Tanaka, A. Okubo, H. Kinouchi, K. Mizoi, T. Hama, A. Suzuki, F. Hamada, M. Otaka, Y. Shoji, and G. Takada. 2002. Characterization of the 105-kDa molecular chaperone. Identification, biochemical properties, and localization. *European journal of biochemistry / FEBS* 269: 5632-5641.
147. Morris, A. M., M. A. Watzky, and R. G. Finke. 2009. Protein aggregation kinetics, mechanism, and curve-fitting: a review of the literature. *Biochimica et biophysica acta* 1794: 375-397.
148. Mayer, M. P., and B. Bukau. 2005. Hsp70 chaperones: cellular functions and molecular mechanism. *Cellular and molecular life sciences : CMLS* 62: 670-684.
149. Mayer, M. P. 2013. Hsp70 chaperone dynamics and molecular mechanism. *Trends in biochemical sciences* 38: 507-514.
150. Bracher, A., and J. Verghese. 2015. The nucleotide exchange factors of Hsp70 molecular chaperones. *Front Mol Biosci* 2: 10.
151. Trott, A., L. Shaner, and K. A. Morano. 2005. The molecular chaperone Sse1 and the growth control protein kinase Sch9 collaborate to regulate protein kinase A activity in *Saccharomyces cerevisiae*. *Genetics* 170: 1009-1021.
152. Raviol, H., B. Bukau, and M. P. Mayer. 2006. Human and yeast Hsp110 chaperones exhibit functional differences. *FEBS letters* 580: 168-174.

153. Gowda, N. K., G. Kandasamy, M. S. Froehlich, R. J. Dohmen, and C. Andreasson. 2013. Hsp70 nucleotide exchange factor Fes1 is essential for ubiquitin-dependent degradation of misfolded cytosolic proteins. *Proc Natl Acad Sci U S A* 110: 5975-5980.
154. Gao, X., M. Carroni, C. Nussbaum-Krammer, A. Mogk, N. B. Nillekoda, A. Szlachcic, D. L. Guilbride, H. R. Saibil, M. P. Mayer, and B. Bukau. 2015. Human Hsp70 Disaggregase Reverses Parkinson's-Linked alpha-Synuclein Amyloid Fibrils. *Mol Cell* 59: 781-793.
155. Shorter, J. 2011. The mammalian disaggregase machinery: Hsp110 synergizes with Hsp70 and Hsp40 to catalyze protein disaggregation and reactivation in a cell-free system. *PLoS one* 6: e26319.
156. Erkin, A. M., C. C. Adams, M. Gao, and D. S. Gross. 1995. Multiple protein-DNA interactions over the yeast HSC82 heat shock gene promoter. *Nucleic Acids Res* 23: 1822-1829.
157. Erkin, A. M., C. Szent-Gyorgyi, S. F. Simmons, and D. S. Gross. 1995. The upstream sequences of the HSP82 and HSC82 genes of *Saccharomyces cerevisiae*: regulatory elements and nucleosome positioning motifs. *Yeast* 11: 573-580.
158. Behnke, J., M. J. Mann, F. L. Scruggs, M. J. Feige, and L. M. Hendershot. 2016. Members of the Hsp70 Family Recognize Distinct Types of Sequences to Execute ER Quality Control. *Mol Cell* 63: 739-752.
159. Trott, A., and K. A. Morano. 2004. SYM1 is the stress-induced *Saccharomyces cerevisiae* ortholog of the mammalian kidney disease gene Mpv17 and is required for ethanol metabolism and tolerance during heat shock. *Eukaryotic cell* 3: 620-631.
160. Hampsey, M. 1997. A review of phenotypes in *Saccharomyces cerevisiae*. *Yeast* 13: 1099-1133.
161. Shaner, L., P. A. Gibney, and K. A. Morano. 2008. The Hsp110 protein chaperone Sse1 is required for yeast cell wall integrity and morphogenesis. *Current genetics* 54: 1-11.

162. Brodsky, J. L., E. D. Werner, M. E. Dubas, J. L. Goeckeler, K. B. Kruse, and A. A. McCracken. 1999. The requirement for molecular chaperones during endoplasmic reticulum-associated protein degradation demonstrates that protein export and import are mechanistically distinct. *J Biol Chem* 274: 3453-3460.
163. Sadlish, H., H. Rampelt, J. Shorter, R. D. Wegrzyn, C. Andreasson, S. Lindquist, and B. Bukau. 2008. Hsp110 chaperones regulate prion formation and propagation in *S. cerevisiae* by two discrete activities. *PloS one* 3: e1763.
164. Saxena, A., Y. K. Banasavadi-Siddegowda, Y. Fan, S. Bhattacharya, G. Roy, D. R. Giovannucci, R. A. Frizzell, and X. Wang. 2012. Human heat shock protein 105/110 kDa (Hsp105/110) regulates biogenesis and quality control of misfolded cystic fibrosis transmembrane conductance regulator at multiple levels. *J Biol Chem* 287: 19158-19170.
165. Nagy, M., W. A. Fenton, D. Li, K. Furtak, and A. L. Horwich. 2016. Extended survival of misfolded G85R SOD1-linked ALS mice by transgenic expression of chaperone Hsp110. *Proc Natl Acad Sci U S A* 113: 5424-5428.
166. Song, Y., M. Nagy, W. Ni, N. K. Tyagi, W. A. Fenton, F. Lopez-Giraldez, J. D. Overton, A. L. Horwich, and S. T. Brady. 2013. Molecular chaperone Hsp110 rescues a vesicle transport defect produced by an ALS-associated mutant SOD1 protein in squid axoplasm. *Proc Natl Acad Sci U S A* 110: 5428-5433.
167. Moran, C., G. K. Kinsella, Z. R. Zhang, S. Perrett, and G. W. Jones. 2013. Mutational analysis of Sse1 (Hsp110) suggests an integral role for this chaperone in yeast prion propagation in vivo. *G3 (Bethesda)* 3: 1409-1418.
168. Samaddar, M., A. V. Goswami, J. Purushotham, P. Hegde, and P. D'Silva. 2014. Role of the loop L4,5 in allosteric regulation in mtHsp70s: in vivo significance of domain communication and its implications in protein translocation. *Molecular biology of the cell* 25: 2129-2142.

169. Muralidharan, V., A. Oksman, P. Pal, S. Lindquist, and D. E. Goldberg. 2012. Plasmodium falciparum heat shock protein 110 stabilizes the asparagine repeat-rich parasite proteome during malarial fevers. *Nature communications* 3: 1310.
170. Rakhit, R., S. R. Edwards, M. Iwamoto, and T. J. Wandless. 2011. Evaluation of FKBP and DHFR based destabilizing domains in *Saccharomyces cerevisiae*. *Bioorganic & medicinal chemistry letters* 21: 4965-4968.
171. Iwamoto, M., T. Bjorklund, C. Lundberg, D. Kirik, and T. J. Wandless. 2010. A general chemical method to regulate protein stability in the mammalian central nervous system. *Chem Biol* 17: 981-988.
172. Jaiswal, M., H. Sandoval, K. Zhang, V. Bayat, and H. J. Bellen. 2012. Probing mechanisms that underlie human neurodegenerative diseases in *Drosophila*. *Annu Rev Genet* 46: 371-396.
173. Easton, D. P., Y. Kaneko, and J. R. Subject. 2000. The hsp110 and Grp1 70 stress proteins: newly recognized relatives of the Hsp70s. *Cell stress & chaperones* 5: 276-290.
174. Finka, A., S. K. Sharma, and P. Goloubinoff. 2015. Multi-layered molecular mechanisms of polypeptide holding, unfolding and disaggregation by HSP70/HSP110 chaperones. *Front Mol Biosci* 2: 29.
175. Kelley, L. A., S. Mezulis, C. M. Yates, M. N. Wass, and M. J. Sternberg. 2015. The Phyre2 web portal for protein modeling, prediction and analysis. *Nat Protoc* 10: 845-858.
176. Albanese, V., S. Reissmann, and J. Frydman. 2010. A ribosome-anchored chaperone network that facilitates eukaryotic ribosome biogenesis. *J Cell Biol* 189: 69-81.
177. Koplin, A., S. Preissler, Y. Ilina, M. Koch, A. Scior, M. Erhardt, and E. Deuerling. 2010. A dual function for chaperones SSB-RAC and the NAC nascent polypeptide-associated complex on ribosomes. *J Cell Biol* 189: 57-68.
178. McClellan, A. J., M. D. Scott, and J. Frydman. 2005. Folding and quality control of the VHL tumor suppressor proceed through distinct chaperone pathways. *Cell* 121: 739-748.

179. Doyle, S. M., J. R. Hoskins, and S. Wickner. 2007. Collaboration between the ClpB AAA+ remodeling protein and the DnaK chaperone system. *Proc Natl Acad Sci U S A* 104: 11138-11144.
180. Lum, R., J. M. Tkach, E. Vierling, and J. R. Glover. 2004. Evidence for an unfolding/threading mechanism for protein disaggregation by *Saccharomyces cerevisiae* Hsp104. *J Biol Chem* 279: 29139-29146.
181. Yamagishi, N., K. Goto, S. Nakagawa, Y. Saito, and T. Hatayama. 2010. Hsp105 reduces the protein aggregation and cytotoxicity by expanded-polyglutamine proteins through the induction of Hsp70. *Exp Cell Res* 316: 2424-2433.
182. Knowles, T. P., M. Vendruscolo, and C. M. Dobson. 2014. The amyloid state and its association with protein misfolding diseases. *Nat Rev Mol Cell Biol* 15: 384-396.
183. Ciocca, D. R., N. Cayado-Gutierrez, M. Maccioni, and F. D. Cuello-Carrion. 2012. Heat shock proteins (HSPs) based anti-cancer vaccines. *Curr Mol Med* 12: 1183-1197.
184. Wang, X. Y., X. Chen, M. H. Manjili, E. Repasky, R. Henderson, and J. R. Subjeck. 2003. Targeted immunotherapy using reconstituted chaperone complexes of heat shock protein 110 and melanoma-associated antigen gp100. *Cancer research* 63: 2553-2560.
185. Manjili, M. H., R. Henderson, X. Y. Wang, X. Chen, Y. Li, E. Repasky, L. Kazim, and J. R. Subjeck. 2002. Development of a recombinant HSP110-HER-2/neu vaccine using the chaperoning properties of HSP110. *Cancer research* 62: 1737-1742.
186. Wang, X. Y., and J. R. Subjeck. 2013. High molecular weight stress proteins: Identification, cloning and utilisation in cancer immunotherapy. *International journal of hyperthermia : the official journal of European Society for Hyperthermic Oncology, North American Hyperthermia Group* 29: 364-375.

## **Vita**

Veronica Margarita Garcia was born on July 22<sup>nd</sup>, 1984 in Reynosa, Tamaulipas, Mexico to Miguel Angel García Gracia and María Del Refugio García Barrientos. After graduating from La Joya High School (La Joya, Texas) in 2002, she attended Texas A&M University (College Station, Texas). In December 2006, Veronica received a Bachelor of Science in Bioenvironmental Science with minors in Environmental Soil Science and Spanish. Upon completion of the Bachelor of Science degree, she started working as a Microbiologist at the NASA Lyndon B. Johnson Space Center (Houston, Texas). In August 2010 she enrolled at The University of Texas MD Anderson Cancer Center UTHealth Graduate School of Biomedical Sciences. She joined the laboratory of Kevin A. Morano, Ph.D., in April 2012, where she completed the research for her dissertation.